Luminescence based chronologies on Late Pleistocene loess-palaeosol sequences

- an applied-methodological study on quartz separates -

Sebastian Kreutzer

Dissertation
zur Erlangung des Grades
Doktor der Naturwissenschaften
(Dr. rer. nat.)
an der Fakultät für Biologie, Chemie und Geowissenschaften
der Universität Bayreuth

Gießen im Dezember 2012

Erstellt mit LaTeX

Die vorliegende Arbeit wurde in der Zeit von Oktober 2008 bis Dezember 2012 am Lehrstuhl für Geomorphologie der Universität Bayreuth unter Betreuung von Herrn Prof. Dr. Markus Fuchs angefertigt.

Vollständiger Abdruck der von der Fakultät für Biologie, Chemie und Geowissenschaften der Universität Bayreuth genehmigten Dissertation zur Erlangung des akademischen Grades Doktor der Naturwissenschaften (Dr. rer. nat.).

Amtierende Dekanin: Prof. Dr. Beate Lohnert

Tag des Einreichens der Dissertation: 05.12.2012

Tag des wissenschaftlichen Kolloquiums: 08.02.2013

Prüfungsausschuß

1. Prof. Dr. Markus Fuchs (Justus-Liebig-Universität Gießen, Erstgutachter)
2. Prof. Dr. Ludwig Zöller (Zweitgutachter)
3. Prof. Dr. Stefan Peiffer (Vorsitzender)
4. Prof. Dr. Klaus Bitzer
5. Prof. Dr. Andreas Held

Zusammenfassung

Hintergrund Der Wunsch nach einem tiefgreifenden Verständnis für den Ablauf früherer landschaftsgenetischer, morphologischer Prozesse, bildet einen wichtigen Beweggrund in der Quartärforschung. Im Hinblick auf die Rekonstruktion von Paläolandschafts- und Umweltbedingungen haben sich Lössprofile als unverzichtbare terrestrische Archive herausgestellt. Die Überprüfung einer durch Geländeuntersuchungen identifizierten und klassifizierten Stratigraphie, insbesondere hinsichtlich einer gewünschten Parallelisierung mit anderen Profilen, erfordert numerische Datierungen. Für die Datierung von Lössarchiven hat sich die Lumineszenz-, hier speziell die optisch stimulierte Lumineszenz (OSL-), Datierung als eine der führenden Methoden etabliert. Zudem gibt es, insbesondere in der jüngeren Geschichte der Lössforschung, eine enge Verbindung zwischen der Entwicklung angewandter Verfahren zur Lumineszenzdatierung an Sedimenten und einem verbesserten Verständnis zum zeitlichen Ablauf der Lösssedimentation im Spätpleistozän. Vor diesem Hintergrund können Lössforschung und Forschung zur angewandten Lumineszenzdatierung als korrespondierende Verfahren verstanden werden.

Als Teil des europäischen Lössgürtels befindet sich die Sächsische Löss Region (Saxonian Loess Region) in einer Übergangszone zwischen einem ozeanisch und einem kontinental geprägten Klima. In der sächsischen Lösslandschaft finden sich bis zu 20 m mächtige Ablagerungen von weichselzeitlichem Löss mit zwischengeschalteten Paläoböden. Die erste systematische Lössforschung in Sachsen begann in den späten 1950er Jahren. Seit 2008 wurden im Rahmen eines von der Deutschen Forschungsgemeinschaft (DFG) finanzierten interdisziplinären Forschungsprojektes zur Paläolandschafts- und Umweltrekonstruktion, alte und neue Lössprofile in Sachsen neu geöffnet und systematisch unter Anwendung von Gelände- und Labormethoden untersucht. In diesem Zusammenhang konnten zum ersten Mal an Lössen in Sachsen hoch aufgelöste OSL-Datierungen an fünf Lössprofilen durchgeführt werden. Die Geländearbeiten wurden von einer Arbeitsgruppe der TU Dresden geleitet, die OSL-Datierungen sind Schwerpunkt der hier präsentierten kumulativen Studie.

Neben der Vorstellung neu erstellter Chronostratigraphien ist die vorliegende Datierungsstudie auf einen Vergleich der in der Datierungspraxis üblicherweise herangezogenen Korngrößen ausgelegt. Es wird versucht die Frage zu klären, ob es hinsichtlich der verschiedenen Korngrößen, die aus einer Bulkprobe separiert werden, Unterschiede in den Lumineszenzeigenschaften gibt, welche sich in den Datierungsergebnissen niederschlagen. Konkrete in der Datierungspraxis verwendete Korngrößen sind: (1) Grobkorn (90–200 µm), (2) Mittelkorn (38–63 µm) und (3) Feinkorn (4–11 µm). Unterschiede sind z.B. aufgrund korngrößenabhängiger Transportprozesse zu erwarten. Es werden Datierungsstudien von vier Lössprofilen, drei durchgeführt in Deutschland (Sachsen, Sachsen-Anhalt) und Tschechien, herangezogen und präsentiert.

Als Kombination aus angewandter Datierung und methodischer Untersuchung die Lumineszenzdatierung betreffend, liefert diese Arbeit einen Beitrag zur Erstellung von zuverlässigen

hoch aufgelösten numerischen Chronologien an spätpleistozänen Löss-Paläoboden Sequenzen. Die Datierungen wurden überwiegend an Quarzen durchgeführt.

Aufbau und Methoden In der vorliegenden Arbeit werden sieben Einzelstudien vorgestellt. Eine ausführliche Zusammenfassung liefert Ch. 1. Vier Studien (Ch. 2, 3, 7, 8) stellen numerische Chronologien unter Anwendung der OSL-Datierung vor. Es werden Vergleiche hinsichtlich des Alters, basierend auf den Datierungen verschiedener Korngrößen (und Minerale), vorgestellt. Aus Sachsen werden die Ergebnisse von zwei der im Rahmen dieser Arbeit datierten fünf Lössprofile vorgestellt. Eine Übersicht aller Datierungsergebnisse findet sich im Anhang dieser Arbeit.

Obwohl die Datierungen hauptsächlich auf Quarzpräparaten basieren, kommt in der Studie in Ch. 7 ein neuartiges Datierungsprotokoll, post-IR IRSL (Thomsen et al. 2008) zum Einsatz, das ursprünglich für K-Feldspäte (Korngröße $> 90\,\mu m$) entwickelt wurde und hier an polymineralischen Feinkornpräparaten Anwendung findet. Die Verwendung polymineralischer Feinkornpräparte zur Datierung soll die Gültigkeit der erzielten Ergebnisse an Feinkornquarz unter Anwendung eines weiteren Minerals (hier Mineralgemisch) und eines anderen Messprotokolls sicherstellen.

Zwei weitere Studien (Ch. 4, 5) beschäftigen sich mit technischen Aspekten die während der Untersuchungen relevant wurden. Zum einen wurde im Rahmen dieser Arbeit ein **R** Paket („Luminescence“) zur Datenauswertung und Visualisierung entwickelt und zum anderen konnten Streulichteffekte (cross-bleaching) der Infrarot-LEDs in den genutzten Risø Lumineszenzmessgeräten untersucht und quantifiziert werden.

Die methodische Studie in Ch. 6 geht schließlich unter Anwendung des post-IR IRSL Protokolls an polymineralischen Feinkornpräparaten der Frage nach, ob die übliche Praxis der Verwendung eines gemeinsamen a-Wertes (Effektivität der durch α-Strahlung im Verhältnis der durch β-, γ- oder Röntgenstrahlung induzierten Lumineszenz) für beide Signale (hier IR_{50} und $pIRIR_{225}$) gerechtfertigt ist.

Ergebnisse Die vorliegenden Untersuchungen zeigen, dass unter Verwendung von Feinkornquarzpräparaten zuverlässige und hochaufgelöste Datierungen an Lössen bis zum Eem-Interglazial (MIS 5e, 5d) generell möglich sind. Durch die erstellten hochaufgelösten Chronostratigraphien konnten in den sächsischen Lössprofilen Hiati von ca. 30 ka zwischen der Früh- und der Spätweichselzeit (MIS 3) ausgemacht werden, was sich über sämtliche Profile (sofern die Stratigraphie dies zulässt) verifizieren lässt.

Für untere Dosisbereiche (Äquivalenzdosis bzw. $D_e < 100\,Gy$) zeigen die Ergebnisse zudem eine Altersübereinstimmung innerhalb der Fehler zwischen den untersuchten Korngrößen. Dennoch weisen die Grob- und Mittelkornergebnisse eine hohe Streuung innerhalb der D_e-Verteilungen auf, was für Lösse a priori nicht zu erwarten war und sich in Testmessungen nach künstlicher Signalrückstellung bestätigt. Zum anderen gehen die Quarze der Grob- und Mittelkornfraktion für $D_e > 180\,Gy$ in Sättigung und wurden aus diesem Grund für spätere Datierungen nicht mehr verwendet. Im Gegensatz dazu ist für die Feinkornfraktion nur eine geringe Streuung in der D_e Verteilung beobachtet worden, was allerdings auch aufgrund von Mittelungseffekten zu erwarten war. Interessant hingegen ist die Beobachtung, dass die Feinkornquarzfraktion eine erheblich höhere Sättigungsdosis aufweist. Dies ist in der Literatur bereits

früher beschrieben worden, allerdings gingen diese höheren Sättigungsdosen auch manchmal mit einer Altersunterschätzung einher. Eine Beobachtung, die sich in der vorliegenden Studie nicht bestätigt. Im Gegenteil war eine zuverlässige Datierung bis zum Eem möglich und Test- messungen nach künstlicher Bleichung haben die Reproduzierbarkeit der gegebenen Dosis auch bei höheren Dosen bestätigt. Zusammen mit den Erkenntnissen der Pedo- und Lithostratigraphie sind die Datierungsergebnisse als zuverlässig anzusehen.

Die Datierungen an polymineralischem Feinkorn (Ch. 7) konnten zudem die Ergebnisse der Datierungen an Quarzen bestätigen.

Die Quantifizierung der Streueffekte der Infrarot-LEDs hat nach Messungen auf 10 Geräten in unterschiedlichen Lumineszenzlaboren ergeben, dass dieser Effekt nahezu an allen untersuchten Geräten auftritt und zu erheblichen Verfälschungen bei der Bestimmung der D_e führen kann (mittlerer cross-bleaching Effekt $\sim 0.026\,\%$). Darüber hinaus liegt der beobachtete Streueffekt um eine Größenordnung über dem der ebenfalls im Gerät verbauten blauen LEDs.

Die Ergebnisse der a-Wert Bestimmungen zeigen, dass die mittleren a-Werte für Polymineralisch-Feinkorn für die gemessenen IR_{50} und $pIRIR_{225}$ Signale signifikant (min. um 0.02) voneinander abweichen. Der resultierende a-Wert für das $pIRIR_{225}$ Signal lieferte in den Untersuchungen einen systematisch höheren Wert. Die Ergebnisse der a-Wert Bestimmungen lassen daher den Schluss zu, dass die Nutzung eines einheitlichen a-Wertes für beide Signale des post-IR IR Protokolls zu systematischen Verzerrungen führen kann.

Fazit Im Rahmen dieser Arbeit wurde für die Sächsische Löss Region zum ersten Mal eine umfassende Chronostratigraphie erstellt. Die Lössprofile können nun zuverlässig mit anderen Profilen und Archiven korreliert werden, was neue Erkenntnisse hinsichtlich des Paläoumweltverständnisses erwarten lässt. Die Zuverlässigkeit von Feinkornquarzpräparaten als Dosimeter zur OSL-Datierung an Lössarchiven wurde unter Beweis gestellt. Signifikante Abweichungen zwischen den Altern der Korngrößen, in dem Bereich wo ein Vergleich aufgrund der frühen Signalsättigung der Grob- und Mittelkornfraktion möglich war, wurden nicht beobachtet. Dennoch bleibt die Streuung der Grob- und Mittelkornfraktion ebenso wie die höhere Sättigungsdosis der Feinkornquarze letztlich unerklärt. Hierzu sollten weitere Studien durchgeführt werden.

Als Konsequenz aus den Ergebnissen der Messungen zur Streuung der Infrarot-LEDs hat der Gerätehersteller mittlerweile ein Bauteil entwickelt, welches den Effekt signifikant zu reduzieren vermag (bis hin zu einer 20-fachen Reduzierung; siehe Ch. 5).

Das entwickelte **R** Paket 'Luminescence', welches im Zeitraum der Erstellung dieser Arbeit veröffentlicht wurde und auf einer CD dieser Arbeit beiliegt, ermöglicht bisher nicht realisierbare Auswertungen und konnte für einen Teil der Analysen und zur Erstellung eines großen Teils der in dieser Arbeit präsentierten Grafiken verwendet werden. Mittlerweile wird das Paket von mehreren Personen kontinuierlich weiterentwickelt.

Abschließend ist aufgrund der Ergebnisse der a-Wert Bestimmungen ein Umdenken in der Datierungspraxis unter Anwendung des post-IR IRSL Protokolls zu erwarten, da die Verwendung eines gemeinsamen a-Wertes nicht gerechtfertigt scheint. Zum einen, weil systematische Fehler generell zu vermeiden sind und zum anderen weil auch einige Fragen ungeklärt geblieben sind: So sind z.B. die Ursachen für die beobachteten Unterschiede unklar und müssten zunächst durch

andere Studien bestätigt werden. Die Ergebnisse dieser Arbeit mögen solche Untersuchungen anregen.

Summary

Background Understanding morphological processes that sculpt former terrestrial landscapes is one of the driving rationales in Quaternary research. Loess records have been found to be valuable archives for reconstructing palaeoenvironmental conditions.

However, once identified, characterised and classified by fieldwork, the stratigraphic significance of such records has to be revealed by numerical dating. Luminescence dating, especially optically stimulated luminescence (OSL), is the leading dating approach for establishing chronologies on loess archives. Furthermore, the development of luminescence dating techniques on sediments is closely connected with the history of loess research and vice versa.

As part of the European loess belt the Saxonian Loess Region is located in a transition zone between oceanic dominated western and continental dominated eastern climates. The Saxonian Loess Region comprises up to 20 m thick Weichselian loess accumulations, with intercalated palaeosoils. Loess research in Saxony dates back to the late 1950s. For an interdisciplinary research project funded by the German Research Foundation (DFG), since 2008 the Saxonian Loess Region has been re-investigated by fieldwork and laboratory methods. For the first time, during the work on this thesis, high-resolution numerical chronologies were established in the Saxonian Loess Region on five loess sections using OSL dating on quartz separates. Here, age results of these dating from two sections are presented.

The dating was employed as a comparison of three quartz grain size fractions commonly used for luminescence dating: (1) coarse (90–200 µm), (2) middle (38–63 µm) and (3) fine grain (4–11 µm). As a survey on four loess sections, three from Germany (Saxony and Saxony-Anhalt) and one from the Czech Republic, these studies investigate the question whether the use of different grain size fractions from one sample yield consistent luminescence characteristics and age results.

By combining dating application with methodological investigations, this thesis is intended as contribution towards the establishment of reliable high-resolution numerical chronologies on Late Pleistocene loess-palaeosol sequences based on OSL dating of quartz separates.

Scope and methods In summary seven studies are presented along with an extended summary (Ch. 1). Four studies (Ch. 2, 3, 7, 8) present numerical chronologies using OSL dating techniques on different grain size and (mineral) fractions. Although dating of the quartz fraction is the main focus of this study, in Ch. 7 polymineral fine grain dating results using the post-IR IR protocol (Thomsen et al., 2008) are presented for a comparison.

Two studies (Ch. 4, 5) deal with technical issues that arose during the dating applications. Firstly, an **R** package for luminescence dating data analysis ('Luminescence') was developed and secondly, the cross-bleaching behaviour of IR-LEDs of Risø luminescence readers were quantified.

The study in Ch. 6 treats the question whether the common practice of using an identical α-efficiency (a-value) for the conventional IR_{50} and $pIRIR_{225}$ dating is justified under theoretical and empirical viewpoints.

Results It was found that for the established numerical chronologies on loess the fine grain quartz fraction results in reliable age estimates up to the Eemian (MIS 5e, 5d). The high-resolution dating in Saxony uncovered a prominent hiatus of c. 30 ka between the early and the late Weichselian found in all investigated loess sections in Saxony. The fine grain quartz age results are confirmed by the polymineral fine grain dating.

For lower dose ranges ($D_e < 100$ Gy) age results of all three grain size fractions agree within uncertainties. However, the coarse and middle grain fractions show highly scattered D_e distributions. For higher doses ($D_e > 180$ Gy) the luminescence signals of the coarse and middle grain fractions are in saturation. In contrast, the luminescence signal of the fine grain fraction still grows and is reproducible as shown by test measurements.

The results of a cross-bleaching survey on 10 luminescence readers revealed substantial cross-bleaching behaviour of the IR-LEDs (mean cross-bleaching: ~ 0.026 %), in an order of magnitude higher than for blue LEDs. This may lead to systematic underestimations during D_e determination.

The investigation on the a-values of polymineral fine grain samples gave evidence for significant differences between the mean a-values obtained with the IR_{50} and the $pIRIR_{225}$ signals; at least by 0.02. The a-value obtained with the $pIRIR_{225}$ signal is always higher.

Conclusions For the first time a comprehensive numerical chronology was established for the Saxonian Loess Region. Additionally, it is shown that fine grain quartz separates provide a reliable dosimeter for establishing high-resolution chronologies on loess records. Significant grain size dependent differences in the ages were not observed for dose ranges $D_e < 100$ Gy, where the dating was applied on all three grain size fractions. However, the scatter of the coarse and middle grain fraction as well as the dose response behaviour of the fine grain fraction at higher doses remains unexplained so far. But the outcomes may be subject of further investigations.

As consequence of the cross-bleaching measurements a new component for the luminescence readers was developed by the manufacturer, which is capable to reduce the cross-bleaching of the IR-LEDs up to 20-times (Ch. 5). The developed **R** package 'Luminescence' was launched in the course of this thesis enabling data analysis and visualising options, which had not been available before. The package was intensively used for data analysis and visualising in the presented studies and is continuously under development by a growing developer community.

Finally, for the first time a-values on polymineral fine grain samples were measured using the post-IR IR protocol and it was shown that the practice of using a common a-value for different stimulation temperatures seems not to be justified. But further investigations are needed.

List of Abbreviations

$\dot{D}$	Dose rate in Gy ka^{-1}
λ	Wavelength in nm
ϕ	Stimulation intensity (photon flux) in cm^{-2} s^{-1}
ϕ_{max}	Maximum stimulation intensity in cm^{-2} s^{-1}
σ	Photoionisation cross-section in cm^2
σ	Standard deviation
b	Decay parameter in the context of LM-OSL in s^{-1}
c_v	Coefficient of variation as $\frac{\sigma}{\mu}$
D_e	Equivalent dose in Gy; $1\text{Gy} = \frac{\text{J}}{\text{kg}}$
E	Energy in eV
E_t	Thermal activation energy in eV
I	Luminescence signal intensity
k	Decay rate in s^{-1}
k_B	Botzmann's constant (8.6173324×10^{-5} eV K^{-1})
n	Concentration of trapped charges
n_0	Concentration of trapped charges in m^{-3} at $t = 0$
P	Stimulation period in s
p	Probability of a charge carrier to escape from the trap in s^{-1}
s	Frequency factor in s^{-1}
T	Temperature in K ($0\,°\text{C} \simeq 273.15\,\text{K}$)
t	Time in s
R	Name of the numerical programming language R (here written in bold letters)
CRAN	Comprehensive R Archive Network; http://cran.r-project.org
CW-OSL	Continuous wave optically stimulated luminescence

IR_{50} Infrared light stimulated luminescence; signal recorded at 50°C

IR-RF Infrared radiofluorescence

IRSL Infrared (light) stimulated luminescence

LM-OSL Linearly modulated optically stimulated luminescence

MIS Marine Isotope Stage

OSL Optically stimulated luminescence

$pIRIR_{225}$ Infrared light stimulated luminescence signal; recorded at 225°C after recording an IR_{50} signal

pLM-OSL Pseudo linearly modulated optically stimulated luminescence

post-IR IR Measurement protocol for feldspars according Thomsen et al. (2008); also termed post-IR IRSL or pIRIR

SAR Single aliquot regenerative (-dose protocol)

TL Thermoluminescence or thermally stimulated luminescence

Contents

List of Tables

List of Figures

1 Extended Summary

1.1 Introduction

1.1.1 Background

"Loess is not just the accumulation of dust"

(Pecsi, 1990)

This title of an essay on the definition, chemical and physical characteristics of loess now dates back more than 20 years and it may still be considered as an understatement on the relevance of simple dust that "becomes loess after the passage of a certain amount of time" (Pecsi, 1990, p. 1) and it may be acknowledged as a snippy reply on the question: What makes loess interesting?

Antoine et al. (2013, p. 1) stated for the European loess belt that it should be considered as the "most extensive and continuous continental archive of the Last Glacial". However, it undoubtedly represents one of the fundamental Quaternary sediment archives for understanding and evaluating morphological processes that sculpt former terrestrial landscapes. Furthermore, with the progression of sedimentation, erosion and soil formation, loess-palaeosol sequences result in a pattern that preserves valuable information on the palaeoclimate.

Pecsi (1990, p. 2) stated that loess "covers almost 10 % of the land surfaces", varying in thickness from a few meters up to several tens of meters (e.g. Rousseau et al., 2007). The European loess belt extends over an area from Northern France via Germany, Poland, the Czech Republic, Ukraine, Belarus to Southern Russia (cf. Haase et al., 2007; Fig. 8.1) and is almost located outside of the Fennoscandinavian and Alpine ice sheets (Kukla, 1977; Haase et al., 2007; Rousseau et al., 2007). According to Rousseau et al. (2007) the loess in Europe originated mainly from (distant) dried-out plains (e.g. English Channel, North Sea) and local dust sources (e.g. dried channels, alluvial plains).

Although varying in detail, all definitions on (pure) loess include the aeolian nature of the terrestrial sediment (e.g. Smalley and Vita-Finzi, 1968; Pecsi, 1990; Pye, 1995; Wright, 2001). The deposits consist of silt-sized quartz dominated particles. The modal grain size range varies in the literature (e.g. 20–50 µm: Smalley and Vita-Finzi, 1968 or 2–63 µm: Pye, 1995) and is, as well as the specific mineral composition, a product of a source area and natural variations (cf. Pye, 1995; Rousseau et al., 2007). The appearance is described as unstratified (Pecsi, 1990) "wind-laid sheets" (Smalley and Vita-Finzi, 1968) of pale yellow colouring (e.g. Pye, 1995; Rousseau et al., 2007) for which Smalley and Vita-Finzi (1968) mentioned two major sources (a) glacial/periglacial regions and (b) 'hot' deserts. Accounting for the primary sedimentation process e.g. Pecsi (1990) called for a distinction between (a) 'primary loess' (accumulated by aeolian processes) and (b) 'secondary loess' (redeposited, post depositional translocated), whereas Pye (1995) argued against such a distinction because it does not include the name of the redeposition process. Such emerging discussions appear somehow theoretical but they highlight an interesting aspect: The appearances and the origins of loess deposits are manifold and a single loess record may contain a variety of information on the depositional environment (e.g. Kukla, 1977) and the question of how the process of accumulation occurred and proceeded.

However, loess archives are collections of single records. They are physically spread out, often fragmented, incomplete and comprehensive interpretation and recognition at the local level remain challenging. Pecsi (1990) stated: "Erosional hiatuses are seldom visible to the naked eye." Historically, the above mentioned significance of loess as a climate archive as well as the aeolian origin had not been recognised in the early years of loess research in Europe at the end of the 19th century (cf. Zöller and Semmel, 2001). Thus, the nowadays commonly applied litho- and pedological parallelisation (e.g. Antoine et al., 2001; Jary, 2009; Haesaerts et al., 2010; Meszner et al., 2011) of different loess sections reflects the ongoing research history on loess over a long period of time (cf. Zöller and Semmel, 2001; Rousseau et al., 2007).

This long research history on loess deposits allows us to take up the initial question again and to answer it in a way beyond its relevance for terrestrial palaeoenvironmental research: What makes loess interesting? There are hundreds of loess sections in Europe that have been described in the literature (e.g. Kukla, 1977). They are partly well investigated, stratified and reinvestigated by litho- and pedological methods (e.g. Nussloch/Germany: Antoine et al., 2001, 2009 or Dolní Věstonice/Czech Republic: Klíma et al., 1962; Demek and Kukla, 1969; Kukla, 1975) and provide a profound interregional stratigraphic correlation and understanding (cf. Zöller, 2010; Rousseau et al., 2007). This situation qualifies loess records to developing, testing and refining new methodological investigation approaches and it makes loess sections interesting beyond their palaeoenvironmental implications (e.g. luminescence dating techniques: Timar-Gabor et al., 2012; Vasiliniuc et al., 2012; Thiel et al., 2011b; Schmidt et al., 2011; Novothny et al., 2010 or geochemical/pedological techniques: Zech et al., 2012; Buggle, 2011).

On the other hand, the continuous application of new methods on loess sections leads to an ongoing refinement of existing stratigraphies and revisiting of established theories. This hand-in-hand process is best described with the history of luminescence dating: Loess was the first terrestrial sediment on which this dating method was systematically applied (review article: Roberts, 2008). This complementary link is not a historical accident but accounts for a (still) increasing demand for numerical dating techniques (e.g. Pecsi, 1990) beyond the age limit of e.g. ^{14}C dating (cf. Geyh, 2005) to reveal the stratigraphic significance of the litho- and pedological findings, estimate mass accumulation rates (e.g. Frechen et al., 2003) or to uncover gradients and hiatuses (Ch. 2).

> *"The dating of geological and archaeological events would be easier if the mineral grains that form a sediment could be dated directly"*
>
> (Huntley et al., 1985)

Optical stimulated luminescence (OSL) dating was introduced in 1985 on quartz by Huntley et al. (1985) and in 1988 on K-feldspar, termed infrared light stimulated luminescence (IRSL) by Hütt et al. (1988). Previously, luminescence dating (cf. Sec. 1.3) on loess had been applied using thermal luminescence (TL) dating (review article: Wintle, 1990). The event dated is the last heating. The optical bleaching of the investigated luminescence signal using TL dating is carried out "with less effectiveness" (Aitken, 1998, p. 2) but on loess that presumably had a long exposure to sunlight the method is applicable. However, secondary locally limited translocations or short transport distances may lead to age overestimations due to insufficient signal resetting and constrain the application of TL dating techniques on sediments. For OSL

dating much shorter bleaching times (e.g. Godfrey-Smith et al., 1988; Stokes, 1999) are needed, making OSL dating a powerful numerical dating tool (cf. Stokes, 1999, for further discussion on the advantages of OSL over TL dating on sediments).

Using ubiquitously available mineral grains of quartz or feldspar the method can potentially be employed all over the world. The dated event is the last exposure of the sediment to sunlight and the "geological and archaeological events" (Huntley et al., 1985) are dated directly. Furthermore, OSL dating overcomes tentative problems of other commonly applied dating methods on loess: Other radiometric dating methods (e.g. radiocarbon dating, potassium-argon dating) cannot directly date the depositional event. In addition, unlike for radiocarbon dating, which has been proposed as the main quaternary dating methods for the last c. 50 ka (e.g. Reimer, 2012), it is not linked to the availability of organic matter.

Nevertheless, it took another 15 years to develop the single-aliquot regenerative-dose (SAR) protocol as an efficient, precise and reliable measurement protocol for OSL dating on quartz (Murray and Wintle, 2000). Since then the number of dating studies for the last glacial-interglacial cycle on loess have continuously increased along with the methodological progression of luminescence dating methods (review article: Roberts, 2008).

However, there are still pressing methodological concerns. Within the age range of radiocarbon dating luminescence dating (TL/OSL) provides a highly reliable numerical dating method and its validity can be proved by independent age controls. Beyond the age range of conventional coarse grain (cf. Sec. 1.3 and Fig. 1.7) quartz dating on loess (depending on the dose rate: 50 ka to 80 ka; e.g. Zöller, 2010), dating may fail due to the saturation limit of the dosimeter. For the fine grain fraction of quartz, higher saturation doses (i.e. extended age ranges) are reported (cf. Roberts, 2008) but they seem to underestimate the expected age (e.g. Lowick and Preusser, 2011; Timar et al., 2010). Furthermore, smaller grain sizes may reflect different post-depositional transport processes resulting in differing ages. Here, further investigations are needed.

Higher saturation doses and therefore extended age ranges are enabled by IRSL dating on coarse grain K-feldspars or polymineral (a mixture of minerals) fine grains, but luminescence dating on feldspars suffers from age underestimations due to an anomalous signal loss over time (anomalous fading: Wintle, 1973; Visocekas, 1985). Much effort has been undertaken to overcome this problem by numerical corrections (e.g. Huntley and Lamothe, 2001; Auclair et al., 2003) or adjusted measurement routines (e.g. Kadereit, 2000). An alternative approach of feldspar dating using a new measurement protocol (post-IR IR protocol) was introduced in 2008 by Thomsen et al. (2008). The post-IR IR approach deals with measuring a signal component that is assumed to be less fading affected. Although applied on loess sections (e.g. Vasiliniuc et al., 2012; Thiel et al., 2011a), this method is still under discussion and has not been proven beyond any doubt (e.g. Lowick et al., 2012). In addition, Buylaert et al. (2011) reported unbleachable signal residuals when applying the new protocol which indicated different bleaching characteristics of the investigated luminescence signals.

Accounting for the mineral composition of loess (quartz content in European loess: 40–80 %; Rousseau et al., 2007) and considering the disadvantages of feldspar dating, almost all age results of this thesis have been carried out using OSL dating on quartz. The investigated age range covers the full last-interglacial cycle. The potential differences between the grain

size fractions have been investigated and combined with further methodological investigations. The general objectives of this thesis are provided in the following section.

1.1.2 Objectives

This cumulative thesis is intended as a contribution towards the establishing of reliable high-resolution numerical chronologies based on quartz OSL dating on loess palaeosol-sequences for the last glacial-interglacial cycle. Designed as an applied-methodological study it continues the closely-related progression of luminescence dating and loess research.

1. **Establishing high-resolution chronostratigraphies**

   Luminescence dating has become one the most important numerical dating technique for terrestrial sediment archives but it remains challenging. Although widely applied on Quaternary sediment archives the obtained age results depend on different circumstances that may hamper the dating procedure. (a) The dosimeter used for dating may suffer from bad luminescence characteristics, e.g. dim luminescence signal, domination of improper slowly bleachable signal components or early signal saturation that limit the datable age range. (b) The investigated transport process may not have had sufficiently reset the latent luminescence signal, e.g. due to short travel distances. (c) Uncertainties in the dose rate estimation, e.g. due to radioactive disequilibria.

   The prime objective was to establish a reliable high-resolution numerical chronostratigraphy on Late Pleistocene loess sections in the Saxonian Loess Region using OSL dating.

   The study of Meszner et al. (2011) using IRSL dating on polymineral fine grain (4–11 µm) samples showed the general suitability of the Saxonian Loess Region for luminescence dating and due to the aeolian origin of the loess the luminescence signal was expected to have been fully reset during transport. For the IR-stimulated luminescence signal of the polymineral fine grain fraction it is believed that the measured signal in the violet-blue band is dominated by feldspar minerals. However, it is known from feldspar that it suffers from anomalous fading (Wintle, 1973) that potentially leads to age underestimations.

   For this thesis the strategy was to establish the chronological framework on the mineral quartz and it is hypothesised that a reliable chronostratigraphy can be established up to the Eemian interglacial (MIS 5d, 5e; Shackleton, 2003).

2. **Investigation of luminescence characteristics on different grain size fractions**

   Luminescence dating is widely applied on loess archives but the dating procedure is not that straight forward. For luminescence dating on sediments, in general three different grain size fractions are used: (a) coarse grain (c. 90–250 µm; e.g. Wintle, 2008a), (b) middle grain (c. 38–63 µm; e.g. Lai and Wintle, 2006) and (c) fine grain (4–11 µm; e.g. Roberts, 2008). The selection of a specific grain size for the dating procedure depends on practical (e.g. grain size availability in the target sediment) or methodological considerations (e.g. higher saturation doses for fine grain compared to coarse grain; e.g. Roberts, 2008).

   The question remains whether the selection of a specific grain size fraction for dating from a bulk sample is justified: (a) Different luminescence characteristics for distinct grain size

fractions are mentioned in the literature (e.g. Wang and Miao, 2006; Roberts, 2008; Lai, 2010; Timar-Gabor et al., 2011) and (b) different transport histories and processes may result in different depositional ages for the specific grain fractions (e.g. post-depositional translocation). Systematic investigations on this question were missing at the beginning of this thesis.

The goal was to compare the luminescence characteristics of different quartz grain size fractions and compare the obtained age results.

It is hypothesised that grain size fractions show specific luminescence characteristics due to differences in the dosimeter and therefore result in different luminescence ages.

3. **Methodological investigations**

   Luminescence dating dates back to the 1950s (Daniels et al., 1953; Houtermans and Stauffer, 1957; Grögler et al., 1958) but it has been greatly improved during the last decades (review articles: Wintle, 2008b,a, 2010).

   For example, for quartz Bailey et al. (1997) proposed that the signal of quartz comprises at least three individual signal components with individual bleaching and saturation characteristics. These signal components can be convoluted by mathematical fitting and visualised as peak shape curves by measurements ramping the stimulation power (e.g. LM-OSL measurements) or mathematical transformation of the continuous wave (CW) measurement. Such investigations allow the characterisation of the dosimeter and the estimate whether a dosimeter is suitable for dating or not (e.g. contains an easy bleachable fast component).

   The strategy of this thesis was in general to enhance the combination of methodological analysis and dating applications on loess to evaluate and improve existing attempts towards reliable chronologies on loess deposits.

   It aimed at using different methodological approaches during the dating process to investigate luminescence characteristics and to further methodologically improve the luminescence dating on loess archive.

1.1.3 Thesis scope and format

For this thesis seven studies are selected and presented which were carried out between October 2008 and August 2012 and contributed to international peer-reviewed journals (full list of publications Ch. C). All studies deal with the application of luminescence dating to establish numerical chronologies on loess-palaeosol sequences or focusing on somehow more specific technical or methodological aspects of luminescence dating. The studies should not be considered as insular contributions but comprehensive developments and investigations that became necessary during the research process to cover the objectives of this thesis. The studies can be classified using three categories:

- Dating application (Sec. 1.1.3.1)
- Technical investigations and developments (Sec. 1.1.3.2)

- Methodological investigations (Sec. 1.1.3.3)

This allows the reader to trace the research process, it provides a link between these studies and it outlines the purpose of each study.

Five out of seven manuscripts (Ch. 2–6) were prepared as first author articles including data analysis, writing, scientific discussion, illustration and correspondence with the journal editor if not stated otherwise. For the other two manuscripts (Ch. 7, 8) substantial contributions as co-author were provided. The approximated relative authors contributions to each manuscript are given on the cover sheet of each study. The journal and the publication status are shown on the cover sheet of each study. The summarised (partly so far unpublished) dating results are listed in Ch. A.1 (D_e values and age results) and Ch. A.2 (nuclide concentrations and dose rates).

The following subsections (Sec. 1.1.3.1–1.1.3.3) summarise the main intention of each study. Section 1.2 briefly describes the main research area. Section 1.3 examines the method of luminescence dating in more detail to provide the basic methodological concepts. In Sec. 1.4 the main results of this thesis are presented and discussed and subsequently summarised (Sec. 1.5).

1.1.3.1 Dating application

Most of the presented work was carried out within the framework of the DFG funded research project 'Saxony Loess' (FU 417/7-1 and FU 417/7-2) that was intended to reconstruct the palaeoenvironmental conditions of the Late-Pleistocene in Middle Saxony using loess-palaeosol sequences. As a co-operation between the TU Dresden and the University of Bayreuth the objective of this project was twofold: (a) To establish a litho- and pedostratigraphy (TU Dresden) and (b) to provide a luminescence based high-resolution chronostratigraphy (University of Bayreuth).

Once the loess layers have been identified, characterised and classified by fieldwork, a numerical chronostratigraphy is needed to reveal their full stratigraphic significance. In the framework of the DFG project 'Saxony Loess' on five loess profiles in Saxony and one profile in Saxony-Anhalt numerical chronologies have been established.

To get started the loess section Ostrau as the most complete last glacial-interglacial loess section in Saxony was selected as key location for high-resolution OSL dating.

Chapter 2 introduces a chronostratigraphy based on 20 OSL samples. From each sample three different quartz grain size fractions (coarse, middle and fine grain) were prepared. The study (a) shows the suitability of the Saxonian loess belt for OSL dating on quartz, (b) introduces the OSL based chronostratigraphy and (c) systematically compares the derived quartz coarse (90–200 µm) and fine grain ages (4–11 µm). The OSL ages based on the middle grain quartz fraction (38–63 µm) were not part of this study and are thus briefly presented and discussed in Sec. 1.4.1.1.1.

In preparation of the field trip of the 37th meeting of the German working group on geomorphology to the Saxony-Anhalt loess belt the opportunity arose to reinvestigate the locally important quaternary profile Zeuchfeld. The profile is part of the Middle German Loess Region and is well known for its sandur (Zeuchfeld Sandur) at the base of the profile and the overlying

periglacial deposits (e.g. Ruske, 1961; Meng and Wansa, 2008). To validate the stratigraphical classification of the Saxonian Loess Region introduced by Meszner et al. (2011) a chronostratigraphy for the profile Zeuchfeld was determined for the first time and compared with the findings from the Saxonian Loess Region.

Chapter 3 presents and discusses the dating results as a combination of (a) conventional OSL quartz dating for the loess deposits and (b) innovative feldspar dating using infrared radiofluorescence (IR-RF; Trautmann et al., 1999; Erfurt and Krbetschek, 2003; Erfurt, 2003) for the Zeuchfeld Sandur. Originally, it was intended to continue the systematic age comparison of different quartz grain size fractions on the profile Zeuchfeld. Due to feldspar contamination of the quartz extracts and limited sample material the dating was limited to only one grain size fraction per sample but the differences in the luminescence characteristics are discussed.

Based on the ongoing fieldwork and the comprehensive numerical framework it was finally possible to present a revised composite profile for the Saxonian Loess Region.

Chapter 7 summarises and combines the results from the investigated loess sections in Saxony as an attempt to reconstruct the Pleistocene landscape dynamics. Furthermore, the chronostratigraphy for the loess record Seilitz is introduced. The luminescence dating was almost carried out on fine grain quartz separates. However, to provide a cross-validation of the obtained dating results on the mineral quartz, additionally polymineral fine grains were extracted to apply a, at this then, newly developed dating protocol (post-IR IR protocol; initially: Thomsen et al., 2008) on 5 out of 11 samples.

Chapter 8 is intended as a supplementary dating study. This study introduces a revised chronostratigraphy for the famous loess section Dolní Věstonice in the Czech Republic (e.g. Klíma et al., 1962), well known for its high-resolution loess-palaeosol sequence of the last interglacial-glacial climatic cycle. Carried out between 2009 and 2011, the study deals with luminescence dating on different grain size fractions of quartz separates. It logically continues the combination of field work, dating application and methodological investigations towards reliable numerical frameworks back to the Eemian.

Further related studies (not part of this thesis):

- *Introducing a chronostratigraphy of the profile Gleina in Saxony based on fine grain quartz:*

  Zech, M., Kreutzer, S., Goslar, T., Meszner, S., Krause, T., Faust, D., Fuchs, M., 2013. Technical Note: *n*-Alkane lipid biomarkers in loess: post-sedimentary or syn-sedimentary? Biogeosciences Discuss 9, 9875–9896.
  doi: `http://dx.doi.org/10.5194/bgd-9-9875-2012`

1.1.3.2 Technical investigations and developments

In an ideal manner the research process is a step by step process along a well defined path that finishes the previous step before moving on to the next step. Imbedded in a comprehensive project framework it often requires a multiple step approach to pay attention to more practical aspects or to take into account external forces. Such requirement for intermediate steps may

grow if it turns out that the common approach of data handling and visualisation is no longer feasible to efficiently analyse the produced amount of data.

Chapter 4 deals with a software developed for the numerical programming language **R** (e.g. Hornik and Leisch, 2002; Ligges, 2008). The **R** package ('Luminescence') for luminescence dating data analysis (e.g. LM-OSL component separation or data visualisation) has been continuously developed during the entire time of this thesis. Initially split up over several **R** scripts, the software code was bundled in functions and subsequently provided as **R** package. The package was first released in version 0.1.7 in June 2012 under General Public License (GPL) conditions via the Comprehensive R Archive Network (CRAN). Part of this thesis is the **R** package 'Luminescence' in version 0.2.[1] All included functions with the primary author are given in Ch. A.4.

Chapter 5 accounts for an observation that was made during the luminescence measurements on polymineral fine grain samples from the profile Seilitz (Ch. 7). The measurement of every first subsample (aliquot) yielded substantially higher D_e values. After a series of further test measurements thereof it was hypothesised that the luminescence signal on the adjacent measurements positions were reduced due to a cross-bleaching effect (e.g. Bray et al., 2002) of the used infrared light stimulation head of the luminescence reader. The preliminary results were first presented on the German LED meeting in Innsbruck in 2010 and later confirmed by Hülle (2011). Since the cross-bleaching effect of commonly used Risø TL/OSL readers had never been investigated before, it was decided to conduct a comprehensive series of test measurements on 10 TL/OSL readers over four luminescence laboratories to investigate and quantify the effect of optical 'cross-talk' (cross-bleaching).

Further related studies (not part of this thesis):

- *Investigation of calibration quartz that has also been used for the β-source calibration at the luminescence laboratory in Bayreuth:*

  Kadereit, A. and Kreutzer, S., 2013. Risø calibration quartz – a challenge for β-source calibration. An applied study with relevance for luminescence dating. Measurement 46 (7), 2238–2250.
  doi: `http://dx.doi.org/10.1016/j.measurement.2013.03.005`

- *Investigation of luminescence signals from empty sample carriers used for the luminescence dating application:*

  Schmidt, C., Kreutzer, S., Fattahi, M., Bailey, R.M., Zander, A., Zöller, L., 2011. On the luminescence signals of empty sample carriers. Ancient TL 29 (2), 65–74.

1.1.3.3 Methodological investigations

In a more general approach the progress of scientific knowledge is an ongoing process of hypothesising and evaluating. The emission of light from natural minerals (e.g. quartz or feldspar) is a release of energy previously absorbed by interaction of ionising radiation with matter (cf. Sec. 1.3). For the luminescence dating process (i.e. determination of ages) several

[1] CD in the cover of this thesis or via CRAN: http://cran.r-project.org/web/packages/Luminescence/index.html

considerations have to be made accounting for the type of radiation. Due to different ionisation densities, the luminescence induced per unit Gy of α-radiation varies from that of β- and γ-radiation. In the luminescence dating practise this behaviour is expressed as α-efficiency or a-value (cf. Aitken, 1985b) and is also relevant for fine grain dating (for details cf. Sec. 1.3).

For the cross-validation of the fine grain quartz ages carried out on the profile Seilitz the polymineral fine grain fraction was used applying the post-IR IR protocol (Thomsen et al., 2008). This protocol is proposed to be less affected by fading because it measures two infrared light stimulated luminescence signals, the second, less fading affected signal, is measured at higher temperatures. However, for the dose rate calculation it is assumed that a common a-value (α-(radiation)-efficiency; cf. 1.3.1.1) can be used for both signals. This raised the question if this common practise using a fixed a-value is justified.

Chapter 6 deals with this more fundamental concern by presenting empirical results of a-values measured with the post-IR IR protocol along with theoretical considerations using the polymineral fine grain fraction. The obtained a-values of this study have been further used for the age calculation in Ch. 7

A complete list of all a-values measured for fine grain quartz and polymineral separates are given in Ch. A.3.

Further related studies (not part of this thesis):

- *Methodological investigations on amorphous/microcrystalline SiO_2 using the R package 'Luminescence' and the LM-OSL approach:*

  Schmidt, C. and Kreutzer, S., 2013. Optically stimulated luminescence of amorphous/microcrystalline SiO_2 (silex): basic investigations and potential in archeological dosimetry. Quaternary Geochronology 15, 1–10.
  doi: `http://dx.doi.org/10.1016/j.quageo.2013.01.005`

- *Investigation of the luminescence characteristics of the local quartz using TL and LM-OSL techniques:*

  Fuchs, M., Kreutzer, S., Fischer, M., Sauer, D., Sørensen, R., 2012. OSL and IRSL dating of raised beach sand deposits along the southeastern coast of Norway. Quaternary Geochronology 10, 195–200.
  doi: `http://dx.doi.org/10.1016/j.quageo.2011.11.009`

1.2 Regional setting

As mentioned, one of the prime objectives of the overarching project framework of this thesis was to establish chronologies on loess records in Saxony (Germany) using luminescence dating technologies. Two of the presented dating applications (Ch. 2, 7) were carried out in the Saxonian Loess Region (Saxony/Germany) and for the technical and methodological studies mostly samples from loess records in Saxony were taken (Ch. 4, 5, 6).

As part of the European loess belt (e.g. Haase et al., 2007; Antoine et al., 2013) the Saxonian Loess Region is located on the northern foothills of the Erzgebirge in a transition zone between oceanic dominated western and continental dominated eastern climates. The Saxonian Loess

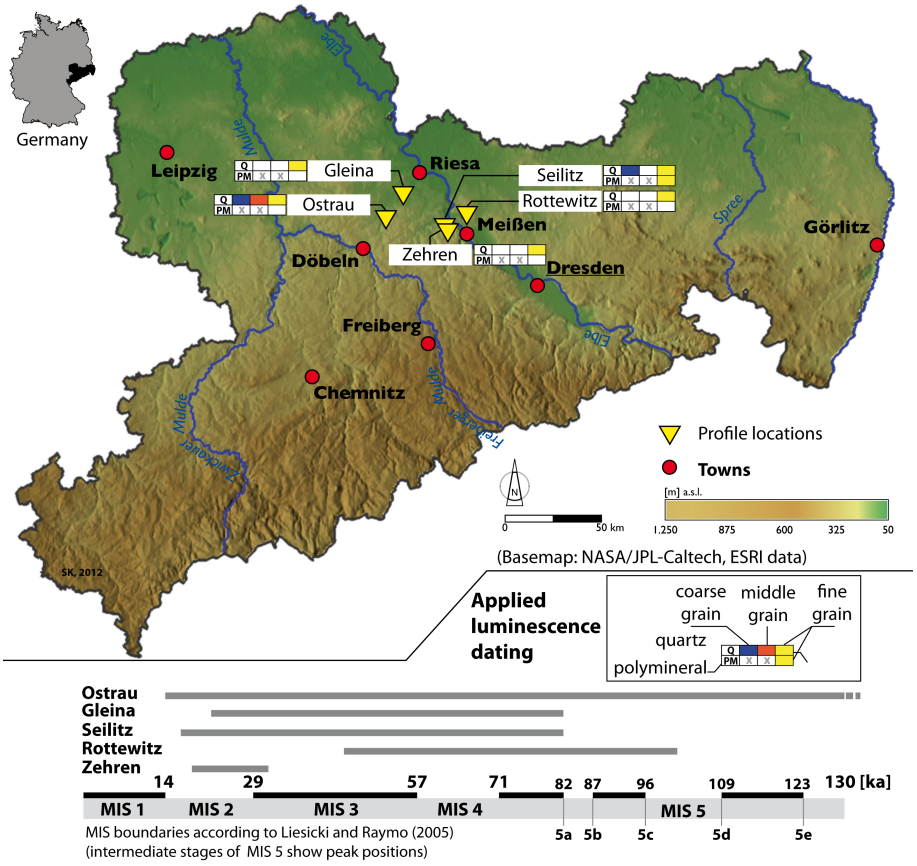

Figure 1.1: Research area in Saxony/Germany with profile locations. The applied luminescence dating (used mineral and grain size fractions) and the age range (minimum and maximum extent) covered by luminescence dating as Marine Isotope Stages (MIS) for each investigated loess record are shown. MIS stages according to Lisiecki and Raymo (2005).

Region relates to the local major geographic region 'Sächsisches Hügelland' (e.g. Lieberoth, 1959). It is featured by abrupt changes between loess deposits and glacial and glaciofluvial sediments with intercalated pedocomplexes of various intensities. The up to 20 m thick bodies of loess contain loess and reworked loess from the last glacial-interglacial cycle (Meszner et al., 2011). The recent mean annual temperature in the research are in Saxony is ∼8–9 °C with a total mean precipitation between ∼600 mm and ∼750 mm per year (1961–1990; Bernhofer and Goldberg, 2008).

The significance of the regional Weichselian loess accumulations were noticed at the beginning of the last century (cf. Meszner et al., 2011). However, first intensified palaeopedologic and stratigraphic investigations go back to the late 1950s (Lieberoth, 1959) and were continued during the following years (e.g. Lieberoth, 1962; Haase, 1963; Lieberoth, 1964; Lieberoth and Haase, 1964; Haase, 1968). Since 2004 the loess records in Saxony have been subjected to systematic investigations using a multi-methodological approach and since 2008 these efforts have given rise to the DFG project 'Saxony Loess' to combine litho-, pedo- and chronostratigraphic

findings.

An overview of the investigated loess sections in the Saxonian Loess Region along with the applied luminescence dating is provided in Fig. 1.1. The figure shows the chosen mineral and grain size fraction for each profile and the approximated covered age ranges[2] investigated by luminescence dating are given as Marine Isotope Stages (MIS). Almost all investigated profiles, except the profile Rottewitz, are located on the western side of the river Elbe. An additional map showing the loess distribution is provided with Fig. 7.1.

The different regional settings of the accompanying investigated loess records Zeuchfeld (Ch. 3) and Dolní Věstonice (Ch. 8) are given in Sec. 3.2, Fig. 3.1 and Sec. 8.1, Fig. 8.1.

1.3 Luminescence dating

This section briefly summarises the basic concepts of the luminescence phenomenon and dating procedure. The section aims at providing (1) an overview in a general manner and (2) focusing attention on some aspects relevant for this thesis.

1.3.1 The luminescence phenomenon

Luminous effects are well-known from every day experience: Warning plates are still visible when the light is switched off or bicycle reflectors seem to flash when they are illuminated. However, not every illumination effect should be termed 'luminescence'. Whereas the first observation on the warning plate is probably related to some kind of phosphorescence, the latter one is just a reflection.

Although first observations of the luminescence phenomena are believed to date back to far eastern and classical antiquity (cf. Newton, 1957) and the first written description is attributed to Sir Robert Boyle in 1664 (e.g. Newton, 1957; Yukihara and McKeever, 2011), the term 'luminescence' was introduced by Eilhardt Wiedemann. The German physicist used the term in 1888/1889 to distinguish between light emitted during heating of solids to incandescence and light emission that does not correspond to the actual temperature and therefore is independent of the thermal background (e.g. Newton, 1957; Mahesh et al., 1989; Yukihara and McKeever, 2011). The first effect is occasionally called 'hot light', the latter one 'cold light'. According to the process of light excitation (in the visible or near visible range), the term luminescence has undergone several classifications such as 'thermoluminescence' (thermally stimulated luminescence), 'photoluminescence' (light emission caused by light radiation) or 'triboluminescence' (light excitation by grinding; cf. Mahesh et al., 1989). To distinguish the phenomena by the time it takes for the emission to takes place after stimulation (delay) the terms 'fluorescence' ($t \lesssim 10^{-8}$ s) and 'phosphorescence' ($t \gtrsim 10^{-8}$ s) were used (cf. McKeever, 1988). The optically stimulated luminescence (OSL) phenomenon used for dating in this thesis is referred to as phosphorescence phenomenon (photophosphorescence, Yukihara and McKeever, 2011) and should not be mixed up with the related term 'photoluminescence', which is used for prompt light emission. For the latter one no prior energy absorption by ionising radiation is necessary and thus the emission intensity is independent of the previously stored energy (cf. Bøtter-Jensen et al., 2003b; Yukihara and McKeever, 2011). In contrast, the emission intensity of the OSL signal is (amongst others) a function of the absorbed energy (over time).

[2] The given age ranges do not mean that the profiles contain the complete age information. They just indicate the minimum and maximum age extent of the investigated part of the profile.

1.3.1.1 Theoretical background

The theory of luminescence dating is based on the observation that crystalline solids (conductors and semiconductors) are capable to store energy from radiation emitted by naturally occurring traces of radioactive nuclides and their decay products (^{238}U,^{235}U, ^{232}Th, ^{40}K,^{87}Rb) and cosmic rays (primary muons; Prescott and Hutton, 1994). Therefore, the light emitted by the stimulation process (e.g. thermal or optical) is just absorbed energy that is released. The process of energy storage and release is commonly described using the energy band model. Within crystalline solids sets of discrete energy levels constitute "periodically varying potentials" (McKeever, 1988, p. 20) of allowed zones ('bands') of energy states for electrons. The energy bands are separated by energy gaps. For semiconductors and insulators the zone between the uppermost energy level filled with electrons (valence band) and the next (partly) unfilled band (conduction band) is called 'forbidden zone'. The width of the forbidden zone, i.e. the distance between valence and conduction band is specified as the energy (E_g in eV) needed to surmount this potential barrier (e.g. for quartz $\sim$8.5 eV; Bailey and McKeever, 2012).

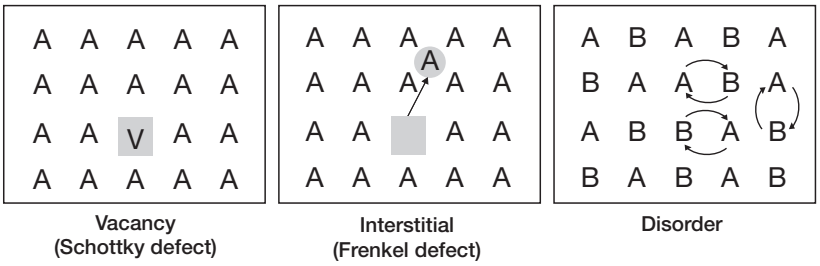

Figure 1.2: Intrinsic point defects redrawn from Mahesh et al. (1989).

An ideal crystal would never exhibit any capability of storing energy. However, any disturbance in the periodicity of the crystal, like structural defects and/or impurities within the lattice, causes localised energy states in the forbidden zone (e.g. McKeever, 1988; Demtröder, 2005; Bailey and McKeever, 2012). The literature distinguishes between intrinsic and extrinsic defects (McKeever, 1988). Intrinsic defects (Fig. 1.2) are point defects like vacancies or missing atoms (Schottky defects), interstitials (Frenkel defects), atomic disorders or an aggregation of these defects (Mahesh et al., 1989; Furetta, 2010). Extrinsic or impurity related defects are substitutionals or interstitials caused by impurities (e.g. Mahesh et al., 1989; Furetta, 2010), i.e. additions not belonging to the regular crystal structure such as the replacement of Si^{4+} by Al^{3+} in a quartz crystal (cf. Preusser et al., 2009).

The defect-induced localised energy states provide discrete energy levels of positive net charge in case of electron traps within the forbidden zone (gap) of the crystal where an electron, displaced from the valence band by ionising radiation and migrating through the crystal lattice, can become trapped (process of energy storage). Therefore, these energy levels (centres) are called 'electron traps' or 'recombination centres'. Traps are located near the band edges, whereas recombination centres are situated towards the middle of the band gap (McKeever, 1988; Bailey and McKeever, 2012). Once an electron is freed from the valence band a cation vacancy is induced and might get trapped in a defect center of opposite charge ('hole trap'; Bailey and McKeever, 2012; McKeever, 1988). In Figure 1.3 the basic principle of excitation and recombination can described by two models: The Schön-Klasen scheme (Fig. 1.3a) and the

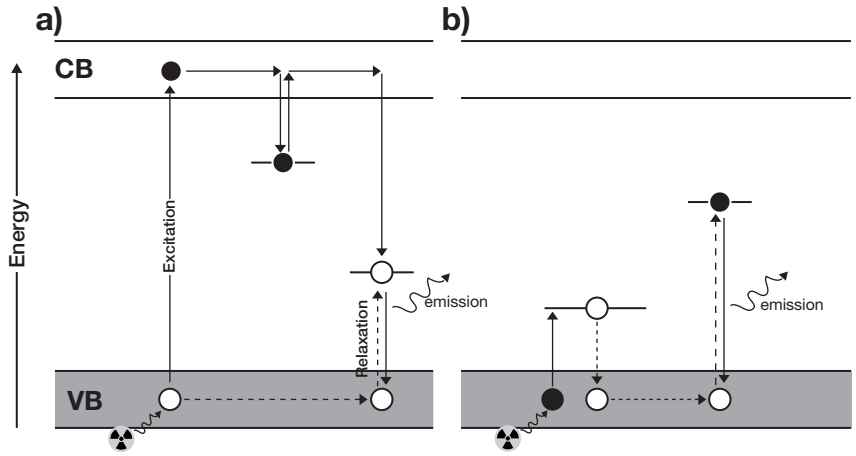

Figure 1.3: Energy band diagram with modifications redrawn from Bailey and McKeever (2012). Recombination schemes are shown according to Schön-Klasen (a) as recombination of an electron with a trapped hole and Lambe-Klick (b) as a mobile hole with a trapped electron. Solid lines show electrons, dashed lines hole transfers, respectively. VB = valence band, CB = conduction band. Details see main text.

Lambe-Klick scheme (Fig. 1.3b). In both cases an electron is evicted from the valence band by ionising radiation. Differences occur in the recombination process. In the Schön-Klasen scheme the recombination process is described as relaxation of the electron from an excited state to the ground state (valence band), accompanied by a photon emission. In the Lambe-Klick scheme the photon emission is induced by a mobile hole that "migrates to the vicinity of a trapped electron which then returns to the valence band" (Bailey and McKeever, 2012, p. 9).[3]

The mean time an electron spends in a trap can be approximated (1^{st} order kinetics) with the Arrhenius equation (e.g. Furetta, 2010):

$$\tau = s^{-1} \exp\left(\frac{E_t}{k_B T}\right) \tag{1.1}$$

where s is the frequency factor in s^{-1}, E_t the thermal activation energy in eV, k_B is Boltzmann's constant (8.617×10^{-5} eV K^{-1}) and T the temperature in K. The frequency factor is the attempt-to-escape frequency and therefore the interaction of the electron with the crystal lattice (Furetta, 2010). The probability for the charge carrier to escape from the trap is:

$$p = \frac{1}{\tau} \tag{1.2}$$

As luminescence dating is based on the principle of energy storage in the form of electrons trapped at excited energy states, this relationship becomes fundamentally important for this discussion of luminescence dating. The mean (life) time an electron spends in a trap is finite and should be, however, greater than the investigated age range. For example, a trap depth

[3]For further details the reader is referred to the original literature: Schön (1942); Klasens (1946); Lambe and Klick (1955).

of $E = 1.74\,\mathrm{eV}$ with a frequency factor of $s = 8.9 \times 10^{13}\,\mathrm{s}^{-1}$ would result in a lifetime of $\sim 292\,\mathrm{Ma}$ at $T = 20\,^{\circ}\mathrm{C} = 293.15\,\mathrm{K}$.[4] Compared with the usually investigated age range of a few hundred ka, this value seems sufficient for using luminescence dating on quartz. Aitken (1985b) suggests a lifetime 10 times the age of the sample.

For TL the trap depth is related to the corresponding TL peaks (i.e. luminescence intensity with temperature) in the glow curve which was first recognised by Urbach (1930). However, once an electron is trapped at an excited state the energy needed to free the electron again from the trap is lower than the energy to excite another electron from the valence band. The eviction process (stimulation) is caused again by energy transfer, here heating (TL) or optical stimulation (OSL). In the simplest (single electron trap) case, the released electron travels via conduction band and recombines with a hole at a lower energy state (near the edge of the valence band). This process is accompanied by the release of a photon in the visible or near visible spectrum.

Indeed, the process of recombination is much more complex and many other schemes (re-trapping, non-radiative recombination, direct transitions via tunnelling) for this kind of "lattice relaxation" (Bailey and McKeever, 2012, p. 11) are thinkable depending on stimulation conditions, i.e. temperature and stimulation wavelength and not last on the dosimeter itself, but this has to be beyond the scope of this section. To summarise, the eviction and recombination process can be related to different emission energies and the process of recombination is not always accompanied by the release of a photon in the visible spectrum. The wavelength emitted is characteristic of the investigated mineral and related to the defects in the crystal lattice mentioned above (McKeever, 1988).

For natural quartz several kinds of imperfections and impurities lead to a broad complex emission spectrum depending on the type of stimulation and the trap-centre pairs, i.e. the energy required to evict an electron from the trap and "the energy loss required for the recombination centre to relax to a lower energy state" (Bailey and McKeever, 2012, p. 10). The stimulation and detection wavelengths relevant for luminescence dating were summarised by the spectral investigations of Krbetschek et al. (1997). However, the emission does not occur continuously over the entire visible and near visible (visible plus UV, infrared) spectrum but is characterised by several mineral specific emission wavelength windows. With regard to the chronometric application, luminescence dating utilises this observation by selecting specific stimulation and detection wavelengths. For example OSL dating on quartz is mainly carried out using optical stimulation in the blue band and detection in the UV band (cf. Sec. 1.3.3.3 for technical details). Chapter B in the appendix provides a chart of the commonly used mineral related emission and detection wavelengths along with the characteristics of the used optical filters.[5]

The last paragraph of this section focusses in more detail on what was mentioned just briefly at the beginning: The energy storage process in the crystal by trapping charge carriers is induced by energy transfer due to external or internal (e.g. from internal U) radiation. Depending on the type of radiation, α, β and γ (and cosmic rays), different types of lattice interactions occur. Of paramount interest is the amount of energy loss when radiation passes through the

[4] Values according to Singarayer and Bailey (2003) for the fast component of quartz.

[5] Note: The chart provides a simplified view as it does not distinguish between optical and thermal stimulation, nor are all possible stimulation wavelengths or filter characteristics shown. Spectral wavelength ranges according to Stöcker (2010)

crystal lattice; it depends on the character of the irradiation (e.g. energy, mass) as well as on the composition of the traversed matter (e.g. density). During radioactive decay different types of radiation (α, β and γ) are emitted, differing in their mean range in matter ($\gtrsim 20\,\mu m$ for α-particles, $\sim 2\,mm$ for β-particles and $\sim 30\,cm$ for γ-rays for standard rock;Stolz, 2005; Aitken, 1985a) and the type of energy transfer. Charged particles, such as α- and β-particles, lose energy due to a number of atomic collisions. Photons (γ- and X-rays) may be directly absorbed with the first collision, releasing a (secondary) charged particle travelling through the matter (Bailey and McKeever, 2012; Stolz, 2005). Depending on the photon energy different kinds of interaction processes are possible: photoelectric effect (absorption of the photon), Compton effect (scattering of the photon) and pair production (absorption of a photon by an electron and release of electron/positron pair).

With regard to luminescence dating, the different types of radiation-dependent lattice interactions result in specific ways of energy transfer. Beta- and γ-radiation or X-rays show a low ionisation density (or low linear energy transfer, LET) and high efficiency, expressed as induced luminescence per unit of energy. In contrast, heavy charged α-particles have a high ionisation density (e.g. Zimmerman, 1972; Jain et al., 2007), but lower luminescence efficiency and a higher probability of defect creation, i.e. creating new traps; e.g. Kalefezra and Horowitz (1982).

1.3.1.2 Towards a dating application

The recognition of the proportional relationship between the amount of absorbed energy and the amount of released luminescence during heating in the 1950s resulted in early investigations on dosimetric applications (cf. McKeever, 1988). First applied on alkali halides in 1953, Daniels et al. (1953) suggested the application for luminescence in terms of environmental dosimetry, as follows: "Any new method for dating rocks and minerals is well worth exploring, [...]" (Daniels et al., 1953, p. 349). The first dating applications using TL were carried out on meteorites by Houtermans and Stauffer (1957) and continued by Grögler et al. (1958) and e.g. Aitken et al. (1964). Following applications of TL dating were carried out almost exclusively in archaeological sciences. Dating of sediments emerged in the late 1970s and early 1980s, with loess being one of the first sediments to which luminescence (TL) dating was applied (review articles: Wintle, 1980, 1990). With the introduction of optical dating on quartz (Huntley et al., 1985) and later feldspar (Hütt et al., 1988), however, this "progenitor" (Aitken, 1998, p. v) has been favoured by OSL dating due to shorter bleaching times needed for the signal resetting.

The principle of luminescence (here OSL) dating on sediments is shown in Fig. 1.4. Natural minerals such as quartz or feldspars work like a battery that can be continuously charged and released. Charging is induced by environmental radiation when the sediment is buried. Sunlight exposure during sediment transport processes (e.g. aeolian) releases the energy until the mineral grains are covered again. The energy release process can be induced in the laboratory using artificial light sources.[6] The natural signal growth is assumed approximately following an exponential saturating function (cf. Eq. 1.10) due to a decrease of available free electron traps with increasing dose.

The (cumulative) absorbed dose, i.e deposited energy by ionisation radiation per unit mass, is called palaeodose (natural dose), since it cannot be directly read from the mineral, but only

[6] To avoid confusion: The linear luminescence signal growth in Fig. 1.4 is a graphic simplification.

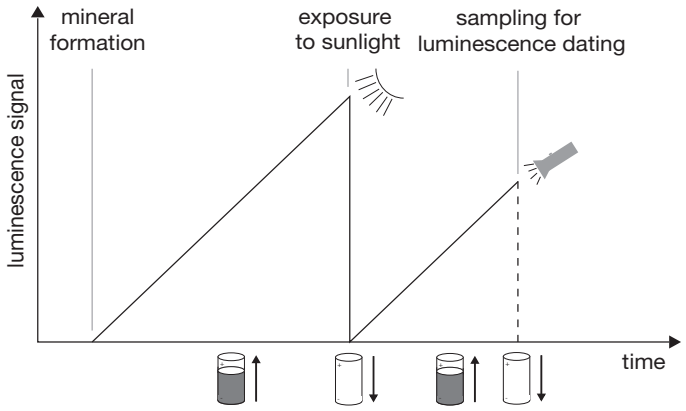

Figure 1.4: The principle of luminescence dating, show the luminescence signal growth and depletion over geologic time scales. The battery symbol indicates the energy storage and release process. Similar figures can be found in e.g. Preusser et al., 2008; Fuchs, 2001.

indirectly by measuring the emitted photon flux and calculating an equivalent dose (D_e given in Gy, see also Sec. 1.3.3.4). The energy emitted per time from natural U,Th, Rb, K and cosmic rays is called dose rate ($\dot{D}$ in Gy ka^{-1}). The resulting age equation (Eq. 1.3) is a simple division of these two parameters (for technical remarks cf. Sec. 1.3.3.6):

$$Age\ [ka]\ =\ \frac{D_e\ [Gy]}{\dot{D}\ [Gy\ ka^{-1}]} \tag{1.3}$$

However, as a drawback to the previous sections, to act as a proper dosimeter for luminescence dating applications the mineral (or more specifically the investigated luminescence signal) has to fulfil some (amongst other) requirements:

- Bleachability: The latent luminescence signal has to be reset in sufficient time with regard to the investigated transport process of the sediment, i.e. question of light sensitive electron traps zeroing prior to subsequent burial.
- Capacity: The saturation dose of the dosimeter should cover the investigated age range corresponding to the dose rate specific for the sediment, i.e. question of the number of available light sensitive electron traps.
- Stability: The signal used for dating has to be stable over the time range of interest: Thermally (i.e. question of lifetime of the electron traps) and athermally, i.e. question of possible electron transitions via tunnelling; anomalous fading: Wintle (1973).
- Practicality: The mineral should occur with sufficient quantity in the target sediment and should be separable from the bulk sediment.

Quartz fulfils these criteria. Mineral grains of quartz are nearly ubiquitous in loess (cf. Sec. 1.1.1) and quartz has proven to be a stable and reliable dosimeter for loss dating (cf. Roberts, 2008).

1.3.2 Luminescence signals

Of particular interest for every kind of luminescence application is the obtained shape of the signal curve, i.e. luminescence intensity versus stimulation temperature (TL) or stimulation time (OSL). For TL the appearing temperature related peaks are associated with distinct types of electron traps (e.g. McKeever, 1988) and the curve peaks may be intuitively interpreted as singular signals (if not overlapping).

In contrast, a typical OSL curve obtained under constant stimulation power ($\lambda_{stimulation} \neq \lambda_{detection}$) appears to be somehow featureless. Assuming a single type of electron trap and 1st order kinetics (i.e. no re-trapping) the obtained continuous wave (CW)-OSL monotonically decaying signal curve should follow a single exponential function of the general type (cf. Bailey and McKeever, 2012):

$$I(t)_{CW} = n_0 k \ \exp(-kt) \tag{1.4}$$

with n_0 the initially trapped charge at $t = 0$ and k as the decay constant in s^{-1}. Logarithmic calculus results in a linear function:

$$\ln(I(t)_{CW}) = \ln(n_0 k) - kt \tag{1.5}$$

With regard to the measured CW-OSL signal from a natural sample, however, it becomes apparent that this assumption might be misleading. Figure 1.5 shows a CW-OSL signal following the Eq. 1.4, the inset shows the log count values which graphically follows a linear function. Contrary, the measured CW-OSL signal reveals a still decaying exponential-like rather than a linear shape.

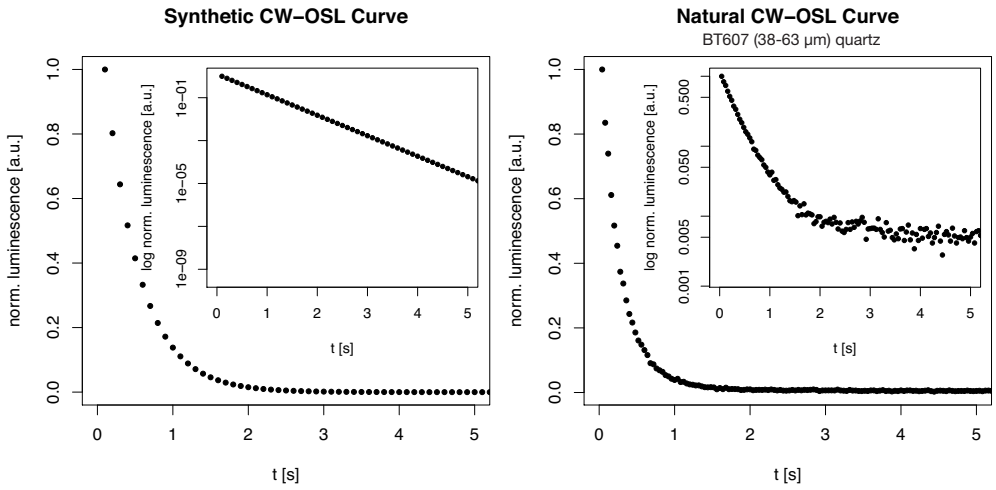

Figure 1.5: Synthetic CW-OSL assuming a single electron trap and 1st order kinetics and natural CW-OSL curves (BT607, middle grain quartz). The insets show the curve with log signal values.

The CW-OSL signal comprises a finite number of individual signal components as reported by Smith and Rhodes (1994). Bailey et al. (1997) postulated that quartz consists of, at least,

three distinct signal components and due to the individual bleaching characteristics he termed them as 'fast', 'medium' and 'slow'. Later the nomenclature was extended by terms like 'ultra fast' and the slow components have been further separated numerically, i.e. 'slow 1'/'s 1', 'slow 2'/'s 2' and 'slow 3'/'s 3' (cf. Jain et al., 2003; Singarayer and Bailey, 2003). The sum signal of Eq. 1.6 can therefore be written as a linear combination of j exponential functions:

$$I_{CW}(t) = \sum_{i=1}^{j} n_{0_i} k_i \exp(-k_i t) \tag{1.6}$$

The distinct signal components are associated with individual types of electron traps (cf. Bailey, 2001) with different bleaching and dose response characteristics that give rise to the sum signal. OSL dating aims to investigate signal components that have been sufficiently bleached during transport and can be measured reproducibly. The so called fast component was found to meet these requirements. In OSL dating on quartz, it is tempted to isolate the fast component for D_e determination. Several approaches of more or less practical relevance have been suggested to isolate the fast decaying signal component, e.g. by early background subtraction (Ballarini et al., 2007) or direct measurement using infrared light stimulation (Bailey, 2010). Although other (less bleachable) components may be used for dating when a dominant fast component is missing (e.g. Singarayer and Bailey, 2003; Singarayer, 2002), the underlying assumption is that the signal is dominated by the fast component. However, this is in most cases hardly visible from the sum CW-OSL curve without mathematical fitting procedures. In 1996, Bulur (1996) presented an alternative read-out method by ramping the stimulation intensity over time, termed as linear modulation technique (LMT or LM-OSL). The linear ramp is given as:

$$\phi(t) = \frac{\phi_{\max}}{P} t \tag{1.7}$$

with ϕ_{max} as the maximal stimulation intensity in $cm^{-2}\,s^{-1}$, P the stimulation period in s. The resulting peak-shaped curve can be described as:

$$I_{LM}(t) = \sum_{i=1}^{j} n_{0_i} \frac{b_i}{P} t \ \exp\left(-\frac{b_i t^2}{2P}\right) \tag{1.8}$$

with b the detrapping probability

$$b = \sigma \phi_{\max} \tag{1.9}$$

Sigma (σ) is the photoionisation cross-section in cm^2 and a fundamental parameter associated with distinct components resulting in a release of electrons from traps/components with increasing optical stability (i.e. decreasing detrapping probability) during the measurement. Figure 1.6 shows a comparison of resulting CW-OSL and LM-OSL for similar underlying assumptions.

Nevertheless, Bos and Wallinga (2012, p. 752) pointed out that the modulation of the "stimulation power does not result in better separation of quartz OSL components", but it may help to visualise the OSL signal components to understand the signal to sum contribution as a function of the stimulation time. To keep the measurement time as short as possible mathematical transformation methods can be used to obtain so called pseudo LM-OSL curves,

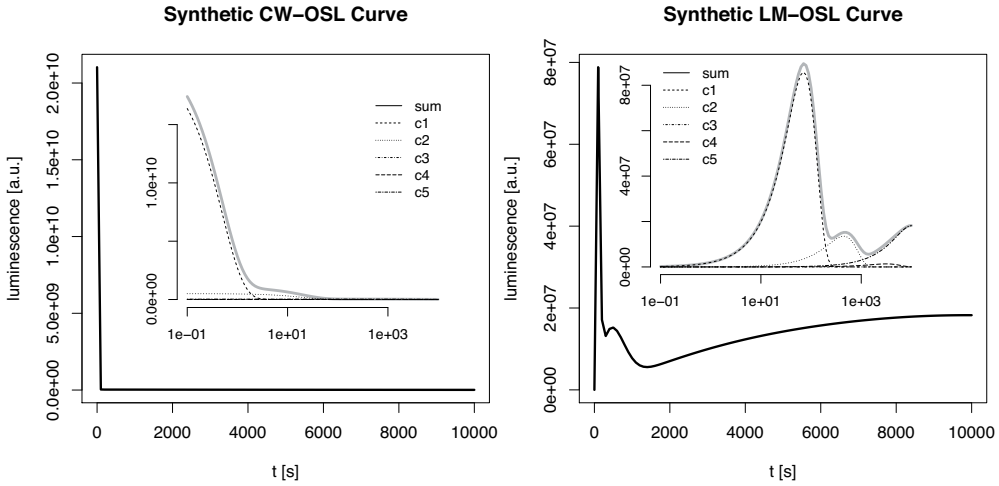

Figure 1.6: Synthetic 1st-order kinetics CW-OSL (Eq. 1.6) and LM-OSL (Eq. 1.8) curves comprising 5 signal components: $n_{1,\ldots,5} = \{1\times10^{10}, 1\times10^{10}, 1\times10^{4}, 0.7\times10^{10}, 0.3\times10^{12}\}$ and $b_{1,\ldots,5} = \{2, 0.05, 0.01, 0.001, 0.0001\}$. The insets show the plots on a log scale.

which were first suggested by Bulur (2000). Bos and Wallinga (2012) presented additional methods with advantages and disadvantages concerning the preferred component to be visualised.

During this thesis several LM-OSL measurements were carried out to investigate the signal characteristics of the quartz separates and to ensure a domination of the sum signal by a fast decaying signal component. Automatic LM-OSL fitting routines have therefore been implemented along with CW-OSL fitting and the transformation methods suggested by Bulur (2000) and Bos and Wallinga (2012).

1.3.3 Dating practise

In this section the basic technical procedures used for the dating application on quartz are presented. Most of the sample preparation and measurements were employed at the luminescence laboratory in Bayreuth. A few samples were partly prepared (Ch. 3) and/or measured at other laboratories. For the differences in general procedure the reader is referred to the specific study.

1.3.3.1 Sample collection

Two methods of sample collection have been established in the dating routine: (a) Sampling during nighttime with sampling directly into opaque plastic bags or (b) sampling during daytime using steel cylinders of varying sizes. For both methods the profile has previously to be carefully cleaned to locate the distinct sedimentary units of each section. Sampling during nighttime is carried out using a red light headlamp ($\lambda = 640\ \Delta\ 20\,\mathrm{nm}$) and after removing the daylight affected sediment layer. For the sampling procedure during daytime the light-exposed sediment

material is removed in the laboratory under subdued red light conditions ($\lambda = 640\ \Delta\ 20$ nm). On the investigated loess sections the sampling was mostly carried out during nighttime after preparing the section for luminescence dating sampling. The advantage compared to daytime sampling is that thin layers (horizons) can be sampled and the amount of the sampled material is normally not problematic. In contrast, for daytime sampling the amount of material is limited to the size of the cylinder as well as the diameter. However, practical reasons, accessibility and/or safety reasons may require daytime sampling.

Sample material for dosimetry (i.e. to determine ^{238}U, ^{232}Th and ^{40}K nuclide concentrations) were taken by random sampling from the surrounding $\sim$ 30 cm. In rare cases the outer daylight affected material from both sides of the steel cylinders were used.

1.3.3.2 Sample preparation

Sample preparations were carried out under subdued red light conditions ($\lambda = 640\ \Delta\ 20$ nm). First, the samples were wet sieved to extract the wanted grain size fractions used for dating. Typically used sieve sizes were: 200 µm, 90 µm, 63 µm and 38 µm. The fine grain fraction (4–11 µm) was separated from the fraction < 90 µm by settling applying Stokes' law. The used grain size fractions to which luminescence dating is typically applied are shown in Fig. 1.7 with their corresponding particle size classes.

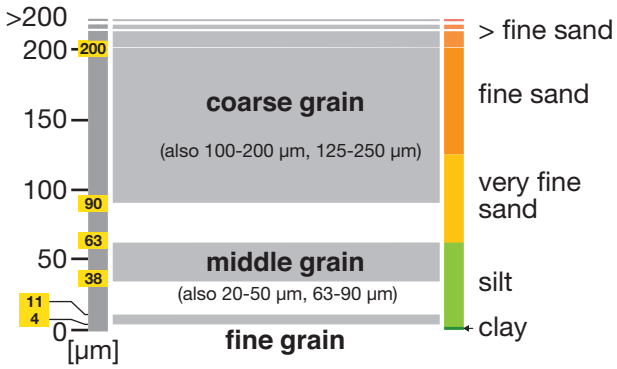

Figure 1.7: Typical grain size fractions used for luminescence dating and their corresponding particle size classes (Chesworth, 2008).

Subsequently, the samples were chemically treated to destroy carbonates and organic material using HCl (10 % and 30 %) and H_2O_2 (10 % and 30 %). The following procedures vary for the prepared grain size fractions:

(I) Coarse grain (90–200 µm) Heavy minerals and feldspars were separated using density separation with heavy-liquid solution (lithium heteropolytungstate or sodium polytungstate) with densities of $\rho = 2.75$ g cm^{-3} and $\rho = 2.62$ g cm^{-3}, respectively. To remove the α-irradiated outer layer (Fleming, 1970) and remove any remaining feldspar contaminations the coarse grain extracts were etched for 45 min in HF (48 %) or 60 min in HF (40 %) and subsequently washed in HCl (10 %) and distilled water.

(II) Middle grain (38–63 µm) The (polymineral) middle grain fraction was etched in untreated H_2SiF_6 (34 %) for at least 14 days to extract the quartz minerals. Quartz grains were subsequently washed in HCl (10 %) and distilled water (e.g. Lai et al., 2009).

(III) Fine grain (4–11 µm) To extract the mineral quartz the (polymineral) fine grain fraction was etched in three day pre-treated H_2SiF_6 (34 %)[7] for three up to six days and subsequently washed in HCl (10 %) and distilled water (cf. Fuchs et al., 2005; Berger et al., 1980). For the study on polymineral fine grain at the profile of Seilitz (Ch. 7) a part of the material was not etched.

After etching, the quartz separates were again sieved (coarse grain: 90 µm, middle grain: 38 µm) or settled using Atterberg cylinders to remove grains smaller than the wanted grain size. The purity of the quartz extracts was tested by IR stimulation (IRSL/OSL ratio $< 2\,\%$).[8]

1.3.3.3 Measurement equipment

Except the radiofluorescence measurements in Ch. 3 all luminescence measurements were carried out on commercially available Risø TL/OSL DA-12 (cf. Ch. 5), DA-15 or DA-20 readers (Bøtter-Jensen, 1997; Bøtter-Jensen et al., 2000, 2003a)[9]. All readers were fitted with a EMI 9235Q UV sensitive photomultiplier tube and a $^{90}Sr/^{90}Y$ β-source. Dose rates are typically in the range between c. 5 Gy min^{-1} and c. 10 Gy min^{-1}. Luminescence was stimulated with blue LEDs ($\lambda = 470\ \Delta\ 20$ nm, up to 40 mW cm^{-2}) and IR LEDs ($\lambda = 870\ \Delta\ 40$ nm, up to 135 mW cm^{-2}). For luminescence detection in the ultra-violet region (quartz) a 7.5 mm Hoya U340 filter and for the violet-blue band (polymineral, feldspar) a 3 mm Chroma D410/30x interference filter (410 Δ 15 nm) or a blue filter combination (BG3, GG400, BG3, BG39) with comparable transmission window were used (cf. Ch. B in the appendix for the detailed filter characteristics of the Hoya U340 and Chroma D410/30x filter).

For the three investigated grain size fractions different sample carriers were used. As shown in Fig. 1.8 the number of accommodated grains on the sample carrier varies with the grain size. The coarse and middle grain fractions were fixed on the aluminium cups using silicone oil. The fine grain fraction was adhesively fixed on aluminium disc as α-thin layers. Approximately 2 mg of sample material were settled on each disc.

For α-irradiation (a-value estimation) two mono-energetic α-sources from the luminescence laboratory in Bayreuth were used: (a) A built-in ^{241}Am α-source of one Risø reader delivering (8.7 Gy min^{-1} to fine grain on aluminium discs) and (b) an external α-source (Littlemore, type 721/B) comprising six ^{241}Am α-sources each delivering 1.25 Gy min^{-1} to fine grains on aluminium discs. The ^{241}Am sources deliver α-particles with energies of 3.7 MeV. The sources had been calibrated against the track-length calibrated α-source from the former Forschungsstelle Archaeometrie at the Max-Planck Institute of Nuclear Science in Heidelberg / Germany. For all measurements aluminium discs were used. The irradiation was carried out under vacuum

[7] Pretreatment procedure according to Syers et al. (1968) to remove any traces of HF.

[8] Note: The rejection criterion is not based on the so called 'IR depletion ratio' suggested by Duller (2003). For the purity tests the samples were first measured using IR stimulation at 125 °C and subsequently using blue stimulation at 125 °C. The net signal integrals of both shine down curves were used to obtain the IRSL/OSL ratio. The signals were measured in the UV band using a Hoya U340 filter. A preheat of 200 °C or 220 °C was applied previous to the IR stimulation.

[9] A technical drawing of the measurement chamber is shown in Fig. 5.1.

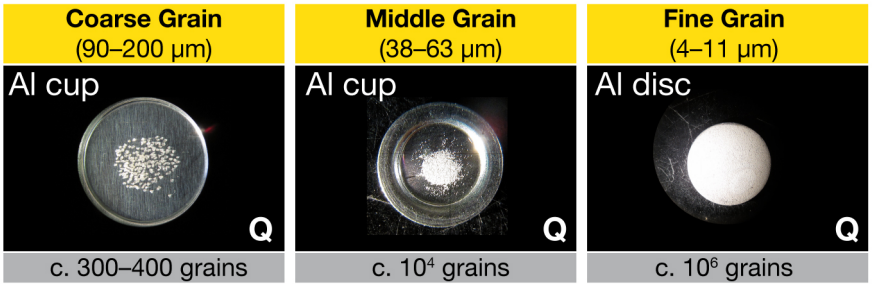

Figure 1.8: Typical aliquot sizes of different grain size fractions used for luminescence dating. Depending on the grain size Al cups or Al discs are used. The pictures show quartz separates.

($< 10^{-2}$ mbar) conditions.

U, Th and K concentrations for dose rate determination were measured using thick-source α-counting for the U and Th contents (Zöller and Pernicka, 1989) and ICP-MS (BayCEER Bayreuth) for the K concentration. Additionally, low-level high-resolution γ-ray-spectrometry was carried out for U,Th and K concentrations in external laboratories (details given in studies).

1.3.3.4 D_e estimation

Since the absorbed dose in Gy cannot be directly measured a reference system is used to evaluate the palaeodose ("the dose that the sample received during antiquity", Aitken, 1985b) by comparing natural luminescence signals with artificially induced signals. For OSL dating in general two different approaches for palaeodose estimation have been developed: The additive and the regeneration method. Regarding the additive method, incrementally increasing artificial doses are added on top of the natural dose using different sets of multiple aliquots, before measuring the resulting luminescence intensity. For the regeneration method the natural signal is recorded and then increasing artificial (regeneration) doses are administered on previously bleached aliquots (cf. Aitken, 1998). In contrast to the additive method the regeneration method can be applied on just one single aliquot to obtain the D_e of a sample. The applied measurement protocol thus comprises several cycles of heating, stimulation and dosing. However, the luminescence response to a certain dose for the same aliquot can change due to sensitisation effects (e.g. cf. Chen and Pagonis, 2011). In 2000, Murray and Wintle (2000) introduced the single aliquot regenerated (SAR) dose protocol which corrects for sensitivity changes by measuring a separate luminescence signal induced by a constant test dose after recording the regenerated signals.

All measurements carried out for this thesis are based on the SAR approach on single aliquots. A generalised SAR protocol is given in Tab. 1.1. Before the protocol is applied for D_e determination, a series of routine test measurements is employed to figure out the optimal protocol parameters, which are sample dependent. A parameter that is usually altered according to such series of test measurements is the preheat temperature. Preheats are needed to empty light sensitive shallow traps that may contribute to the regenerated but not to the natural

luminescence signal due to a lower lifetime of electrons in those traps (cf. Wintle and Murray, 2006). For this thesis, during combined preheat and dose recovery tests the natural signal was first bleached and subsequently an artificial dose was administered. SAR measurements using different preheat temperatures test are aimed at testing the reproducibility of a given dose. The preheat temperature that showed the best reproducibility was chosen for the final protocol.

Table 1.1: Generalised single aliquot regenerated (SAR) dose protocol according to Murray and Wintle (2000).

#	Treatment	Observation
1	[regenerative dose (β-irradiation)]*	
2	preheat@(180,...,260 °C) for 10 s	
3	blue stimulation@125 °C for 40 s	L_n, L_x
4	test dose (β-irradiation)	
5	cutheat to 160 °C	
6	blue stimulation@125 °C for 40 s	T_n, T_x
7	return to step 1	

*skipped for the first cycle

L_n: natural luminescence signal; T_n: corresponding natural test signal

L_x: regenerated luminescence signal; T_x: corresponding regenerated test signal

Regeneration points are set to enclose the expected range of the D_e. For the employed measurements at least six regeneration points (four dose points, one repeated dose point and one zero dose point) were set. For higher D_e ($\gtrsim$ 200 Gy) more dose points were used. However, there is no upper limit but additional dose points may substantially increase the measurement time, particularly for samples with high natural D_es.

Along with the mentioned parameters in general every parameter (e.g. read and/or cutheat temperature) can be altered to increase the reliability of the protocol or to meet previously defined rejection criteria, as long as the principle of the underlying sequence (progression of regenerated signal and corrected signal) remains unchanged (cf. Wintle and Murray, 2006, for further details). Determining the D_e means plotting L_x/T_x values against the dose to obtain so called 'growth' or 'dose response' curves. Finally, mathematical fitting is applied to the data points and the D_e can be directly calculated from the fitted function by iteration procedures (for exponential plus linear function see below). Since it is assumed that the growth of the luminescence signal with dose can be approximated as an exponentially saturating process because the electron traps become saturated at higher doses (e.g. Yukihara and McKeever, 2011), the process is mathematically described as:

$$f(x)_{EXP} = a\left(1 - \exp\left(-\frac{(x+c)}{b}\right)\right) \tag{1.10}$$

where a describes the saturation dose level, b the onset of saturation and c the y-offset. Parameter b is called D_0 value and suggested as rejection criterion for reliable D_e determination ($D_e < 2D_0$; Wintle and Murray, 2006). However, in nature the system is not that simple and a single exponentially saturating signal growth is the exception rather than the rule (e.g. for discussion: Bailey and McKeever, 2012; Chen and Pagonis, 2011; Bøtter-Jensen et al., 2003b) and the fit is often not satisfactory. Therefore, for the dating practise two other functions are

commonly used, i.e. an exponential plus linear function (Eq. 1.11) and a double exponential function (Eq. 1.12):

$$f(x)_{EXP+LIN} = a\left(1 - \exp\left(-\frac{(x+c)}{b}\right) + (gx)\right) \tag{1.11}$$

$$f(x)_{EXP+EXP} = a_1\left(1 - \exp\left(-\frac{(x+c_1)}{b_1}\right)\right) + a_2\left(1 - \exp\left(-\frac{(x+c_2)}{b_2}\right)\right) \tag{1.12}$$

For Eq. 1.12 it is convenient to assume c to be 0 to make the fitting procedure more stable.[10]

Although Eq. 1.11 seems to be an appropriate adjustment to the data, for higher dose ranges it remains physically meaningless (cf. Sec. 1.4). Accounting for an increased interest in higher dose ranges, i.e. dating 'older' sediments, in the literature the application of double saturating exponential functions has emerged (e.g. Pawley et al., 2010; Timar-Gabor et al., 2012; Lowick and Preusser, 2011; Berger and Chen, 2011). Even the need for a second exponential function is empirically acknowledged to describe the signal growth at higher doses (cf. Sec. 1.10), the mechanism is unexplained and the validity for the dating practise is still under discussion (cf. Timar-Gabor et al., 2012).

D_e estimations for this thesis were carried out using the software *Analyst* version 3.24b (Duller, 2007). For dose response curve fits for high dose experiments ($\geqslant 1$ kGy) the function `plot_GrowthCurve()` from the **R** package 'Luminescence' was used (Ch. 4).

1.3.3.5 $\dot{D}$ estimation

The age equation used for luminescence dating (Eq. 1.3) depends on two fundamental values: The equivalent dose (D_e) and the dose rate ($\dot{D}$). The total dose rate can be described as a sum function of components related to different types of irradiation:

$$\dot{D}_{Total} = \dot{D}_\alpha + \dot{D}_\beta + \dot{D}_\gamma + \dot{D}_{Cosmic} \tag{1.13}$$

As mentioned above, the dose rate results from traces of natural radioactive nuclides and cosmic rays. Due to the specific ranges of the different types of radiation in matter, the calculations applied for the specific grain size fractions used for dating differ, i.e. due to etching of the outer rim for coarse grain dating the α-dose rate is neglected. In contrast, the fine grains are small compared to the mean natural α-particle range ($\gtrsim 20\,\mu$m for $\rho = 2.6$ g cm^{-3}, e.g. Aitken, 1985b) and considered as being fully penetrated by α-particles (e.g. Zimmerman, 1971, 1972). However, as mentioned before, the amount of luminescence induced by α-particles is different from that of β- and γ-radiation or X-rays. Thus, the determination of the so called 'a-value' was systematically applied for the fine grain dating for this thesis. For the middle grain fraction the a-value was deduced from the fine grain fraction and the volume unaffected by α-radiation was neglected.

[10] This should be done carefully in the case of high recuperation rates.

Nuclide concentrations were converted to dose rates using the conversion factors from Adamiec and Aitken (1998). For the sake of consistency of ages obtained from the Saxonian Loess Region, the re-evaluated conversion factors published by Guérin et al. (2011) during the work on this thesis were not applied. The internal dose rate for quartz separates was assumed to be negligible according to the high external dose rate normally determined for loess deposits (cf. Vandenberghe et al., 2008, for investigations on the internal radioactivity in quartz). Cosmic dose rates were calculated according to Prescott and Hutton (1994). The moisture content, which significantly influences the total dose rate due to attenuation of radiation effects, was estimated by: (a) measuring the recent moisture content of the sediment by drying and (b) considerations on the upper moisture saturation level of the sediment matrix and sedimentological findings (e.g. hints of soil wetness).

1.3.3.6 Age calculation

Luminescence ages in principle are calculated according to Eq. 1.3. Nevertheless, as mentioned in the previous section, different parameters have to be included. This was done by using an *MS Excel™* sheet developed by Prof. Dr. Markus Fuchs and Dr. Annette Kadereit for age calculation. This was used in most cases. In addition, the age calculation software *ADELE* (Kulig, 2005) was used (details are given in the studies).

Apart from that, lots of efforts have been undertaken in the OSL dating literature to apply statistical methods to the D_e and/or age distribution to deduce the 'true' burial dose and the D_e error (cf. Galbraith and Roberts, 2012). But the application of such methods has to be justified. This might be the case if heterogenous or insufficient bleaching is expected in a fluvial environment and if dating on small aliquots was performed, i.e. using as few grains as possible on each aliquot down to just a single grain per aliquot. For loess deposits a priori no insufficient bleaching is expected due to the windblown origin of the sediment. However, secondary translocation processes might possibly cause such effects. The dating applied to coarse grain quartz showed large scattered D_e distributions (Sec. 1.4.1); but also during dose recovery tests. The tried minimum dose/age models (e.g. Fuchs and Lang, 2001; Woda and Fuchs, 2008) yield unrealistic young ages (data not shown) and have not been further applied.

Since almost all presented chronologies are essentially based on quartz fine grain dating comprising $\sim 10^6$ grains per disc and for this the application of such statistical methods is not feasible, the obtained D_e for every sample was calculated as the mean of individual D_es from single aliquots and the standard deviation was taken as error.

1.4 Results & discussions

1.4.1 Dating application

This thesis comprises four dating studies on loess sections in Saxony/Germany (Ch. 2 and Ch. 7), Saxony-Anhalt/Germany (Ch. 3) and Jihomoravský kraj/Czech Republic (Ch. 8), combining dating applications with methodological investigations. In this section the main outcomes of each study and overlapping results are summarised. For methodological details on the luminescence dating (e.g. individual results of preheat tests, dosimetry etc.) the reader is referred to the studies themselves.

1.4.1.1 Main dating results

Chapter 2 presents the first dating results derived through this thesis as a comparison of ages obtained for two quartz grain size fractions (coarse grain: 90–200 µm and fine grain: 4–11 µm). To determine a high-resolution numerical framework on the Saxonian Loess Region 20 samples were taken form the profile Ostrau (1.2) in Saxony/Germany. For every sample three grain size fractions (coarse, middle and fine grain) were prepared. The dating results for the coarse and fine grain fraction are presented with this study and listed in Tab. 2.2 and Fig. 2.8. The general suitability of the Saxonian Loess Region for luminescence dating on quartz is shown.

The OSL ages of the two grain size fractions (coarse and fine grain) are consistent within a 2σ error range for the upper part of the profile and are in stratigraphic order. From the dating it was observed that the profile in Ostrau is divided by a hiatus into two parts. In the upper part of the profile the samples yielded D_e estimates < 100 Gy (c. < 30 ka) and D_e values > 180 Gy (c. > 60 ka) in the lower part. With other words: The entire MIS 3 (29–57 ka; Lisiecki and Raymo, 2005) is missing in this loess record.

In the lower part of the profile the coarse grain quartz fraction is in saturation, resulting in unreliable age estimates, whereas the fine grain quartz fraction shows no saturation behaviour but underestimates the expectations from the litho- and pedostratigraphy. Therefore, the fine grain quartz ages should be taken as minimum values. Additionally, an adjusted SAR protocol for the fine grain quartz fractions was applied using higher cutheat and read temperatures (cf. Sec. 2.3.3). In contrast to the previous findings for the fine grain quartz fraction, the obtained OSL ages are in good agreement with the litho- and pedostratigraphy, but the reasons are unknown and further investigations are needed.

Chapter 3 was conducted (a) as an accompanying study to evaluate the stratigraphic classification of the Saxonian Loess Region presented by Meszner et al. (2011) on a nearby loess section (Zeuchfeld, Fig. 3.1) in Saxony-Anhalt and (b) as a preliminary dating study on this loess section for which numerical dating results had been missing so far.

It was found that the quartz mineral fraction (middle and fine grain) from the section is suitable for OSL dating up to at least 116 ka. The ages (Fig. 3.2 and Tab. 3.1,3.2) increase with depth and confirm the previously assumed Weichselian age with the Eemian soil (MIS 5e, 5d) at the base for the upper periglacial deposits of the profile (Ruske, 1961; Meng and Wansa, 2008). For the underlying fluvioglacial deposits (Zeuchfeld Sandur) luminescence dating on the potassium rich coarse grain feldspar (K-feldpar) fraction using infrared-radiofluorescence (IR-RF) shows good luminescence behaviour. However, the IR-RF age (323 ± 70 ka) overestimates the expected age of the Zeuchfeld Sandur, which is believed to be of Saalian age (MIS 8 to MIS 6, Eis; Eissmann, 1997; Litt et al., 2006). The quartz coarse grain fraction of this layer yields a saturation age of 179 ± 51 ka but should be treated carefully due the saturated luminescence signal.

Chapter 7 was conducted as a comprehensive study combining sedimentological findings from 7 loess sections in the Saxonian Loess Region with dating results from the profiles Ostrau and Seilitz to re-evaluate and extend the pronounced stratigraphic classification published by Meszner et al. (2011).

For the profile Seilitz 11 samples were dated using the fine grain quartz fraction and in addition for 5 samples ages are obtained using the post-IR IR protocol (Thomsen et al., 2008) on the polymineral fine grain fraction (e.g. Thiel et al., 2011a). Ages increase with depth

from 18.3 ± 2.2 ka at the top (BT706) to 72.8 ± 7.6 ka at the base of the profile (BT715). As previously observed on the profile Ostrau the profile is divided into two parts by a hiatus (BT714: < 30 ka and BT715: > 70 ka). The age results of the quartz fine grain dating are confirmed by the (fading corrected) post-IR IR dating results. Numerical dating results of the profile Seilitz are listed in Tab. 7.3 (ages) and Tab. 7.2 (dosimetry). Figure 7.4 provides a synopsis of the results for the profiles Ostrau and Seilitz.

The dating study on the loess section Dolní Věstonice (Ch. 8) continued and intensified the monomineralic dating approach to establish a reliable high-resolution chronology for the last glacial-interglacial cycle as a comparison of three grain size fractions (coarse, middle and fine grain). To overcome the previously reported problem of age underestimation for the Weichselian Early Glacial loess on this section (Musson and Wintle, 1994; Zöller et al., 1994; Frechen et al., 1999), 15 samples were prepared for OSL dating on the coarse, middle and fine grain quartz fraction. Due to the signal saturation of the coarse and middle grain quartz fractions, for samples yielding an age > 45 ka (> 150 Gy) only the fine grain quartz fraction was used for age determination (for further discussion see below).

Samples, were all grain size fractions were measured, the derived ages are the same within errors and therefore a mean age was calculated (Fig. 8.2 and Tab. 8.1, 8.2). Almost all age estimates are in stratigraphic order except one sample from the base of the profile (BT752) that underestimates the assumed pre-Weichselian age. The reasons for this age underestimation remain unknown.

1.4.1.1.1 Supplementary data: Dating results middle grain fraction

The study on the loess profile Ostrau was limited to the coarse and the fine grain quartz fractions. An important aspect that should not be overlooked is that, as mentioned in Sec. 1.1.1, loess has its modal grain size range in the silt fraction (for the Saxonian Loess Region cf. Meszner et al., 2011). The choice of the grain size for luminescence dating depends on the grain size availability in the target sediment and practical considerations, e.g. time for sample preparation (cf. Sec. 2.1). Besides this, specific grain size fractions can result in differing luminescence ages due to differences in the transport processes (cf. discussion in Sec. 2.5). In the conclusion of Ch. 2 it was announced that also the middle grain (38–63 µm) quartz fraction will be measured. Figure 1.9 shows the, so far unpublished, middle grain quartz ages along with the age results from the coarse and the fine grain fractions.

Numerical results are listed in the appendix: Sec. A.1 (ages) and Sec. A.2 (dose rates and nuclide concentrations). Within errors all three grain size fractions yield similar age results. Though it can be concluded that the fine grain quartz fraction can be used to establish the chronological framework (see also Ch. 8). For the lower part of the profile no middle grain quartz ages were obtained due to the signal saturation of the dosimeter (for further discussion see below). Surprisingly, it was found that the D_e distributions of the middle grain quartz fraction are highly scattered (data not shown). Compared with the coarse grain aliquots, the number of settled grains on each aliquot is two orders of magnitude larger and lower scatter was expected due to an averaging effect. The reasons for the differences could not be further investigated in the framework of this thesis but may serve as a subject for further studies.

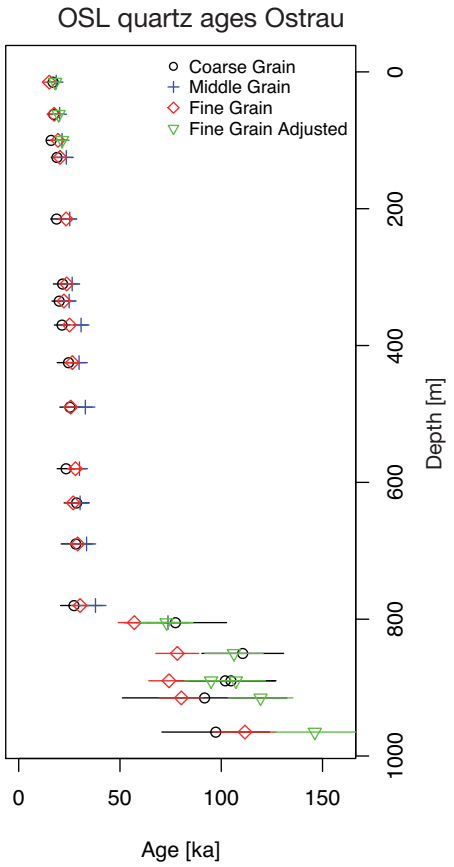

Figure 1.9: Quartz OSL ages for three different grain size fractions from the profile Ostrau. Numerical data are given in Sec. A.1

1.4.1.2 Methodological aspects

The dating studies deal with two major methodological issues: (a) comparison of the different grain size fractions used for dating, (b) establishing reliable chronologies using quartz separates up to the Eemian and therefore beyond the pronounced age range for quartz dating on loess deposits (e.g. Zöller, 2010; Roberts, 2008).

In Chapter 2 shows that the D_e distributions of the coarse grain fractions are highly scattered (cf. Fig. 2.4). This quartz behaviour in the Saxonian Loess Region was also observed in the study on the profile Zeuchfeld (Ch. 3). Here, the quartz coarse and middle grain fractions show a high scatter in the D_e distributions, which does not seem to be correlated with the stratigraphical position. It is perhaps not surprising that $\sim 10^6$ grains (fine grain) on an aliquot (Fig. 1.8) show lower scatter than an aliquot comprising only a couple of hundred grains (coarse grain) and the differences may originated from an average effect of the luminescence signal. These variations may reflect differences in the bleaching history, i.e. mixture of grains deposited over different time periods or insufficient bleaching during reworking or secondary translocation (cf. Fuchs and Wagner, 2003; Duller, 1994). However, the scatter also occurred during the combined preheat and dose recovery tests (profile Ostrau: Fig. 2.2, profile Dolní Věstonice:

Fig. 8.4). These observations indicate that the scatter results from the dosimeter itself and is probably not related to secondary translocation processes (e.g. insufficient signal bleaching during the second transport) or post sedimentary mixture effects (mixed ages). The possibility of different source areas to explain the observed discrepancies by the transport processes (local and distant transport) could not be further investigated.

The large scatter in the D_e distributions of the middle grain fraction (Sec. 1.4.1.1.1) may originate from a combined effect arising from technical difficulties (e.g. non-mono-layer on the sample carrier) and the dosimeter characteristics itself because due to the number of grains on the discs an averaging effect would be expected.

LM-OSL and pLM-OSL investigations performed for selected samples using the **R** package 'Luminescence' (Ch. 4) from the profiles Ostrau (unpublished observation), Zeuchfeld (Fig. 3.7 and Fig. 3.9) and Dolní Věstonice (Fig. 8.7) show that all investigated samples (independent of the grain size fraction) consist of a dominant, easy to bleach and fast decaying signal component. According to that one would a priori expect similar signal characteristics for every grain size fraction, but this observation may be misleading. The LM-OSL investigations have not been performed systematically on all samples during this thesis and an additional component based age determination could not be accomplished due to time restrictions. Nevertheless, such investigations are technically possible with the **R** package 'Luminescence' developed during this thesis and the observations can serve for further studies.

Aside from the discrepancies in the D_e (age) distributions between the grain size fractions, the comparative studies (Ch. 2, 3,8) show grain size dependent differences in the saturation behaviour. For example, for the profile Ostrau (Ch. 2) the luminescence signal of the coarse grain fraction is in saturation in the lower part of the profile (cf. Fig. 2.3), which is, however, in accordance with the expectations from the literature (cf. Roberts, 2008), whereas the fine grain quartz signal still grows. Similar observations for fine grain quartz have been made by Timar-Gabor et al. (2012, 2011) and confirmed in the dating study on the loess section Dolní Věstonice (Ch. 8). The results face on three issues:

(1) The fine grain quartz growth curves have been almost best fitted by using an exponential plus linear function (Eq. 1.11), implying a physically meaningless infinite growth of the luminescence signal in the dosimeter. Furthermore, Wintle and Murray (2006) suggested that the D_e should not exceed $2D_0$ to avoid large uncertainties in the D_e. Using an exponential plus linear function, the linear term prohibits the application of such rejection criteria as the D_0 value strongly depends on the fitting.

Nevertheless, in the studies the exponential plus linear function has been chosen as best fit for the dataset in the investigated dose range covering the expected natural D_e and it was hypothesised that the applied fitting results in reliable D_e estimations. These were confirmed by preheat plateau and dose recovery tests as well as high-dose experiments (Fig. 1.10).

The high-dose experiments (up to $\sim 1.1\,\mathrm{kGy}$) on the fine grain quartz demonstrate that the rejection criterion $D_e < 2D_0$ is fulfilled, and combined with the agreement of the age results with the litho- and pedostratigraphic findings it is concluded that fine grain quartz dating provided reliable age estimates for the investigated loess sections.

(2) However, the studies from Timar-Gabor et al. (2012); Lowick and Preusser (2011); Timar-Gabor et al. (2011) found increasing age underestimation of the fine grain quartz up

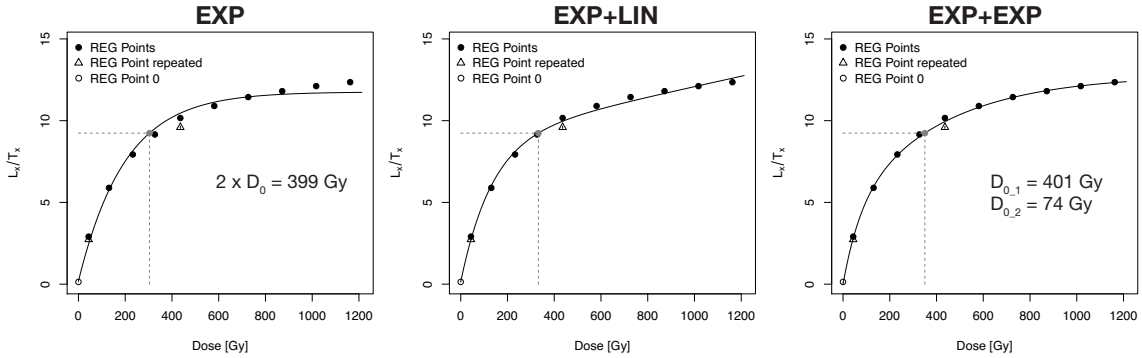

Figure 1.10: High dose growth curves for fine grain quartz sample BT754 (cf. Ch. 8) fitted with different functions. The $2D_0$ value for the EXP and the EXP+EXP fit are shown within the plots.

to and beyond the Eemian.[11] Although differences for the applied protocol for fine grain were observed for the dating study on the loess section in Ostrau (Ch. 2), in general and in combination with the sedimentological findings, it is believed that the fine grain quartz fraction gives reliable age estimates for the investigated loess records. Furthermore, this is confirmed by the comparison of quartz and polymineral fine grain ages on the profile Seilitz (Ch. 7), which are in accordance within uncertainties. Therefore, the reasons for the reported observations could not be ruled out during the conducted studies and may be sample dependent. The OSL dating of the profiles Zehren, Gleina and Rottewitz (Fig. 1.1) were carried out using only fine grain quartz separates (dating results: Ch. A Sec. A.1 and Sec. A.2 in the appendix).

(3) In contrast, of paramount importance is the observed grain size saturation characteristic of the quartz fine grain fraction. In Sec. 2.5 two explanations are presented for the differences between the grain size fractions: (a) the burial history of the different grain size fractions (e.g. more bleach and dose cycles combined with different source areas) and (b) the increase of electron traps (i.e. atomic displacements) as a result of α-activity with time (Odom and Rink, 1989; Rink and Odom, 1991; Weeks, 1956). It should be noted that this remains highly speculative and the work of Kalefezra and Horowitz (1982) for TL raises doubt if this is still a proper explanation, as they found that atomic displacement does not seem to significantly increase the TL efficiency. Nevertheless, a separate OSL study using fine grain quartz separates should be conducted to investigate the effect of heavy-charged α particles for the saturation behaviour of fine grain quartz.

1.4.1.3 Establishing chronologies: A synthesis

In summary, the dating work for this thesis (along with the hitherto unpublished results) reveals the stratigraphic significance for the investigated loess sections by establishing reliable high-resolution chronologies based on OSL dating. For the Saxonian Loess Region this led to a revised composite profile and supports a qualitative approach to reconstruct the Late

[11] Lowick and Preusser (2011) provide additional studies, but it should be noted that not all of these studies deal with fine grain (4–11 µm) quartz.

Pleistocene landscape dynamic.

The study in Ch. 7 provides a summarised view of these results. It was found that the Saxonian Loess Region encompasses five stratigraphic units. Unit V $>$ 120 ka), covers pre-Eemian sediments and Eemian soil formation followed by unit IV ($<$ 120 ka to 60 ka), consisting of compacted pedostratigraphic layers. Due to the high-resolution luminescence dating it was possible to uncover a hiatus of at least 30 ka, which is assigned to unit III ($<$ 30 ka) and covered by the Gleinaer Complex, a local (arctic brown) soil complex first described for the Gleina section by Lieberoth (1963) (cf. Ch. 7 and Meszner, 2008). The slightly decreasing ages of unit II ($<$ 30 ka to $>$ 22 ka) over a couple of meters of the profile indicate a high aeolian dynamic during the last glacial maximum (LGM). Unit I ($<$ 18 ka) represents the top of the composite profile. The presented pattern was also found at the nearby loess section Zeuchfeld in Saxony-Anhalt, where the loess accumulation started latest at c. 70 ka and resumed, following a depositional hiatus, between $<$ 30 ka and 22 ka.

Due to a different local preservation situation the results of Dolní Věstonice illustrate the landscape dynamic in much more detail, but in general with a similar pattern (Fig. 8.2). The basal part of the profile comprises Eemian soil on pre-Eemian calcareous loess followed by a humic soil complex. On top of the laminated sandy loess, a brown soil complex is followed again by thick laminated sandy loess, indicating high accumulation of loess. In contrast to the Saxonian Loess Region, the OSL dating uncovered two hiatuses: The first hiatus is indicated at the transition zone between the lower sandy loess and the brown soil complex ($<$ 50.6 $\pm$ 3.5 ka, transition unit 6 to 7) the second was found between the brown soil complex (unit 6 to 4) and the reinserted loess accumulation (unit 3) and may be related to the hiatus found in the Saxonian Loess Region.

1.4.2 Technical investigations and developments

Two primary technical studies (Ch. 4 and 5) were carried out to deal with emerging technical problems and challenges.

The 1st technical study was conducted to handle upcoming amount of data. To allow for intensive data analysis and visualisation for the work of this thesis, scripts for the numerical programming language **R** were written (Ch. 4). To share the developed scripts with the luminescence dating community, the previously singular **R** scripts were encapsulated into functions and bundled within a separate **R** package ('Luminescence'; Ch. 4). The package can be installed and loaded into the **R** environment; it provides functions that work as small applications within the **R** environment. The source code of the scripts is always available and the calculations are transparent for the user. Along with the **R** code, a documentation file for every function is provided as well as additional example data.[12]

The package comprises 22 individual functions (Ch. A.4) for luminescence dating data analysis. It is not intended to replace existing, commonly used software solutions for routine luminescence dating like the *Analyst* (Duller, 2007) but it provides tools for a flexible and unconventional data handling combined with a high-quality graphic output. For example, the function `readBIN2R()` directly imports so called BIN-files[13] into the **R** environment. The files contain the measurement raw data from the Risø TL/OSL luminescence reader and can be used for further analyses. In **R** the function is called (details: Sec. 4.2.1):

[12] CD in the cover of this thesis or via CRAN: http://cran.r-project.org/web/packages/Luminescence/index.html
[13] *.bin - binary file format

```
,
readBIN2R('[path]/MeasurementData.BIN')
```

Another implemented function allows extensive LM-OSL curves analysis and visualisation. With the introduction of the `fit_LMCurve()`, it was the first time that an automated and scalable solution for LM-OSL analysis had been provided (details: Sec. 4.2.3). For example, the analysis simply started by calling:

```
,
> fit_LMCurve(values=values.curve,n.
+ components=3,log_scale="x")
```

Since the **R** package 'Luminescence' was being developed over the entire time of this thesis and is continuously under development after the original publication presented in Ch. 4, the functions within the package have been further improved, extended and new functions have been added. Some of the functions were developed by other authors or in cooperation with other authors (cf. Ch. A.4). The functions added by the author of this thesis after the publication of the study (Ch. 4) are listed in Tab. 1.2. Due to the dimension of the entire project it is not possible to provide all details of the package. For details of each function the reader is referred to the manual of the package. Substantial changes from version to version (e.g. bug-fixes, improvements) are documented in **R** package itself.

Table 1.2: Selected additional functions in the **R** package 'Luminescence' since vers. 0.1.7

#	Name	Description
1	`CW2pHMi()`	Transforms a CW-OSL curve in a pHM-OSL curve via interpolation under hyperbolic modulation conditions (Bos and Wallinga, 2012)
2	`CW2pLMi()`	Transforms a CW-OSL curve in a pLM-OSL curve via interpolation under linear modulation conditions (Bos and Wallinga, 2012)
3	`CW2pPMi()`	Transforms a CW-OSL curve in a pPM-OSL curve via interpolation under parabolic modulation conditions (Bos and Wallinga, 2012)
4	`fit_CMCurve()`	Nonlinear Least Squares Fit for CW-OSL Curves

The functions of the package along with self-written **R** scripts were intensively used for almost all presented studies except the first study (Ch. 2).

The 2nd technical study investigates measurement artefacts. Considerable evidence suggested that during the dating application for the study in Ch. 7 on polymineral fine grain samples using IR stimulation, the measurement results were systematically biased. Test measurements for the D_e estimation showed that the first position of every measurement yielded substantially higher D_e values, which may lead to significant age underestimations. The luminescence readers used for the measurements accommodate up to 48 aliquots on a carousel in a single measurement chamber (Fig. 5.1). Due to this construction and the small distance

between the single aliquot positions (17 mm), the adjacent positions are potentially affected by cross-talk effects (cross-irradiation of the β-source, cross-bleaching of the LEDs arrays; cf. Fig. 1.11).

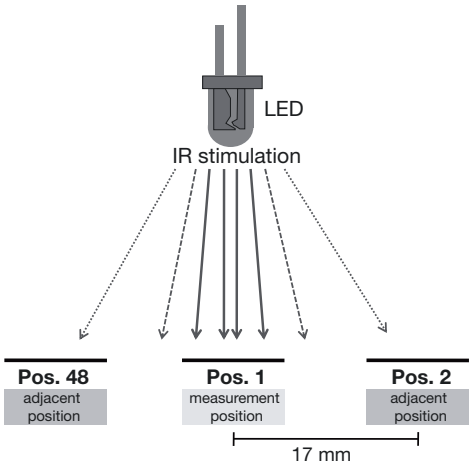

Figure 1.11: Sketch of the cross-bleaching principle redrawn from Bray et al. (2002) and Hülle (2011).

This behaviour is confirmed by previous studies (e.g. Bray et al., 2002; Bøtter-Jensen et al., 2000). However, the cross-bleaching of the IR-LEDs had never been investigated before. Particularly, with regard to the 'run 1 at a time' option that carries out all measurement steps on one aliquot before moving to the next position, this may become an issue. The 'run 1 at a time' option is usually applied for feldspar measurements (IR stimulation) to hold the elapsed time between irradiation and stimulation constant in order to account for the anomalous fading. The experiments were carried out on Risø TL/OSL DA-12, DA-15 and DA-20 readers in four laboratories.

The results show that the cross-bleaching value of the IR LEDs on adjacent positions is systematically higher than observed for blue LEDs for all investigated DA-15 and DA-20 readers (Fig. 5.4). The cross-bleaching values range from $< 0.0001\,\%$ to $0.1279 \pm 0.0167\,\%$ and vary markedly between the readers. In comparison, the cross-bleaching values derived for the blue LEDs range from $0.0019\,\%$ to $0.0176\,\%$, which is an order of magnitude lower than for the IR-LEDs. The results show no dependence of the cross-bleaching on the stimulation power but rather a variation with the sample carrier used (higher values for steel discs than for steel cups: Tab. 5.2). The reasons for the higher cross-bleaching values for the IR LEDs than for the blue LEDs as well as the notably higher cross-bleaching values for the investigated reader ID 189 (Fig. 5.4) in comparison to other investigated readers have remained unclear so far.

However, in order to account for this problem during this study a newly designed bottom flange for the LED stimulation head was developed by the measurement manufacturer Risø (Fig. 5.6). This bottom flange reduces the cross-bleaching value on the adjacent position by the factor of ~ 20 (Tab. 5.2).

In addition, it is recommended to split the sequence into different measurement sets to reduce the number of measurement steps carried out on one position before moving to the next

or to use only every 2nd position on the sample carousel. To allow an estimation of how much (cumulative/total) stimulation time on the measurement position is acceptable for a given threshold value of signal reduction on the adjacent position (blue and IR LEDs), in Fig. 5.7 isoline plots for signal reduction on adjacent position vs. cross-bleaching values are provided.

For this study all measurements were carried out using only every 2nd position on the sample carousel and previous measurements had been checked carefully for measurement artefacts. However, for the quartz measurements no substantial cross-bleaching effect was observed.

1.4.3 Methodological investigations

Methodological investigations were carried out in a survey on a-values of polymineral fine grain samples in Ch. 6.

Feldspar provides an alternative if quartz is not available in the target sediment or not sufficient for dating purposes (e.g. early saturation, domination of slow bleachable signal component). As feldspar suffers from anomalous fading, which leads to age underestimations with the development of the the post-IR IRSL (pIRIR) protocol by Thomsen et al. (2008), a method was suggested to circumvent this limitation by measuring at higher temperatures and detecting a signal component that is less affected by fading. For age calculation recent studies (e.g. Thiel et al., 2011a; Schatz et al., 2012; Buylaert et al., 2011) assumed that the α-efficiency of the polymineral fine grain fraction allows the application of an identical value for both signals (IR_{50} and $pIRIR_{225}$ or $pIRIR_{290}$).

To characterise the a-value of the IR_{50} and $pIRIR_{225}$ various a-value measurements were carried out (Ch. 6). The study was twofold: The 1st part was an empirical study of the a-value determination applying the (regenerated) pIRIR protocol at 225 °C for three methods of signal resetting (optical, end of SAR cycle, heating); it treated the α-dose as unknown. This SAR-based approach might be called 'conventional' since it has been previously applied on fine grain quartz (e.g. Tribolo et al., 2001; Mauz et al., 2006; Lai et al., 2008). The 2nd part investigated the a-value at higher dose regions using α- and β-irradiation to obtain uncorrected dose response curves and extrapolate the a-value based on the determined mathematical fit.

The a-values of five polymineral fine grain samples were investigated. The empirical results show that the mean a-value of the polymineral fine grain fraction differs significantly for the IR_{50} and the $pIRIR_{225}$ signals, at least by 0.02. The $pIRIR_{225}$ a-value is always higher than the IR_{50} a-value (Fig. 6.2, numerical values: Tab. 6.2). Nevertheless, a dependency of the a-values on the chosen method of signal resetting was observed. The results indicate that this dependency for the method of optical signal resetting generally arises from apparent residual signals (cf. for optical bleaching Fig. 6.9). Although for the signal resetting method 'end of SAR cycle' a finally convincing explanation is still missing, the results indicate a correlation between the applied fitting, insufficiently corrected sensitivity changes and the (lower) a-values.

It is further shown that the α- and β-induced growth curves show a similar trend for the IR_{50} and the $pIRIR_{225}$ signals with flatter curves for the $pIRIR_{225}$ signal (Fig. 6.3). The different curve shapes for the β-induced growth curves for the IR_{50} and the $pIRIR_{225}$ signals are in accordance with findings from previous observations (e.g. Thiel et al., 2011a).

The measurements for the synthetic growth curves were carried out on three polymineral

fine grain samples. The determined synthetic growth curves show that the a-value increases with higher doses up to the onset of saturation of the β-radiation induced luminescence signal Fig. 6.6). Consistent high-dose behaviour was found (Fig. 6.5 and Fig. 6.6) compared with results previously reported in the literature for quartz. From these data it is hypothesised that the energy density model for the α-effectiveness is valid for polyminerals determined with the pIRIR protocol. The a-values obtained with the 'conventional' approach and the uncorrected growth curves are in accordance within in errors (Fig. 6.7).

The practical significance of the findings is revealed in Sec. 6.5 by comparing ages calculated with identical a-values with ages calculated using differing a-values. The calculation shows that the assumption of a common a-value for the IR_{50} and the $pIRIR_{225}$ signal results in a (mean) age overestimation of the $pIRIR_{225}$ ages of around 8–10 %. It should be noted that this calculation is just valid for assumed parameters and all a-values of this study are measured for samples from one single loess record.

Nevertheless, with this study it was shown that the use of identical a-values for the IR_{50} and the $pIRIR_{225}$ signal seems not to be justified and leads to systematic errors in the luminescence ages. The physical reasons for the differences between the a-values obtained with the IR_{50} and the $pIRIR_{225}$ signals remained unknown so far and further investigations are needed.

1.5 Conclusions

Loess records are considered as most important terrestrial sediment archives to reconstruct palaeoenvironmental conditions of the last glacial-interglacial cycle and loess research has a long lasting history. Establishing reliable chronologies to reveal the stratigraphic findings on loess records remains, however, one of the driving rationales. Luminescence dating provides one of the most important dating methods for loess archives and by determining the time elapsed since the last exposure to light on natural mineral grains of quartz and feldspar, it can trace the morphological process itself.

The broad intention of this cumulative applied-methodological thesis was to provide a contribution towards the establishment of reliable high-resolution numerical chronologies on loess palaeosol-sequences for the last glacial-interglacial cycle using OSL dating on quartz separates. In the past, OSL dating on quartz has in general proved its capability for loess dating. However, different grain size fractions (coarse, middle and fine grain) are used for luminescence dating and it remained unclear, if the use of a specific grain size fraction influences the age results. Furthermore, different luminescence characteristics are reported in the literature, especially for the fine grain quartz fraction, i.e. higher saturation doses.

With this cumulative thesis seven single studies were presented. Four studies (Ch. 2, 3, 7, 8) were focussed on the applications of luminescence dating by establishing chronologies on loess sections in Germany and the Czech Republic. Different quartz grain size fractions were investigated. Two studies (Ch. 4, 5) dealt with technical aspects that arose during the work on this thesis, to provide additional tools for data analysis (Ch. 4) and to overcome pressing technical problems (Ch. 5). One study (Ch. 5) investigated fundamental methodological aspects by presenting empirical results on the α-efficiency for polymineral fine grain samples measured with the post-IR IR protocol designed for feldspar dating. The individual results can

be summarised as follows:

- **Dating application**
  - For the first time, a comprehensive numerical chronology for the Saxonian Loess Region based on OSL quartz separates has been established. The dating application enabled the re-evaluation of the existing composite profile, now encompassing five units. Furthermore, the high resolution dating uncovered a hiatus of at least 30 ka (end of MIS 4 to end of MIS 3). Highest sedimentation rates were found for the MIS 2.
  - The established chronologies in Zeuchfeld (Saxony-Anhalt/Germany) and in Dolní Věstonice (Jihomoravský kraj/Czech Republic) confirmed the general pattern observed in the Saxonian Loess Region.
  - The comparison of quartz coarse, middle and fine grain ages gave similar results within uncertainties, so far as the luminescence signal for the coarse and middle grain fraction is not in saturation ($D_e \lesssim 100$ Gy).
  - Based on pedo- and lithostratigraphical findings the fine grain quartz separates have been proven as reliable dosimeter back to the Eemian.
  - High dose experiments on fine grain quartz showed that the applied exponential plus linear function for growth curve fitting is valid for the investigated dose range.
  - Differences in the dose response characteristics for used grain size fractions remained unexplained.
- **Technical investigations and developments**
  - An **R** package ('Luminescence') was developed comprising several functions for efficient luminescence data analysis and visualisation.
  - Investigations on the cross-bleaching behaviour of IR-LEDs confirmed a significant cross-talk effect in an order of magnitude higher than for the blue LEDs. This effect was quantified for the first time. A new component, developed by the manufacturer, was confirmed to be capable to reduce the cross-bleaching effect significantly.
- **Methodological investigations**
  - For the first time a-values for polymineral fine grains measured with the post-IR IR protocol were presented.
  - Investigations on the a-value of polymineral fine grains using the post-IR IR protocol showed differences in the obtained a-values for the IR_{50} and the $pIRIR_{225}$ signal by a least 0.02.
  - The $pIRIR_{225}$ signal gave always higher a-values.
  - It is not appropriate to a priori use identical a-values for the IR_{50} and the $pIRIR_{225}$ signals and it is recommended to measure the a-value for every sample separately.

Several questions emerged that could not been answered or further investigated in the framework of this study. The following points may serve as possible starting place for further studies:

- The application of double exponential functions for growth curve fitting is still under discussion. Further investigations using high dose experiments should been carried out along with modelling approaches that improve understanding of the dose response characteristics of quartz. Along with spectral measurements it should be investigated, if the age underestimation for the fine grain fraction at higher doses observed in the literature (e.g. Timar-Gabor et al., 2011) may be induced by shifts in the detection wavelength (drifting out of the detection window).

- The higher dose response characteristics for the fine grain fraction remained unexplained. Odom and Rink (1989), Rink and Odom (1991) reported a growth of electron traps as a product of α-activity with time. They found that α-recoils (recoil effect) are capable to increase the electron trap density in the dosimeter by displacement of Si and O atoms resulting from elastic collisions from α-emitting impurities. The recoil effect has ranges of 30–40 nm (e.g. Gögen and Wagner, 2000) and should be valid for all grain fractions. This limits the approach to explain the differences in the shape of the growth curves by α-recoils. However, a previous work by Weeks (1956) has shown defect formation in the crystal lattice by fast neutron bombardment. The common approach for coarse grain quartz OSL dating etches the outer layer which was exposed to α-radiation to remove the α-affected layer. Due to their small grain character the fine grain quartz fraction is usually considered as fully affected by external α-particles. The saturation limit of the fine grain fraction may have been gotten enhanced by such irradiation induced defect formation.

  Although the study of Kalefezra and Horowitz (1982) emphasises that the amount of induced vacancies may be negligible and not be capable to significantly increase the number of traps, it would be worthwhile to conduct an empirical study using fine grain quartz separates to prove the hypothesis that heavy charged α-particles are not responsible for the higher saturation dose observed for the fine grain fraction.

- Systematically LM-OSL investigations on all different grain size fractions could not been carried out due to time restrictions. However, the developed **R** package now allows comprehensive data analysis. Two aspects should be investigated: (a) The variations of the component to sum contribution for the different grain size fractions for the same sample, (b) D_e values should be obtained from distinct signal components for comparison.

- The function `fit_LMCurve()` in the **R** package works with a simplified start parameter estimation based on findings from the literature. However, this may hamper the application due to the fact that the fitting may be forced to a local rather than a global minimum. A start parameter estimation based on a genetic algorithm should be included (cf. Adamiec et al., 2006).

- The study on the a-values of polymineral fine grain samples was limited to samples from one loess section and to the IR_{50} and $pIRIR_{225}$ signal. The outcomes of this study should be: (a) repeated with samples from other sections, (b) carried out using the IR_{50} and the $pIRIR_{290}$ signal.

- The investigation on the a-values on polymineral fine grain showed that the a-values increase with dose. Furthermore, the shape of the growth curves differs for distinct types of irradiation. In the laboratory the artificial irradiation is almost carried out using β- or

X-ray radiation. Nevertheless, the latent luminescence signal in the nature is induced in a mixed radiation field. A study using combined α- and β-irradiation should investigate growth curve shapes under mixed irradiation conditions, to uncover potential differences.

Extended Summary: References

Adamiec, G., Aitken, M.J., 1998. Dose-rate conversion factors: update. Ancient TL 16, 37–50.

Adamiec, G., Bluszcz, A., Bailey, R.M., Garcia-Talavera, M., 2006. Finding model parameters: Genetic algorithms and the numerical modelling of quartz luminescence. Radiation Measurements 41, 897–902.

Aitken, M.J., 1985a. Alpha particle effectiveness: numerical relationship between systems. Ancient TL 3, 22–25.

Aitken, M.J., 1985b. Thermoluminescence dating. Studies in archaeological science, Academic Press.

Aitken, M.J., 1998. An Introduction to Optical Dating. Oxford University Press.

Aitken, M.J., Tite, M.S., Reid, J., 1964. Thermoluminescent Dating of Ancient Ceramics. Nature 202, 1032–1033.

Antoine, P., Rousseau, D.D., Degeai, J.P., Moine, O., Lagroix, F., Kreutzer, S., Fuchs, M., Hatté, C., Gauthier, C., Svoboda, J., Lisa, L., 2013. High-resolution record of the environmental response to climatic variations during the last interglacial-glacial cycle in Central Europe: the loess-palaeosol sequence of Dolní Věstonice (Czech Republic). Quaternary Science Reviews 67, 17–38.

Antoine, P., Rousseau, D.D., Moine, O., Kunesch, S., Hatté, C., Lang, A., Tissoux, H., Zöller, L., 2009. Rapid and cyclic aeolian deposition during the Last Glacial in European loess: a high-resolution record from Nussloch, Germany. Quaternary Science Reviews 28, 2955–2973.

Antoine, P., Rousseau, D.D., Zöller, L., Lang, A., Munaut, A.V., Hatté, C., Fontugne, M., 2001. High-resolution record of the last Interglacial-glacial cycle in the Nussloch loess-palaeosol sequences, Upper Rhine Area, Germany. Quaternary International 76/77, 211–229.

Auclair, M., Lamothe, M., Huot, S., 2003. Measurement of anomalous fading for feldpsar IRSL using SAR. Radiation Measurements 37, 487–492.

Bailey, R.M., 2001. Towards a general kinetic model for optically and thermally stimulated luminescence of quartz. Radiation Measurements 33, 17–45.

Bailey, R.M., 2010. Direct measurement of the fast component of quartz optically stimulated luminescence and implications for the accuracy of optical dating. Quaternary Geochronology 5, 559–568.

Bailey, R.M., McKeever, S.W.S., 2012. Theory of luminescence dating, in: Krbetschek, M.R. (Ed.), Luminescence Dating: An introduction and handbook. Springer, pp. 1–25. The chapter is part of a book, which is so far unpublished.

Bailey, R.M., Smith, B.W., Rhodes, E.J., 1997. Partial Bleaching and the decay from characteristics of quartz OSL. Radiation Measurements 27, 123–136.

Ballarini, M., Wallinga, J., Wintle, A.G., Bos, A.J.J., 2007. A modified SAR protocol for optical dating of individual grains from young quartz samples. Radiation Measurements 42, 360–369.

Berger, G.W., Chen, R., 2011. Error analysis and modelling of double saturating exponential dose response curves from SAR OSL dating. Ancient TL 29, 9–14.

Berger, G.W., Mulhern, P.J., Huntley, D.J., 1980. Isolation of silt-sized quartz from sediments. Ancient TL 11, 8–9.

Bernhofer, C., Goldberg, V., 2008. Sachsen im Klimawandel - Eine Analyse. Freistaat Sachsen.

Bos, A.J.J., Wallinga, J., 2012. How to visualize quartz OSL signal components. Radiation Measurements 47, 752–758.

Bøtter-Jensen, L., 1997. Luminescence techniques: Instrumentation and methods. Radiation Measurements 27, 749–768.

Bøtter-Jensen, L., Andersen, C.E., Duller, G.A.T., Murray, A.S., 2003a. Developments in radiation, stimulation and oberservation facilities in luminescence measurements. Radiation Measurements 37, 535–541.

Bøtter-Jensen, L., Bulur, E., Duller, G.A.T., Murray, A.S., 2000. Advances in luminescence instrument systems. Radiation Measurements 32, 523–528.

Bøtter-Jensen, L., McKeever, S.W.S., Wintle, A.G., 2003b. Optically Stimulated Luminescence Dosimetry. Optically Stimulated Luminescence Dosimetry, Elsevier Science B.V.

Bray, H.E., Bailey, R.M., Stokes, S., 2002. Quantification of cross-irradiation and cross-illumination using a Risø TL/OSL DA-15 reader. Radiation Measurements 35, 275–280.

Buggle, B., 2011. Reconstruction of the Late and Mid-Pleistocene climate and landscape history in SE-Central Europe. Ph.D. thesis. Universität Bayreuth.

Bulur, E., 1996. An Alternative Technique For Optically Stimulated Luminescence (OSL) Experiment. Radiation Measurements 26, 701–709.

Bulur, E., 2000. A simple transformation for converting CW-OSL curves to LM-OSL curves. Radiation Measurements 32, 141–145.

Buylaert, J.P., Thiel, C., Murray, A.S., Vandenberghe, D.A.G., Yi, S., Lu, H., 2011. IRSL and post-IR IRSL residual doses recorded in modern dust samples from the Chinese Loess Plateau. Geochronometria 38, 432–440.

Chen, R., Pagonis, V., 2011. Thermally and Optically Stimulated Luminescence - A Simulation Approach. Thermally and Optically Stimulated Luminescence A Simulation Approach, John Wiley & Sons, Ltd.

Chesworth, W., 2008. Encyclopedia of soil science. Encyclopedia of earth sciences series, Springer.

Daniels, F., Boyd, C.A., Saunders, D.F., 1953. Thermoluminescence as a Research Tool. Science 117, 343–349.

Demek, J., Kukla, J. (Eds.), 1969. Periglazialzone, Löss und Paläolithikum der Tschechoslowakei. Tschechoslowakische Akademie der Wissenschaften, Geographisches Institut in Brno, Brno.

Demtröder, W., 2005. Experimentalphysik 3. Atome, Moleküle und Festkörper, Experimentalphysik. 3rd ed., Springer.

Duller, G.A.T., 1994. Luminescence dating of poorly bleached sediments from Scotland. Quaternary Science Reviews 13, 521–524.

Duller, G.A.T., 2003. Distinguishing quartz and feldspar in single grain luminescence measurements. Radiation Measurements 37, 161–165.

Duller, G.A.T., 2007. Analyst. , URL: `http://www.nutech.dtu.dk/english/~/media/Andre_Universitetsenheder/Nutech/Produkter%20og%20services/Dosimetri/radiation_measurement_instruments/tl_osl_reader/manuals/analyst_manual_v3_22b.ashx`. unpublished software manual.

Eissmann, L., 1997. Das quartäre Eiszeitalter in Sachsen und Nordostthüringen. Altenburger Naturwissenschaftliche Forschungen, Altenburg.

Erfurt, G., 2003. Infrared luminescence of Pb^{+} centres in potassium-rich feldspars. physica status solidi (a) 200, 429–438.

Erfurt, G., Krbetschek, M.R., 2003. IRSAR - A single-aliquot regenerative-dose dating protocol applied to the infrared radiofluorescence (IR-RF) of coarse- grain K-feldspar. Ancient TL 21, 35–42.

Fleming, S.J., 1970. Thermoluminescent dating: refinement of the quartz inclusion method. Archaeometry 12, 133–143.

Frechen, M., Oches, E.A., Kohfeld, K.E., 2003. Loess in Europe - mass accumulation rates during the Last Glacial Period. Quaternary Science Reviews 22, 1835–1857.

Frechen, M., Zander, A., Cílek, V., Ložek, V., 1999. Loess chronology of the Last Interglacial/Glacial cycle in Bohemia and Moravia, Czech Republic. Quaternary Science Reviews 18, 1467–1493.

Fuchs, M., 2001. Die OSL - Datierung von Archäosedimenten zur Rekonstruktion anthropogen bedingter Sedimentumlagerung. Ph.D. thesis. Ruprechts-Karls-Universität Heidelberg.

Fuchs, M., Lang, A., 2001. OSL dating of coarse-grain fluvial quartz using single-aliquot protocols on sediments from NE Peloponnese, Greece. Quaternary Science Reviews 20, 783–787.

Fuchs, M., Straub, J., Zöller, L., 2005. Residual luminescence signals of recent river flood sediments: A comparison between quartz and feldspar of fine- and coarse-grain sediments. Ancient TL 23, 25–30.

Fuchs, M., Wagner, G.A., 2003. Recognition of insufficient bleaching by small aliquots of quartz for reconstructing soil erosion in Greece. Quaternary Science Reviews 22, 1161–1167.

Furetta, C., 2010. Handbook of Thermoluminescence. Handbook of Thermoluminescence. 2nd ed., World Scientific.

Galbraith, R.F., Roberts, R.G., 2012. Statistical aspects of equivalent dose and error calculation and display in OSL dating: An overview and some recommendations. Quaternary Geochronology 11, 1–27.

Geyh, M.A., 2005. Handbuch der physikalischen und chemischen Altersbestimmung. 1st ed., Wissenschaftliche Buchgesellschaft.

Godfrey-Smith, D.I., Huntley, D.J., Chen, W.H., 1988. Optical dating studies of quartz and feldspar sediment extracts. Quaternary Science Reviews 7, 373–380.

Gögen, K., Wagner, G.A., 2000. Alpha-recoil track dating of Quaternary volcanics. Chemical Geology 166, 127–137.

Grögler, N., Houtermans, F.G., Stauffer, H., 1958. Radiation damage as a research tool for geology and prehistory, in: 5° Rassegna Internazionale Elettronica E Nucleare, Supplemento Agli Atti Del Congresso Scientifico, Sezione Nucleare. pp. 5–15.

Guérin, G., Mercier, N., Adamiec, G., 2011. Dose-rate conversion factors: update. Ancient TL 29, 5–9.

Haase, D., Fink, J., Haase, G., Ruske, R., Pecsi, M., Richter, H., Altermann, M., Jäger, K.D., 2007. Loess in Europe—its spatial distribution based on a European Loess Map, scale 1:2,500,000. Quaternary Science Reviews 26, 1301–1312.

Haase, G., 1963. Stand und Probleme der Lößforschung in Europa. Geographische Berichte 8.

Haase, G., 1968. Die Lössrandstufe in Nordsachsen, in: Periglazial-Löß-Paläolithikum, Exkursionsführer der VII. Hauptversammlung der Geographischen Gesellschaft der DDR, Leipzig.

Haesaerts, P., Bachner, M., Borziac, I., Chirica, V., Damblon, F., Drozdov, N., Koulakovska, L., Pirson, S., 2010. New insight on the environmental background and the chronology of the early upper palaeolithic in Central Europe, in: Neugebauer-Maresch, C., Owen, L.R. (Eds.), New Aspects of the Central and Eastern European Upper Palaeolithic - methods, chronology, technology and subsistence, pp. 9–25.

Hornik, K., Leisch, F., 2002. Vienna and R: Love, marriage and the future. Festschrift - 50 Jahre Österreichische Statistische Gesellschaft , 61–70.

Houtermans, F.G., Stauffer, H., 1957. Thermolumineszenz als Mittel zur Untersuchunug der Temperatur - und Strahlungsgeschichte von Mineralien und Gesteinen. Helvetica Physica Acta 30, 274–277.

Hülle, D., 2011. Lumineszenzdatierung von Sedimenten zur Rekonstruktion der jungquartären Landschaftsentwicklung in der Mongolei. Ph.D. thesis. Universität zu Köln. Köln.

Huntley, D.J., Godfrey-Smith, D.I., Thewalt, M.L.W., 1985. Optical dating of sediments. Nature 313, 105–107.

Huntley, D.J., Lamothe, M., 2001. Ubiquity of anomalous fading in K-feldspars and the measurement and correction for it in optical dating. Canadian Journal of Earth Sciences 38, 1093–1106.

Hütt, G., Jaek, I., Tchonka, J., 1988. Optical dating: K-Feldspars optical response stimulation spectra. Quaternary Science Reviews 7, 381–385.

Jain, M., Andersen, C.E., Hajdas, W., Edmund, J.M., Bøtter-Jensen, L., 2007. OSL response to proton irradiation in some natural dosemeters: Implications for martian sediment dating. Nuclear Instruments and Methods in Physics Research Section A: Accelerators, Spectrometers, Detectors and Associated Equipment 580, 652–655.

Jain, M., Murray, A.S., Bøtter-Jensen, L., 2003. Characterisation of blue-light stimulated luminescence components in different quartz samples: implications for dose measurement. Radiation Measurements 37, 441–449.

Jary, Z., 2009. Periglacial markers within the Late Pleistocene loess–palaeosol sequences in Poland and Western Ukraine. Quaternary International 198, 124–135.

Kadereit, A., 2000. IR-OSL-datierte Kolluvien als Archive zur Rekonstruktion anthropogen bedingter Landschaftsveränderungen. - Das Fallbeispiel Bretten-Bacherbach/Kraichgau. Ph.D. thesis. Ruprecht-Karls-Universität Heidelberg.

Kalefezra, J., Horowitz, Y., 1982. Heavy charged particle thermoluminescence dosimetry: Track structure theory and experiments. The International Journal of Applied Radiation and Isotopes 33, 1085–1100.

Klasens, H.A., 1946. Transfer of Energy Between Centres in Zinc Sulphide Phosphors. Nature 158, 306–307.

Klíma, B., Kukla, G., Ložek, V., de Vries, H., 1962. Stratigraphie des Pleistozäns und Alter des paläolithischen Rastplatzes in der Ziegelei von Dolní Věstonice (Unter-Wisternitz). Anthropozoikum , 93–145.

Krbetschek, M.R., Götze, J., Dietrich, A., Trautmann, T., 1997. Spectral information from minerals relevant for luminescence dating. Radiation Measurements 27, 695–748.

Kukla, G., 1975. Loess stratigraphy of Central Europe, in: Butzer, K.W., Isaac, G.L. (Eds.), After the Australopithecines. Mouton Publishers, The Hague, pp. 99–188.

Kukla, G.J., 1977. Pleistocene land—sea correlations I. Europe. Earth-Science Reviews 13, 307–374.

Kulig, G., 2005. Erstellung einer Auswertesoftware zur Altersbestimmung mittels Lumineszenzverfahren unter besonderer Berücksichtigung des Einflusses radioaktiver Ungleichgewichte in der 238-U-Zerfallsreihe. Master's thesis. Inst. F. Informatik, TU Bergakademie Freiberg.

Lai, Z., 2010. Chronology and the upper dating limit for loess samples from Luochuan section in the Chinese Loess Plateau using quartz OSL SAR protocol. Journal of Asian Earth Sciences 37, 176–185.

Lai, Z., Kaiser, K., Brückner, H., 2009. Luminescence-dated aeolian deposits of late Quaternary age in the southern Tibetan Plateau and their implications for landscape history. Quaternary Research 72, 421–430.

Lai, Z., Wintle, A.G., 2006. Locating the boundary between the Pleistocene and the Holocene in Chinese loess using luminescence. The Holocene 16, 893–899.

Lai, Z., Zöller, L., Fuchs, M., Brückner, H., 2008. Alpha efficiency determination for OSL of quartz extracted from Chinese loess. Radiation Measurements 43, 767–770.

Lambe, J., Klick, C., 1955. Model for Luminescence and Photoconductivity in the Sulfides. Physical Review 98, 909–914.

Lieberoth, I., 1959. Beobachtungen im nordsächischen Lößgebiet. Zeitschrift für Pflanzenernährung Düngung Bodenkunde 86, 141–155.

Lieberoth, I., 1962. Die jungpleistozänen Lösse Sachsens im Vergleich zu denen anderer Gebiete: Ein Beitrag zur Würmchronologie. Petermanns Geographischen Mitteilungen 106, 188–198.

Lieberoth, I., 1963. Lößsedimentation und Bodenbildung während des Pleistozäns in Sachsen. Geologie 12, 149–187.

Lieberoth, I., 1964. Bodenbildung aus Löß während des Pleistozäns und Holozäns in Sachsen. Ph.D. thesis. Universität Leipzig.

Lieberoth, I., Haase, G., 1964. Lößexkursion Nordsachsen, in: Haase, G., Ruske, R. (Eds.), 3. Arbeitstagung der Subkommission für Lößstratigraphie der INQUA - Exkursionsführer, Leipzig.

Ligges, U., 2008. Programmieren mit R (Statistik und ihre Anwendungen). 3rd ed., Springer Berlin Heidelberg.

Lisiecki, L.E., Raymo, M.E., 2005. A Pliocene-Pleistocene stack of 57 globally distributed benthic $\delta\ ^{18}O$ records. Paleoceanography 20.

Litt, T., Behre, K.E., Meyer, K.D., Wansa, H.J.S., 2006. Stratigraphische Begriffe für das Quartär des norddeutschen Vereisungsgebietes. E & G, Quaternary Science Journal 1/2, 7–65.

Lowick, S.E., Preusser, F., 2011. Investigating age underestimation in the high dose region of optically stimulated luminescence using fine grain quartz. Quaternary Geochronology 6, 33–41.

Lowick, S.E., Trauerstein, M., Preusser, F., 2012. Testing the application of post IR-IRSL dating to fine grain waterlain sediments. Quaternary Geochronology 8, 33–40.

Mahesh, K., Weng, P.S., Furetta, C., 1989. Thermoluminescence in solids and its application. Thermoluminescence in solids and its application, Nuclear Technology Publishing, England.

Mauz, B., Packman, S.C., Lang, A., 2006. The alpha effectiveness in silt-sized quartz: New data obtained by single and multiple aliquot protocols. Ancient TL 24, 47–52.

McKeever, S.W.S., 1988. Thermoluminescence of Solids. Cambridge Univ Press.

Meng, S., Wansa, S., 2008. Sediments and processes at the borderline of Saalian glaciation southwest of Halle (Saale). Zeitschrift der Deutschen Gesellschaft für Geowissenschaften 159, 205–220.

Meszner, S., 2008. Lösse in Sachsen - Neue Untersuchungen zur Stratigraphie der weichseleiszeitlichen Lösse in der Region um Lommatzsch. Master's thesis. Fakultät Forst-, Geo- und Hydrowissenschaften, Institut für Geographie, Lehrstuhl für Physische Geographie, Technische Universisät Dresden.

Meszner, S., Fuchs, M., Faust, D., 2011. Loess-Paleosol-Sequences from the loess area of Saxony (Germany). E & G, Quaternary Science Journal 60, 47–65.

Murray, A.S., Wintle, A.G., 2000. Luminescence dating of quartz using an improved single-aliquot regenerative-dose protocol. Radiation Measurements 32, 57–73.

Musson, F.M., Wintle, A.G., 1994. Luminescence dating of the loess profile at Dolní Vestonice, Czech Republic. Quaternary Science Reviews 13, 411–416.

Newton, H.E., 1957. A history of luminescence from the earliest times until 1900. Philadelphia, American Philosophical Society.

Novothny, Á., Frechen, M., Horváth, E., Krbetschek, M.R., Tsukamoto, S., 2010. Infrared stimulated luminescence and radiofluorescence dating of aeolian sediments from Hungary. Quaternary Geochronology 5, 114–119.

Odom, A.L., Rink, W.J., 1989. Natural accumulation of Schottky-Frenkel defects: Implications for a quartz geochronometer. Geology 17, 55–58.

Pawley, S.M., Toms, P., Armitage, S.J., Rose, J., 2010. Quartz luminescence dating of Anglian Stage (MIS 12) fluvial sediments: Comparison of SAR age estimates to the terrace chronology of the Middle Thames valley, UK. Quaternary Geochronology 5, 569–582.

Pecsi, M., 1990. Loess is not just the accumulation of dust. Quaternary International 7/8, 1–21.

Prescott, J.R., Hutton, J.T., 1994. Cosmic ray contributions to dose rates for luminescence and ESR dating: Large depths and long-term time variations. Radiation Measurements 23, 497–500.

Preusser, F., Chithambo, M.L., Götte, T., Martini, M., Ramseyer, K., Sendezera, E.J., Susino, G.J., Wintle, A.G., 2009. Quartz as a natural luminescence dosimeter. Earth-Science Reviews 97, 184–214.

Preusser, F., Degering, D., Fuchs, M., Hilgers, A., Kadereit, A., Klasen, N., Krbetschek, M.R., Richter, D., Spencer, J.Q.G., 2008. Luminescence dating: basics, methods and applications. Eiszeitalter und Gegenwart (Quaternary Science Journal) 57, 95–149.

Pye, K., 1995. The nature, origin and accumulation of loess. Quaternary Science Reviews 14, 653–667.

Reimer, P.J., 2012. Refining the Radiocarbon Time Scale. Science 338, 337–338.

Rink, W.J., Odom, A.L., 1991. Natural alpha recoil particle radiation and ionizing radiation sensitivities in quartz detected with EPR: Implications for geochronometry. International Journal of Radiation Applications and Instrumentation. Part D. Nuclear Tracks and Radiation Measurements 18, 163–173.

Roberts, H.M., 2008. The development and application of luminescence dating to loess deposits: a perspective on the past, present and future. Boreas 37, 483–507.

Rousseau, D.D., Derbyshire, E., Antoine, P., Hatté, C., 2007. LOESS RECORDS | Europe, in: Elias, S.A. (Ed.), Encyclopedia of Quaternary Science. Elsevier, pp. 1440–1456.

Ruske, R., 1961. Gliederung des Pleistozäns im Geiseltal und in seiner Umgebung. Geologie , 152–168.

Schatz, A.K., Buylaert, J.P., Murray, A., Stevens, T., Scholten, T., 2012. Establishing a luminescence chronology for a palaeosol-loess profile at Tokaj (Hungary): a comparison of quartz OSL and polymineral IRSL signals. Quaternary Geochronology 10, 68–74.

Schmidt, E.D., Frechen, M., Murray, A.S., Tsukamoto, S., Bittmann, F., 2011. Luminescence chronology of the loess record from the Tönchesberg section: A comparison of using quartz and feldspar as dosimeter to extend the age range beyond the Eemian. Quaternary International 234, 10–22.

Schön, M., 1942. Zum Leuchtmechanismus der Kristallphosphore. Zeitschrift für Physik 119, 463–471.

Shackleton, N., 2003. Marine Isotope Substage 5e and the Eemian Interglacial. Global and Planetary Change 36, 151–155.

Singarayer, J.S., 2002. Linearly modulated optically stimulated luminescence of sedimentary quartz: physical mechanisms and implications for dating. Ph.D. thesis. University of Oxford.

Singarayer, J.S., Bailey, R.M., 2003. Further investigations of the quartz optically stimulated luminescence components using linear modulation. Radiation Measurements 37, 451–458.

Smalley, I., Vita-Finzi, C., 1968. The formation of fine particles in sandy deserts and the nature of 'desert' loess. Journal of Sedimentary Petrology 38, 766–774.

Smith, B.W., Rhodes, E.J., 1994. Charge movements in quartz and their relevance to optical dating. Radiation Measurements 23, 239–333.

Stöcker, H., 2010. Taschenbuch der Physik. Formeln, Tabellen, Übersichten. 6th ed., Harri Deutsch Verlag.

Stokes, S., 1999. Luminescence dating applications in geomorphological research. Geomorphology 29, 153–171.

Stolz, W., 2005. Radioaktivität: Grundlagen - Messung - Anwendungen. Radioaktivität: Grundlagen - Messung - Anwendungen. 5th ed., Vieweg+Teubner.

Syers, J.K., Chapman, S.L., Jackson, M.L., 1968. Quartz isolation from rocks, sediments and soils for dtermination of oxygen isotopes composition. Geochimica et Cosmochimica Acta 32, 1022–1025.

Thiel, C., Buylaert, J.P., Murray, A., Terhorst, B., Hofer, I., Tsukamoto, S., Frechen, M., 2011a. Luminescence dating of the Stratzing loess profile (Austria) - Testing the potential of an elevated temperature post-IR IRSL protocol. Quaternary International 234, 23–31.

Thiel, C., Buylaert, J.P., Murray, A.S., Terhorst, B., Tsukamoto, S., Frechen, M., Sprafke, T., 2011b. Investigating the chronostratigraphy of prominent palaeosols in Lower Austria using post-IR IRSL dating. E & G, Quaternary Science Journal 60, 137–152.

Thomsen, K.J., Murray, A.S., Jain, M., Bøtter-Jensen, L., 2008. Laboratory fading rates of various luminescence signals from feldspar-rich sediment extracts. Radiation Measurements 43, 1474–1486.

Timar, A., Vandenberghe, D., Panaiotu, E.C., Panaiotu, C.G., Necula, C., Cosma, C., van den haute, P., 2010. Optical dating of Romanian loess using fine-grained quartz. Quaternary Geochronology 5, 143–148.

Timar-Gabor, A., Vandenberghe, D.A.G., Vasiliniuc, S., Panaoitu, C.E., Panaiotu, C.G., Dimofte, D., Cosma, C., 2011. Optical dating of Romanian loess: A comparison between silt-sized and sand-sized quartz. Quaternary International 240, 62–70.

Timar-Gabor, A., Vasiliniuc, S., Vandenberghe, D.A.G., Cosma, C., Wintle, A.G., 2012. Investigations into the reliability of SAR-OSL equivalent doses obtained for quartz samples displaying dose response curves with more than one component. Radiation Measurements 10, 75–80.

Trautmann, T., Krbetschek, M.R., Dietrich, A., Stolz, W., 1999. Feldspar radioluminescence: a new dating method and its physical background. Journal of Luminescence 85, 45–58.

Tribolo, C., Mercier, N., Valladas, H., 2001. Alpha sensitivity determination in quartzite using an OSL single aliquot procedure. Ancient TL 19, 47.

Urbach, F., 1930. Zur Lumineszenz der Alkalihalogenide II. Messungsmethoden; erste Ergebnisse; zur Theorie der Thermolumineszenz. Sitzungsberichte der Akademie der Wissenschaften in Wien, Mathematisch-Naturwissenschaftliche Klasse, Abt. IIa, Mathematik, Astronomie, Physik, Meteorologie und Technik 139, 363–372.

Vandenberghe, D., De Corte, F., Buylaert, J.P., Kučera, J., van den haute, P., 2008. On the internal radioactivity in quartz. Radiation Measurements 43, 771–775.

Vasiliniuc, S., Vandenberghe, D.A.G., Timar-Gabor, A., Panaiotu, C., Cosma, C., van den haute, P., 2012. Testing the potential of elevated temperature post-IR IRSL signals for dating Romanian loess. Quaternary Geochronology 10, 75–80.

Visocekas, R., 1985. Tunnelling Radiative Recombination in Labradorite: Its Association With Anomalous Fading Of Thermoluminescence. Nuclear Tracks And Radiation Measurements 10, 521–529.

Wang, X., Miao, X., 2006. Weathering history indicated by the luminescence emissions in Chinese loess and paleosol. Quaternary Science Reviews 25, 1719–1726.

Weeks, R.A., 1956. Paramagnetic Resonance of Lattice Defects in Irradiated Quartz. Journal of Applied Physics 27, 1376–1381.

Wintle, A.G., 1973. Anomalous Fading of Thermoluminescence in Mineral Samples. Nature 245, 143–144.

Wintle, A.G., 1980. Thermoluminescence dating: a review of recent applications to non-pottery materials. Archaeometry 22, 113–122.

Wintle, A.G., 1990. A review of current research on TL dating of loess. Quaternary Science Reviews 9, 385–397.

Wintle, A.G., 2008a. Fifty years of luminescence dating. Archaeometry 50, 276–312.

Wintle, A.G., 2008b. Luminescence dating: where it has been and where it is going. Boreas 37, 471–482.

Wintle, A.G., 2010. Future Directions of Luminescence Dating of Quartz. Geochronometria 37, 1–7.

Wintle, A.G., Murray, A.S., 2006. A review of quartz optically stimulated luminescence characteristics and their relevance in single-aliquot regeneration dating protocols. Radiation Measurements 41, 369–391.

Woda, C., Fuchs, M., 2008. On the applicability of the leading edge method to obtain equivalent doses in OSL dating and dosimetry. Radiation Measurements 43, 26–37.

Wright, J.S., 2001. Desert loess versus glacial loess: quartz silt formation, source areas and sediment pathways in the formation of loess deposits. Geomorphology 36, 231–256.

Yukihara, E.G., McKeever, S.W.S., 2011. Optically Stimulated Luminescence. Optically Stimulated Luminescence, Wiley.

Zech, M., Kreutzer, S., Goslar, T., Meszner, S., Krause, T., Faust, D., Fuchs, M., 2012. Technical Note: *n*-Alkane lipid biomarkers in loess: post-sedimentary or syn-sedimentary? Biogeosciences Discussions 9, 9875–9896.

Zimmerman, D.W., 1971. Thermoluminescent dating using fine grains from pottery. Archaeometry 13, 29–52.

Zimmerman, D.W., 1972. Relative thermoluminescence effects of alpha- and beta-radiation. Radiation Effects 14, 81–92.

Zöller, L., 2010. New approaches to European loess: a stratigraphic and methodical review of the past decade. Central European Journal of Geosciences 2, 19–31.

Zöller, L., Oches, E.A., McCoy, W.D., 1994. Towards a revised chronostratigraphy of loess in Austria with respect to key sections in the Czech Republic and in Hungary. Quaternary Geochronology 13, 465–472.

Zöller, L., Pernicka, E., 1989. A note on overcounting in alpha-counters and its elimination. Ancient TL 7, 11–14.

Zöller, L., Semmel, A., 2001. 175 years of loess research in Germany - long records and "unconformities". Earth-Science Reviews 54, 19–28.

2 Study I

OSL chronostratigraphy of a loess-palaeosol sequence in Saxony/Germany using quartz of different grain sizes

Sebastian Kreutzer[1,2,*], Markus Fuchs[1], Sascha Meszner[3], Dominik Faust[3]

[1]Department of Geography, Justus-Liebig-University Giessen, 35390 Giessen, Germany
[2]Geographical Institute, University of Bayreuth, 95440 Bayreuth, Germany
[3]Institute of Geography, Dresden University of Technology, 01062 Dresden, Germany

[*]corresponding author: sebastian.kreutzer@geogr.uni-giessen.de

Quaternary Geochronology
Year: 2012, Volume: 10, Pages: 102–109
- published -
http://dx.doi.org/10.1016/j.quageo.2012.01.004

Contributions to the manuscript

	SK	MF	SM	DF	MFi	DR
Sampling	50 %	-	50 %	-	-	-
Sample pre-treatment	90 %	-	-	-	10 %	-
OSL Measurement	95 %	-	-	-	5 %	-
Dosimetry BT (including preparation)	40 %	-	-	-	60 %	-
Manuscript preparation	100 %	-	-	-	-	-
Comments to improve the manuscript	-	80 %	5 %	5 %	5 %	5 %

If not stated otherwise abbreviations are the initials from the authors.
MFi: Manfred Fischer (technician luminescence laboratory Bayreuth)
DR: PD Dr. Daniel Richter (researcher luminescence laboratory Bayreuth)

Abstract

Luminescence dating is one of the leading techniques to establish chronologies for loess-palaeosol sequences and has been successfully applied to different minerals and grain size fractions. Using optical stimulated luminescence (OSL) from quartz, we present for the first time a high resolution chronology for the loess section Ostrau in Saxony/Germany. We compare OSL ages derived from two different grain size fractions, coarse (90–200 µm) and the fine grain (4–11 µm) separates. Our results show that the loess section is divided into two parts, separated by a hiatus. OSL samples from the upper part of the loess section show equivalent doses of $D_e < 100$ Gy. D_e values > 180 Gy are observed for the lower part of the loess section. The coarse and fine grain ages agree and also fit to the litho- and pedostratigraphy for the upper part of the profile. For the lower part of the profile the coarse grained quartz OSL is in saturation. The fine grained quartz OSL is not saturated but it appears that the fine grain OSL ages underestimate the sedimentation age. Approaches to explain the D_e differences between the grain size fractions are presented (e.g. post-depositional translocation, dosimetry). A modified SAR protocol for the fine grain fraction produced ages that are in good agreement with expected ages based on litho- and pedostratigraphy. Although further investigations are needed, our results show the suitability of the Saxonian loess belt for OSL dating.

3 Study II

Chronology of the Quaternary profile Zeuchfeld in Saxony-Anhalt / Germany - a preliminary luminescence dating study

Sebastian Kreutzer[1,2,*], Tobias Lauer[3], Sascha Meszner[4], Matthias Krbetschek[5], Dominik Faust[4], Markus Fuchs[1],

[1]Department of Geography, Justus-Liebig-University Giessen, 35390 Giessen, Germany
[2]Geographical Institute, University of Bayreuth, 95440 Bayreuth, Germany
[3]Institute of Geography, Johannisallee 19a, 04103 Leipzig, Germany
[4]Institute of Geography, Dresden University of Technology, 01062 Dresden, Germany
[5]Senckenberg Ges. f. Naturforschung Frankfurt/M., Museum f. Mineralogie und Geologie Dresden, Sektion Lumineszenz / Inst. f. Angew. Physik TU Freiberg, Leipziger Str. 23, 09596 Freiberg, Germany

*corresponding author: sebastian.kreutzer@geogr.uni-giessen.de

Zeitschrift für Geomorphologie
Year: 2014, Volume: 58, Suppl. 1, Pages: 5–26
- published -
http://dx.doi.org/10.1127/0372-8854/2012/S-00112

Contributions to the manuscript

	SK	TL	SM	MK	DF	MF
Profile stratigraphy	-	10 %	80 %	-	10 %	-
Sampling	-	100 %	-	-	-	-
Sample pre-treatment	40 %	60 %	-	-	-	-
OSL measurement	75 %	25 %	-	-	- %	-
RF measurement	-	75 %	-	25 %	-	-
Manuscript preparation	80 %	15 %	5 %	-	-	-
Comments to improve the manuscript	-	5 %	20 %	10 %	5 %	60 %

If not stated otherwise abbreviations are the initials from the authors.

Abstract

Climatic signals are considered as well preserved in loess records. To assess their significance in a local and global context a reliable numerical chronology is needed. Luminescence dating provides an established dating method on natural mineral grains of quartz and feldspar by measuring the last time of the daylight exposure. For the field trip of the 37th meeting of the German working group on geomorphology to the Saxony-Anhalt loess belt, the upper part of the Quaternary profile Zeuchfeld has been reinvestigated. The profile is well known for its sandur (Zeuchfeld Sandur) situated at the base of the profile, assumed to be of Late Saalian age (MIS 6). Here, OSL quartz age estimates for the overlying loess deposits from the last glacial-interglacial cycle are reported. Furthermore, the underlying sandur has been sampled for conventional SAR dating on quartz and IR-RF dating on potassium rich feldspar. The OSL age estimates have been determined for three commonly used quartz grain size fractions (coarse, middle and fine grain). The results suggest at least two phases of loess deposition and preservation around 70 ka and 30 ka to 22 ka confirmed by previous assumptions based on field work and recent pedo- and lithostratigraphic correlation. In contrast, the quartz SAR and the IR-RF measurements from the underlying sandur yield a substantially older (pre-Saalian) age. The reasons for the assumed age overestimation and the details of the luminescence dating results are presented and discussed.

4 Study III

Introducing an R package for luminescence dating analysis

Sebastian Kreutzer[1,2,*], Christoph Schmidt[3], Margret C. Fuchs[4], Michael Dietze[5], Manfred Fischer[2], Markus Fuchs[1]

[1]Department of Geography, Justus-Liebig-University Giessen, 35390 Giessen, Germany
[2]Geographical Institute, University of Bayreuth, 95440 Bayreuth, Germany
[3]Institute for Geography, University of Cologne, 50923 Cologne, Germany
[4]Department of Geology, TU Bergakademie Freiberg, 09599 Freiberg, Germany
[5]Institute of Geography, TU Dresden, 01069 Dresden, Germany

*corresponding author: sebastian.kreutzer@geogr.uni-giessen.de

Ancient TL
Year: 2012, Volume: 30(1), Pages: 1–8
- published -
http://www.aber.ac.uk/en/media/departmental/iges/ancienttl/pdf/vol30no1/ATL---Kreutzer.pdf

Contributions to the manuscript

	SK	CS	MCF	MD	MFi	MF
R-Coding (Package)	90 %	-	5 %	5 %	-	-
Package manual	80 %	-	10 %	10 %	-	-
Manuscript preparation	55 %	15 %	10 %	10 %	5 %	5 %

If not stated otherwise abbreviations are the initials from the authors.

Abstract

For routine luminescence dating applications the commonly used Risø readers are bundled with analysis software, such as *Viewer* or *Analyst*. These software solutions are appropriate for most of the regular dating and publication jobs, and enable assessment of luminescence characteristics and provide basic statistical data treatment. However, for further statistical analysis and data treatments, this software may reach its limits. In such cases, open programming languages are a more appropriate approach. Here, we present the **R** package 'Luminescence' for a more flexible handling of luminescence data and related plotting purposes, using the statistical programming language **R**. The **R** language as well as the package and the source code are provided under the General Public License (GPL) conditions and are available for free. The basic functionality of the package is described along with three application examples.

This package is not an alternative to the existing software (*Analyst*, *Viewer*) but may provide a collection of additional tools to analyse luminescence data and serve as a platform for further contributions.

5 Study IV

Quantification of cross-bleaching during infrared (IR) light stimulation

Sebastian Kreutzer[1,2,*], Daniela Hülle[3], Kristina Jørkov Thomsen[4], Alexandra Hilgers[5], Annette Kadereit[4], Markus Fuchs[1],

[1]Department of Geography, Justus-Liebig-University Giessen, 35390 Giessen, Germany
[2]Geographical Institute, Geomorphology, University of Bayreuth, 95440 Bayreuth, Germany
[3]Institute of Geography, University of Cologne, 50923 Cologne, Germany
[4]Center for Nuclear Technologies, Technical University of Denmark, Risø Campus, DK-4000 Roskilde, Denmark
[5]Heidelberger Lumineszenzlabor, Geographisches Institut der Universität Heidelberg, Im Neuenheimer Feld 348, 69120 Heidelberg, Germany

*corresponding author: sebastian.kreutzer@geogr.uni-giessen.de

Ancient TL
Year: 2013, Volume: 31 (1), Pages: 1–10
- published -
http://www.aber.ac.uk/en/media/departmental/iges/ancienttl/pdf/vol31no1/kreutzer_atl31(1)_1.pdf

Contributions to the manuscript

	SK	DH	KJT	AH	AK	MF
CB analytics	60 %	10 %	20 %	-	10 %	-
CB measurements	40 %	20 %	20 %	5 %	5 %	-
Manuscript preparation	80 %	10 %	10 %	-	-	-
Comments to improve the manuscript	-	20 %	50 %	10 %	5 %	15 %

If not stated otherwise abbreviations are the initials from the authors.

Abstract

The cross-bleaching behaviour of automated Risø TL/OSL (DA-12, DA-15, DA-20) luminescence readers is investigated. By design, up to 24 or 48 aliquots can be stored on a carousel in a single measurement chamber. Due to this construction, irradiation or illumination on one sample may affect the adjacent position resulting in systematic errors. Such cross-talk (cross-bleaching/illumination) has never been quantified explicitly for the infrared (IR) LEDs, although they are intensively used in IRSL measurements of e.g. feldspar and polymineral samples. In IRSL measurements of feldspar or polymineral samples it is important to keep the time constant between the (midpoint of the) irradiation and the subsequent read out to avoid the malign effects of anomalous fading in laboratory constructed dose response curves. This may be achieved by running all measurements for a regular equivalent dose estimation on a single sample before moving to a subsequent sample (e.g. by using the 'run 1 at the time' option in the Risø sequence editor). However, if the measurement sequence is not designed carefully, then using this option may result in a significant depletion of the natural signal on subsequent samples. Here we investigate the size of this reduction due to cross-bleaching from the IR diodes and quantify the cross-bleaching for 10 different Risø TL/OSL readers produced between 1994 and 2011. We find that cross-bleaching from the IR diodes is worse than from the blue diodes. Using the 'run 1 at the time' option can result in significant dose underestimation (1) if the sequence is not split into different sets (2) or if samples are not placed on every 2^{nd} position. In addition, a newly designed flange for the optical unit of the TL/OSL reader is presented which appears to reduce cross-bleaching significantly.

6 Study V

The *a*-value of polymineral fine grain samples measured with the post-IR IRSL protocol

Sebastian Kreutzer[1,2,*], Christoph Schmidt[3],
Regina DeWitt[4], Markus Fuchs[1]

[1]Department of Geography, Justus-Liebig-University Giessen, 35390 Giessen, Germany
[2]Geographical Institute, Geomorphology, University of Bayreuth, 95440 Bayreuth, Germany
[3]Institute of Geography, University of Cologne, 50923 Cologne, Germany
[4]Department of Physics, East Carolina University, NC 27858 Greenville, USA, Denmark

*corresponding author: sebastian.kreutzer@geogr.uni-giessen.de

Radiation Measurements
Year: 2014, Volume: 69, Pages: 18–29
- published -
http://dx.doi.org/10.1016/j.radmeas.2014.04.027

Contributions to the manuscript

	SK	CS	RD	MF
a-value measurements	100 %	-	-	-
a-value analytics	80 %	10 %	10 %	-
Manuscript preparation	100 %	-	-	-
Comments to improve the manuscript	-	30 %	50 %	20 %

If not stated otherwise abbreviations are the initials from the authors.

Abstract

Recent post-IR IRSL (pIRIR) dating studies using polymineral fine grains assumed that the *a*-values obtained for the IRSL signal at 50 °C and the pIRIR signal at higher temperatures (e.g., 225 °C) are identical. However, the *a*-value of a sample depends on the stimulation method, and the assumption mentioned above remains to be tested. Using five polymineral fine grain samples, this study investigates whether a common *a*-value can be used for both the IR and the pIRIR signals. Applying the pIRIR protocol, the *a*-values were measured with three different methods of signal resetting (optical bleaching, end of SAR cycle, heating). In addition, uncorrected α- and β-irradiation induced growth curves were determined for three samples and fitted with single saturating exponential functions. For the investigated samples we found significant mean differences, 0.023 ± 0.012 and higher, in the *a*-values determined for the IR_{50} and $pIRIR_{225}$ signals. Synthetic *a*-values deduced from uncorrected multiple-aliquot dose response curves seem to confirm this observation. Although, in summary, our results indicate that the practice of using a common *a*-value should be carefully re-considered, the physical reasons remain to be determined.

7 Study VI

Late Pleistocene landscape dynamics in Saxony, Germany: Paleoenvironmental reconstruction using loess-paleosol sequences

Sascha Meszner[1,*], Sebastian Kreutzer[2,3],
Markus Fuchs[2], Dominik Faust[1]

[1]Department of Geography, Dresden University of Technology, Helmholtzstr. 10, 01062 Dresden, Germany
[2]Department of Geography, Justus-Liebig-University Giessen, 35390 Giessen, Germany
[3]Geographical Institute, Geomorphology, University of Bayreuth, 95440 Bayreuth, Germany

*corresponding author: sascha.meszner@tu-dresden.de

Quaternary International
Year: 2013, Volume: 296, Pages: 96–107
- published -
http://dx.doi.org/10.1016/j.quaint.2012.12.040

Contributions to the manuscript

	SM	SK	MF	DF	MH
Stratigraphy	90 %	-	-	10 %	-
OSL sampling	50 %	50 %	-	-	-
OSL dating	-	90 %	-	-	10 %
Manuscript preparation	70 %	30 %	-	-	-
Comments to improve the manuscript	-	25 %	40 %	35 %	-

If not stated otherwise abbreviations are the initials from the authors.
MH: Michaela Hoffer (graduate student) did sample preparation during her bachelor thesis

Abstract

Loess archives are of paramount importance for reconstructing regional paleoenvironmental conditions of past glacial periods. The Saxonian Loess Region is an area of transition between the western and the eastern European loess belt. With this contribution, a documented loess-paleosol composite profile for the Saxonian Loess Region is extended, and a new chronostratigraphy, established by high-resolution OSL dating of two profiles, is described. In addition, for the first time OSL age estimates for the loess paleosol sequence at Seilitz are presented for the quartz and polymineral fine grain fraction. Based on the presented composite profile climatic and environmental conditions (e.g. wind speed, temperature) are deduced. Based on high-resolution OSL dating it is possible to identify a hiatus spanning c. 30 ka. This gap is located in the Gleina Complex where an underlying layer shows an age of c. 60 ka and the upper layer an age of c. 30 ka. Additionally, two periods of strong loess accumulation with ages of c. 70–60 ka and 30–18 ka could be identified. There is a general trend of grain size coarsening-up towards the Late Glacial which shows a maximum at c. 21 ka. Correlations with French, western German and Polish loess sections are discussed.

8 Study VII

The loess sequence of Dolní Věstonice, Czech Republic: A new OSL based chronology of the Last Climatic Cycle

Markus Fuchs[1,*], Sebastian Kreutzer[1,2], Denis Rousseau[3], Pierre Antoine[4], Christine Hatté[5], France Lagroix[6], Olivier Moine[5], Caroline Gauthier[7], Jiri Svoboda[8] Lenka Lisa[9]

[1]Department of Geography, Justus-Liebig-University Giessen, 35390 Giessen, Germany
[2]Geographical Institute, University of Bayreuth, 95440 Bayreuth, Germany
[3]UMR CNRS, Ecole Normale Supérieure de Paris, Laboratoire de Météorologie Dynamique, France
[4]UMR CNRS, Laboratoire de Géographie Physique, France
[5]UMR 1572 CEA/CNRS, Laboratoire des Sciences du Climat et de l'Environnement, France
[6]University of Paris Diderot, Institut de Physique du Globe de Paris, France
[7]UMR 1572 CEA/CNRS, Laboratoire des Sciences du Climat et de l'Environnement, France
[8]Masaryk University, Faculty of Science, Czech Republic
[9]Academy of Sciences, Institute of Geology, Czech Republic

*corresponding author: markus.fuchs@geogr.uni-giessen.de

Boreas
Year: 2013, Volume: 42 (3,) Pages: 664–667
- published -
http://dx.doi.org/10.1111/j.1502-3885.2012.00299.x

Contributions to the manuscript

	MF	SK	other co-authors	others
Stratigraphy	-	-	100 %	-
OSL sampling	50 %	25 %	25 %	-
OSL dating	15 %	85 %	-	-
Manuscript preparation	80 %	5 %	15 %	-
Comments to improve the manuscript	-	10 %	90 %	-

If not stated otherwise abbreviations are the initials from the authors.

Abstract

The Dolní Věstonice loess section in the Czech Republic is well known for its high-resolution loess–palaeosol sequence of the last interglacial–glacial climatic cycle (Upper Pleistocene). The loess section is situated in a climatic transition zone between oceanic and continental climates and is therefore of great value in reconstructing past regional climate conditions and their interaction with climate systems, in particular that of the North Atlantic. Based on a combination of optically stimulated luminescence (OSL) ages, stratigraphic field observations and magnetic susceptibility measurements, a chrono-climatic interpretation of the Dolní Věstonice loess section is presented. To establish a reliable Upper Pleistocene chronology, a quartz OSL approach was applied for equivalent dose (D_e) determination. Monomineralic quartz extracts of three distinct grain sizes, fine (4–11 µm), middle (38–63 µm) and coarse (90–200 µm), were used and compared. Within error limits, the calculated OSL ages are the same for the different grain sizes, and the OSL ages are in stratigraphic order. The established OSL chronology is in agreement with a Weichselian litho- and pedostratigraphy. The Dolní Věstonice loess section is characterized by four pedosedimentary subsequences. At the base of the profile, subsequence I is characterized by a distinct Early Glacial soil complex, OSL-dated to c. 110 ka to 70 ka, representing one of the most complete records of environmental change in the European loess belt. Subsequence II is allocated to the Lower Pleniglacial and is characterized by laminated sandy loess. Middle Pleniglacial subsequence III is represented by a brown soil complex, and is followed by the uppermost subsequence IV, characterized by a thick body of laminated sandy loess, indicating strong wind activity and a high sedimentation rate of more than $\sim$1 mm a^{-1} during the Upper Pleniglacial. According to the OSL chronology, as well as to the sedimentological and palaeopedological investigations, it is likely that the sequence at Dolní Věstonice has recorded most of the climatic events expressed in the NGRIP $\delta^{18}O$ reference record between 110 ka and 70 ka.

Appendix - Contents

A Additional tables

A.1 Complete list of luminescence ages

#	ID	Profile	M	Grain Size [µm]	Signal	n	Fit	D_e [Gy]	$\dot{D}_{total}$ [Gy ka^{-1}]	Age [ka]	Reference
1	**BT594**	Seilitz	Q	90–200	BOSL	17/24	EXP	64.81 ± 3.83	2.92 ± 0.16	22.2 ± 3.5	Meszner et al. (2013)
2			Q	4–11	BOSL	12/12	EXP	79.69 ± 1.10	3.58 ± 0.24	22.3 ± 3.0	Meszner et al. (2013)
3	**BT607**	Ostrau	Q	90–200	BOSL	16/24	EXP	54.1 ± 7.0	3.19 ± 0.19	17.0 ± 3.0	Kreutzer et al. (2012)
4			Q	38–63	BOSL	24/24	EXP	57.98 ± 2.05	3.13 ± 0.18	18.5 ± 2.4	unpublished
5			Q	4–11	BOSL	12/12	EXP	54.3 ± 3.8	3.59 ± 0.30	15.1 ± 2.8	Kreutzer et al. (2012)
6			Q	4–11	BOSL[1]	12/12	EXP	64.7 ± 2.4	3.59 ± 0.30	18.0 ± 3.0	Kreutzer et al. (2012)
7	**BT608**	Ostrau	Q	90–200	BOSL	16/24	EXP	51.5 ± 5.4	2.99 ± 0.17	17.3 ± 2.6	Kreutzer et al. (2012)
8			Q	38–63	BOSL	24/24	EXP	61.91 ± 1.51	3.07 ± 0.17	20.2 ± 2.5	unpublished
9			Q	4–11	BOSL	12/12	EXP	61.5 ± 2.4	3.51 ± 0.23	17.5 ± 2.4	Kreutzer et al. (2012)
10			Q	4–11	BOSL[1]	12/12	EXP	68.9 ± 2.4	3.51 ± 0.23	19.7 ± 2.6	Kreutzer et al. (2012)
11	**BT609**	Ostrau	Q	90–200	BOSL	20/24	EXP	45.8 ± 3.2	2.86 ± 0.17	16.0 ± 2.2	Kreutzer et al. (2012)
12			Q	38–63	BOSL	23/24	EXP	63.00 ± 1.83	2.94 ± 0.17	21.4 ± 2.8	unpublished
13			Q	4–11	BOSL	12/12	EXP	64.7 ± 0.8	3.34 ± 0.23	19.4 ± 2.6	Kreutzer et al. (2012)
14			Q	4–11	BOSL[1]	12/12	EXP	71.6 ± 1.6	3.34 ± 0.23	21.4 ± 3.0	Kreutzer et al. (2012)
15	**BT610**	Ostrau	Q	90–200	BOSL	17/20	EXP	51.8 ± 4.8	2.74 ± 0.17	18.9 ± 2.8	Kreutzer et al. (2012)
16			Q	38–63	BOSL	20/24	EXP	66.35 ± 2.41	2.82 ± 0.17	23.5 ± 3.4	unpublished
17			Q	4–11	BOSL	11/12	EXP	65.6 ± 2.2	3.21 ± 0.22	20.4 ± 2.8	Kreutzer et al. (2012)
18	**BT611**	Ostrau	Q	90–200	BOSL	17/24	EXP	51.4 ± 6.0	2.75 ± 0.16	18.7 ± 3.0	Kreutzer et al. (2012)
19			Q	38–63	BOSL	17/18	EXP	71.19 ± 2.54	2.82 ± 0.16	25.2 ± 3.4	unpublished
20			Q	4–11	BOSL	23/24	EXP	75.3 ± 1.8	3.21 ± 0.23	23.4 ± 3.2	Kreutzer et al. (2012)
21	**BT612**	Ostrau	Q	90–200	BOSL	20/24	EXP	60.9 ± 10.8	2.80 ± 0.16	21.7 ± 4.6	Kreutzer et al. (2012)
22			Q	38–63	BOSL	22/24	EXP	76.05 ± 3.08	2.88 ± 0.17	26.4 ± 3.8	unpublished
23			Q	4–11	BOSL	12/12	EXP	78.4 ± 3.4	3.30 ± 0.22	23.7 ± 3.4	Kreutzer et al. (2012)
24	**BT613**	Ostrau	Q	90–200	BOSL	12/24	EXP	54.8 ± 7.4	2.71 ± 0.16	20.2 ± 3.6	Kreutzer et al. (2012)
25			Q	38–63	BOSL	22/24	EXP	69.62 ± 2.00	2.79 ± 0.16	25.0 ± 3.2	unpublished
26			Q	4–11	BOSL	12/12	EXP	70.6 ± 2.0	3.16 ± 0.21	22.3 ± 3.0	Kreutzer et al. (2012)
27	**BT614**	Ostrau	Q	90–200	BOSL	20/24	EXP	58.2 ± 7.8	2.72 ± 0.16	21.4 ± 3.8	Kreutzer et al. (2012)
28			Q	38–63	BOSL	23/24	EXP	85.97 ± 2.31	2.80 ± 0.16	30.8 ± 4.0	unpublished
29			Q	4–11	BOSL	12/12	EXP	80.8 ± 1.4	3.21 ± 0.21	25.1 ± 3.4	Kreutzer et al. (2012)
30	**BT615**	Ostrau	Q	90–200	BOSL	15/24	EXP	65.5 ± 12.6	2.66 ± 0.16	24.6 ± 5.6	Kreutzer et al. (2012)
31			Q	38–63	BOSL	14/15	EXP	81.74 ± 3.00	2.74 ± 0.16	29.8 ± 4.1	unpublished
32			Q	4–11	BOSL	12/12	EXP	83.8 ± 2.0	3.16 ± 0.21	26.5 ± 3.6	Kreutzer et al. (2012)
33	**BT616**	Ostrau	Q	90–200	BOSL	14/24	EXP	67.6 ± 10.4	2.67 ± 0.16	25.3 ± 5.0	Kreutzer et al. (2012)
34			Q	38–63	BOSL	21/24	EXP	90.52 ± 3.49	2.75 ± 0.16	32.9 ± 4.6	unpublished
35			Q	4–11	BOSL	12/12	EXP	81.8 ± 3.0	3.18 ± 0.21	25.7 ± 3.6	Kreutzer et al. (2012)
36	**BT617**	Ostrau	Q	90–200	BOSL	9/24	EXP+LIN	244.5 ± 60.0	2.51 ± 0.15	97.3 ± 26.6	Kreutzer et al. (2012)
37			Q	4–11	BOSL	10/12	EXP+LIN	329.6 ± 3.0	2.95 ± 0.20	111.7 ± 15.4	Kreutzer et al. (2012)

#	ID	Profile	M	Grain Size [µm]	Signal	n	Fit	D_e [Gy]	$\dot{D}_{total}$ [Gy ka^{-1}]	Age [ka]	Reference
38			Q	4–11	BOSL[1]	12/12	EXP+LIN	431.5 ± 6.6	2.95 ± 0.20	146.2 ± 20.2	Kreutzer et al. (2012)
39	**BT618**	Ostrau	Q	90–200	BOSL	4/24	EXP	235.5 ± 100.0	2.57 ± 0.16	91.8 ± 40.6	Kreutzer et al. (2012)
40			Q	4–11	BOSL	12/12	EXP	246.7 ± 6.6	3.07 ± 0.21	80.3 ± 11.0	Kreutzer et al. (2012)
41			Q	4–11	BOSL[1]	12/12	EXP+LIN	366.9 ± 5.0	3.07 ± 0.21	119.4 ± 16.0	Kreutzer et al. (2012)
42	**BT619**	Ostrau	Q	90–200	BOSL	13/24	EXP+LIN	273.6 ± 47.2	2.61 ± 0.16	104.8 ± 22.2	Kreutzer et al. (2012)
43			Q	4–11	BOSL	12/12	EXP	233.6 ± 4.4	3.15 ± 0.21	74.2 ± 10.0	Kreutzer et al. (2012)
44			Q	4–11	BOSL[1]	12/12	EXP+LIN	337.2 ± 8.6	3.15 ± 0.21	107.2 ± 14.6	Kreutzer et al. (2012)
45	**BT620**	Ostrau	Q	90–200	BOSL	17/24	EXP+LIN	288.0 ± 60.6	2.82 ± 0.17	102.0 ± 24.6	Kreutzer et al. (2012)
46			Q	4–11	BOSL	12/12	EXP+LIN	318.3 ± 7.6	3.35 ± 0.23	95.0 ± 13.0	Kreutzer et al. (2012)
47	**BT621**	Ostrau	Q	90–200	BOSL	13/24	EXP+LIN	208.1 ± 62.6	2.69 ± 0.16	77.4 ± 25.2	Kreutzer et al. (2012)
48			Q	38–63	BOSL	22/24	EXP	203.70 ± 7.72	2.76 ± 0.16	73.7 ± 10.4	unpublished
49			Q	4–11	BOSL	12/12	EXP	180.1 ± 6.0	3.15 ± 0.22	57.1 ± 8.0	Kreutzer et al. (2012)
50			Q	4–11	BOSL[1]	12/12	EXP+LIN	230.2 ± 25.6	3.15 ± 0.22	73.0 ± 13.0	Kreutzer et al. (2012)
51	**BT622**	Ostrau	Q	90–200	BOSL	4/24	EXP+LIN	77.9 ± 16.6	2.86 ± 0.17	27.3 ± 6.6	Kreutzer et al. (2012)
52			Q	38–63	BOSL	24/24	EXP	111.30 ± 3.85	2.94 ± 0.18	37.9 ± 4.2	unpublished
53			Q	4–11	BOSL	11/12	EXP	103.0 ± 1.6	3.40 ± 0.23	30.3 ± 4.2	Kreutzer et al. (2012)
54	**BT623**	Ostrau	Q	90–200	BOSL	8/24	EXP+LIN	296.0 ± 40.6	2.68 ± 0.16	110.6 ± 20.2	Kreutzer et al. (2012)
55			Q	4–11	BOSL	12/12	EXP	250.5 ± 2.8	3.20 ± 0.22	78.3 ± 10.6	Kreutzer et al. (2012)
56			Q	4–11	BOSL[1]	12/12	EXP+LIN	340.1 ± 4.6	3.20 ± 0.22	106.3 ± 14.4	Kreutzer et al. (2012)
57	**BT624**	Ostrau	Q	90–200	BOSL	17/24	EXP	79.5 ± 18.0	2.82 ± 0.17	28.2 ± 7.2	Kreutzer et al. (2012)
58			Q	38–63	BOSL	24/24	EXP	97.10 ± 3.27	2.90 ± 0.17	33.5 ± 4.5	unpublished
59			Q	4–11	BOSL	11/12	EXP	96.0 ± 1.6	3.30 ± 0.23	29.1 ± 4.0	Kreutzer et al. (2012)
60	**BT625**	Ostrau	Q	90–200	BOSL	19/24	EXP	78.7 ± 14.4	2.75 ± 0.16	28.6 ± 6.2	Kreutzer et al. (2012)
61			Q	38–63	BOSL	24/24	EXP	85.80 ± 2.59	2.83 ± 0.17	30.3 ± 4.0	unpublished
62			Q	4–11	BOSL	11/12	EXP	87.1 ± 1.8	3.24 ± 0.22	26.9 ± 3.6	Kreutzer et al. (2012)
63	**BT626**	Ostrau	Q	90–200	BOSL	18/24	EXP	62.2 ± 8.8	2.66 ± 0.16	23.4 ± 4.4	Kreutzer et al. (2012)
64			Q	38–63	BOSL	24/24	EXP	82.11 ± 2.60	2.73 ± 0.16	30.0 ± 2.0	unpublished
65			Q	4–11	BOSL	11/12	EXP	88.3 ± 3.4	3.16 ± 0.21	28.0 ± 3.8	Kreutzer et al. (2012)
66	**BT706**	Seilitz	Q	4–11	BOSL	24/24	EXP+LIN	66.07 ± 1.75	3.62 ± 0.23	18.3 ± 2.5	Meszner et al. (2013)
67	**BT707**	Seilitz	Q	90–200	BOSL	14/24	EXP	56.02 ± 3.16	3.05 ± 0.17	18.6 ± 2.9	Meszner et al. (2013)
68			Q	4–11	BOSL	11/12	EXP+LIN	64.20 ± 0.74	3.58 ± 0.19	17.9 ± 2.0	Meszner et al. (2013)
69			PM	4–11	IR_{50}	12/12	EXP	59.78 ± 0.23	3.92 ± 0.21	21.0 ± 2.6 (15.3 ± 1.6)[2]	Meszner et al. (2013)
70			PM	4–11	$pIRIR_{225}$	12/12	EXP	74.13 ± 0.45	4.29 ± 0.24	21.4 ± 2.3 (17.3 ± 1.1)[2]	Meszner et al. (2013)
71	**BT708**	Seilitz	Q	4–11	BOSL	22/24	EXP+LIN	77.59 ± 1.34	3.65 ± 0.22	21.3 ± 2.6	Meszner et al. (2013)
72	**BT709**	Seilitz	Q	4–11	BOSL	9/12	EXP+LIN	74.11 ± 1.16	3.41 ± 0.22	21.7 ± 2.8	Meszner et al. (2013)

#	ID	Profile	M	Grain Size [µm]	Signal	n	Fit	D_e [Gy]	$\dot{D}_{total}$ [Gy ka^{-1}]	Age [ka]	Reference
73	**BT710**	Seilitz	Q	4–11	BOSL	9/12	EXP	71.67 ± 1.21	3.51 ± 0.17	20.4 ± 2.1	Meszner et al. (2013)
74	**BT711**	Seilitz	Q	4–11	BOSL	12/12	EXP+LIN	92.55 ± 0.78	3.46 ± 0.21	26.7 ± 3.3	Meszner et al. (2013)
75		Seilitz	PM	4–11	IR_{50}	12/12	EXP	72.72 ± 0.33	3.80 ± 0.19	26.2 ± 3.0	Meszner et al. (2013)
										(19.1 ± 2.0)[2]	
76		Seilitz	PM	4–11	$pIRIR_{225}$	12/12	EXP	88.20 ± 0.62	4.17 ± 0.21	26.5 ± 3.4	Meszner et al. (2013)
										(21.2 ± 2.1)[2]	
77	**BT712**	Seilitz	Q	4–11	BOSL	12/12	EXP+LIN	83.27 ± 1.12	3.32 ± 0.18	25.1 ± 2.6	Meszner et al. (2013)
78	**BT713**	Seilitz	Q	4–11	BOSL	12/12	EXP+LIN	105.18 ± 1.83	3.40 ± 0.22	31.1 ± 4.1	Meszner et al. (2013)
79			PM	4–11	IR_{50}	12/12	EXP	75.22 ± 0.36	3.72 ± 0.21	27.7 ± 3.4	Meszner et al. (2013)
										(20.2 ± 2.2)[2]	
80			PM	4–11	$pIRIR_{225}$	12/12	EXP	93.14 ± 0.77	4.10 ± 0.23	28.4 ± 3.7	Meszner et al. (2013)
										(22.7 ± 2.6)[2]	
81	**BT714**	Seilitz	Q	4–11	BOSL	12/12	EXP+LIN	101.45 ± 1.09	3.50 ± 0.23	29.1 ± 3.6	Meszner et al. (2013)
82			PM	4–11	IR_{50}	12/12	EXP	78.68 ± 0.51	3.85 ± 0.22	28.0 ± 3.4	Meszner et al. (2013)
										(20.4 ± 2.3)[2]	
83			PM	4–11	$pIRIR_{225}$	12/12	EXP	94.82 ± 0.67	4.23 ± 0.24	28.0 ± 4.2	Meszner et al. (2013)
										(22.4 ± 2.6)[2]	
84	**BT715**	Seilitz	Q	4–11	BOSL	12/12	EXP+LIN	250.22 ± 4.79	3.43 ± 0.17	73.0 ± 7.6	Meszner et al. (2013)
85			PM	4–11	IR_{50}	12/12	EXP	195.09 ± 0.90	3.91 ± 0.20	69.5 ± 8.1	Meszner et al. (2013)
										(50.0 ± 5.1)[2]	
86			PM	4–11	$pIRIR_{225}$	12/12	EXP	245.07 ± 1.06	4.26 ± 0.22	72.3 ± 9.6[2]	Meszner et al. (2013)
										(57.5 ± 5.8)[2]	
87	**BT716**	Zehren	Q	4–11	BOSL	12/12	EXP+LIN	65.91 ± 0.74	3.27 ± 0.18	20.2 ± 2.2	unpublished
88	**BT717**	Zehren	Q	4–11	BOSL	12/12	EXP+LIN	78.77 ± 1.13	3.29 ± 0.20	23.9 ± 2.9	unpublished
89	**BT718**	Zehren	Q	4–11	BOSL	12/12	EXP+LIN	79.65 ± 1.18	3.34 ± 0.21	23.8 ± 3.0	unpublished
90	**BT719**	Zehren	Q	4–11	BOSL	12/12	EXP+LIN	91.43 ± 1.15	3.58 ± 0.22	25.5 ± 3.2	unpublished
91	**BT720**	Zehren	Q	4–11	BOSL	12/12	EXP+LIN	90.21 ± 1.13	3.15 ± 0.17	28.6 ± 3.2	unpublished
92	**BT752**	DV	Q	4–11	BOSL	10/12	EXP+LIN	322.4 ± 5.9	3.05 ± 0.20	105.7 ± 14.4	Fuchs et al. (2012)
93	**BT753**	DV	Q	4–11	BOSL	12/12	EXP+LIN	344.7 ± 1.3	3.16 ± 0.20	108.9 ± 13.6	Fuchs et al. (2012)
94	**BT754**	DV	Q	4–11	BOSL	12/12	EXP+LIN	344.5 ± 3.9	3.28 ± 0.21	104.9 ± 13.6	Fuchs et al. (2012)
95	**BT755**	DV	Q	4–11	BOSL	11/12	EXP+LIN	306.1 ± 2.9	3.39 ± 0.22	90.3 ± 12.0	Fuchs et al. (2012)
96	**BT756**	DV	Q	4–11	BOSL	12/12	EXP+LIN	252.5 ± 1.0	3.43 ± 0.22	73.7 ± 9.4	Fuchs et al. (2012)
97	**BT757**	DV	Q	4–11	BOSL	12/12	EXP+LIN	255.1 ± 2.0	3.58 ± 0.24	71.3 ± 9.8	Fuchs et al. (2012)
98	**BT758**	DV	Q	38–63	BOSL	9/12	EXP+LIN	246.6 ± 10.4	3.77 ± 0.21	65.4 ± 9.2	Fuchs et al. (2012)
99		DV	Q	4–11	BOSL	11/12	EXP	242.5 ± 3.7	3.85 ± 0.25	63.0 ± 8.4	Fuchs et al. (2012)
100	**BT759**	DV	Q	4–11	BOSL	12/12	EXP+LIN	231.9 ± 3.3	4.58 ± 0.31	50.6 ± 7.0	Fuchs et al. (2012)
101	**BT760**	DV	Q	90–200	BOSL	18/41	EXP	146.6 ± 5.8	3.22 ± 0.23	45.6 ± 7.4	Fuchs et al. (2012)

#	ID	Profile	M	Grain Size [µm]	Signal	n	Fit	D_e [Gy]	$\dot{D}_{total}$ [Gy ka^{-1}]	Age [ka]	Reference
102		DV	Q	38–63	BOSL	18/24	EXP+LIN	169.8 ± 4.0	3.88 ± 0.21	43.7 ± 5.6	Fuchs et al. (2012)
103		DV	Q	4–11	BOSL	12/12	EXP	180.6 ± 2.6	3.96 ± 0.27	45.6 ± 6.2	Fuchs et al. (2012)
104	**BT761**	DV	Q	90–200	BOSL	20/45	EXP	96.8 ± 4.4	3.44 ± 0.23	28.1 ± 4.6	Fuchs et al. (2012)
105		DV	Q	38–63	BOSL	20/24	EXP	102.4 ± 3.8	4.17 ± 0.23	24.6 ± 3.2	Fuchs et al. (2012)
106		DV	Q	4–11	BOSL	12/12	EXP	115.8 ± 1.1	4.25 ± 0.27	27.2 ± 3.6	Fuchs et al. (2012)
107	**BT762**	DV	Q	90–200	BOSL	28/48	EXP	83.7 ± 3.2	3.80 ± 0.25	22.1 ± 3.4	Fuchs et al. (2012)
108		DV	Q	38–63	BOSL	19/48	EXP	97.7 ± 3.1	4.58 ± 0.25	21.3 ± 2.8	Fuchs et al. (2012)
109		DV	Q	4–11	BOSL	10/12	EXP	110.5 ± 3.4	4.67 ± 0.30	23.6 ± 3.4	Fuchs et al. (2012)
110	**BT763**	DV	Q	90–200	BOSL	13/48	EXP	79.1 ± 2.7	3.67 ± 0.28	21.6 ± 3.6	Fuchs et al. (2012)
111		DV	Q	38–63	BOSL	18/24	EXP	99.3 ± 3.1	4.39 ± 0.29	22.6 ± 3.2	Fuchs et al. (2012)
112		DV	Q	4–11	BOSL	12/12	EXP	93.7 ± 0.9	4.48 ± 0.32	20.9 ± 3	Fuchs et al. (2012)
113	**BT764**	DV	Q	90–200	BOSL	13/57	EXP	85.7 ± 2.8	3.68 ± 0.24	23.3 ± 3.4	Fuchs et al. (2012)
114		DV	Q	38–63	BOSL	11/24	EXP	87.6 ± 3.2	4.43 ± 0.24	19.8 ± 2.6	Fuchs et al. (2012)
115		DV	Q	4–11	BOSL	12/12	EXP	105.8 ± 1.8	4.52 ± 0.29	23.4 ± 3.2	Fuchs et al. (2012)
116	**BT765**	DV	Q	90–200	BOSL	17/48	EXP	85.4 ± 3.5	3.51 ± 0.22	24.4 ± 3.6	Fuchs et al. (2012)
117		DV	Q	38–63	BOSL	8/19	EXP	84.1 ± 3.2	4.23 ± 0.23	19.9 ± 2.6	Fuchs et al. (2012)
118		DV	Q	4–11	BOSL	12/12	EXP	94.0 ± 1.1	4.31 ± 0.27	21.8 ± 2.8	Fuchs et al. (2012)
119	**BT766**	DV	Q	90–200	BOSL	8/48	EXP	83.0 ± 4.3	3.75 ± 0.23	22.1 ± 3.6	Fuchs et al. (2012)
120	**BT835**	Gleina	Q	4–11	BOSL	12/12	EXP+LIN	80.4 ± 0.69	3.29 ± 0.18	24.5 ± 2.7	Zech et al. (2012)
121	**BT836**	Gleina	Q	4–11	BOSL	12/12	EXP+LIN	71.04 ± 1.14	3.1 ± 0.17	22.9 ± 2.6	Zech et al. (2012)
122	**BT837**	Gleina	Q	4–11	BOSL	12/12	EXP+LIN	89.73 ± 1.72	3.38 ± 0.19	26.5 ± 3.1	Zech et al. (2012)
123	**BT838**	Gleina	Q	4–11	BOSL	12/12	EXP+LIN	88.17 ± 0.92	3.15 ± 0.17	28.0 ± 3.0	Zech et al. (2012)
124	**BT839**	Gleina	Q	4–11	BOSL	12/12	EXP+LIN	87.71 ± 0.99	3.29 ± 0.18	26.6 ± 2.9	Zech et al. (2012)
125	**BT840**	Gleina	Q	4–11	BOSL	12/12	EXP+LIN	132.91 ± 1.33	3.41 ± 0.19	39.0 ± 4.4	Zech et al. (2012)
126	**BT841**[4]	Gleina	-	-	-	-	NV	NV	NV	-	
127	**BT842**	Gleina	Q	4–11	BOSL	12/12	EXP+LIN	161.38 ± 1.25	3.54 ± 0.2	45.6 ± 5.3	Zech et al. (2012)
128	**BT843**[4]	Gleina	-	-	-	-	NV	NV	NV	-	
129	**BT844**	Gleina	Q	4–11	BOSL	12/12	EXP+LIN	235.46 ± 2.41	3.23 ± 0.18	72.8 ± 8.1	Zech et al. (2012)
130	**BT845**[4]	Gleina	-	-	-	-	NV	NV	NV	-	
131	**BT998**	Rottewitz	Q	4–11	BOSL	25/25	EXP+LIN	129.25 ± 2.47	3.54 ± 0.19	36.6 ± 4.2	unpublished
132	**BT999**	Rottewitz	Q	4–11	BOSL	13/13	EXP+LIN	234.11 ± 1.16	3.34 ± 0.18	70.0 ± 7.6	unpublished
133	**BT1000**	Rottewitz	Q	4–11	BOSL	11/12	EXP+LIN	228.66 ± 1.28	3.66 ± 0.20	62.5 ± 6.8	unpublished
134	**BT1001**	Rottewitz	Q	4–11	BOSL	12/12	EXP+LIN	234.62 ± 4.04	3.41 ± 0.18	68.9 ± 7.8	unpublished
135	**BT1002**	Rottewitz	Q	4–11	BOSL	12/12	EXP+LIN	243.25 ± 0.87	3.54 ± 0.19	68.6 ± 7.5	unpublished
136	**BT1003**	Rottewitz	Q	4–11	BOSL	12/12	EXP+LIN	252.66 ± 2.69	3.45 ± 0.19	73.4 ± 8.0	unpublished
137	**BT1004**	Rottewitz	Q	4–11	BOSL	12/12	EXP+LIN	253.71 ± 1.22	3.33 ± 0.18	76.3 ± 8.2	unpublished
138	**BT1005**	Rottewitz	Q	4–11	BOSL	12/12	EXP+LIN	292.33 ± 2.71	3.31 ± 0.19	88.3 ± 10.2	unpublished

#	ID	Profile	M	Grain Size [µm]	Signal	n	Fit	D_e [Gy]	$\dot{D}_{total}$ [Gy ka^{-1}]	Age [ka]	Reference
139	**BT1006**	Rottewitz	Q	4–11	BOSL	12/12	EXP+LIN	305.31 ± 2.29	3.32 ± 0.19	92.0 ± 10.7	unpublished
140	**ZEU I**	Zeuchfeld	Q	4–11	BOSL	12/12	EXP+LIN	74.22 ± 0.74	3.28 ± 0.24	22.6 ± 3.4	Kreutzer et al. (2012A)
141	**ZEU II**[3]	Zeuchfeld	Q	200–240	BOSL	6/48	EXP	82.74 ± 2.25	2.69 ± 0.22	30.7 ± 4.7	Kreutzer et al. (2012A)
142	**ZEU III**	Zeuchfeld	Q	4–11	BOSL	12/12	EXP+LIN	235.63 ± 1.79	3.25 ± 0.24	72.5 ± 10.8	Kreutzer et al. (2012A)
143	**ZEU IV**	Zeuchfeld	Q	38–63	BOSL	17/24	EXP+LIN	224.64 ± 8.66	3.27 ± 0.3	68.7 ± 11.2	Kreutzer et al. (2012A)
144	**ZEU V**	Zeuchfeld	Q	38–63	BOSL	20/24	EXP+LIN	287.11 ± 9.08	2.46 ± 0.24	116.6 ± 21.2	Kreutzer et al. (2012A)
145	**ZEU/SA1**	Zeuchfeld	Q	130–200	BOSL	4/14	EXP+LIN	220.48 ± 17.99	1.23 ± 0.2	179 ± 51 (minimum age)	Kreutzer et al. (2012A)
146	**ZEU/SA1**	Zeuchfeld	KFS	130–200	IR-RF	7/9	stretched EXP	623.95 ± 46.84	1.93 ± 0.19	323 ± 70 (maximum age)	Kreutzer et al. (2012A)

[1]OSL adjusted protocol, cf. Kreutzer et al. (2012)

[2]Age without fading correction, cf. Meszner et al. (2013)

[3]Dating was done by Tobias Lauer

[4]Samples BT841, BT843 and BT845 are duplicated samples for samples BT840, BT842 and BT844 and have not been further treated.

M = Mineral; Q = quartz; PM = polymineral; KFS = K-feldspar

Signal = investigated luminescence signal; BOSL = blue OSL; IR_{50} = IRSL@50 °C; $pIRIR_{225}$ = post IRSL@225 °C; IR-RF = infrared radiofluorescence

Fit = chosen function for dose response curve fitting: EXP = exponential; EXP+LIN = exponential plus linear

NV = no value (not measured)

DV = Dolní Věstonice

The chosen water contents are given in the cited articles.

The total dose rates ($\dot{D}_{total}$) considers cosmic dose rates ($\dot{D}_{cosm.}$; Sec. A.2), a-values (Sec. A.3), attenuation factors and water contents.

The chosen water contents are given in the cited articles. All ages given as mean ± 2σ uncertainty.

A.2 Complete list of nuclide concentrations and cosmic dose rates

#	ID	Profile	α-counting		ICP-MS	γ-ray-spectrometry			$\dot{D}_{cosm.}$	Reference
			Th	U	K	Th	U	K		
			[ppm]	[ppm]	[%]	[ppm]	[ppm]	[%]	[Gy ka^{-1}]	
1	**BT594**	Seilitz	10.66 ± 0.95	3.73 ± 0.29	1.87 ± 0.09	NV	NV	NV	0.13 ± 0.01	Meszner et al. (2013)
2	**BT607**[1]	Ostrau	13.82 ± 0.93	2.58 ± 0.28	1.93 ± 0.19	NV	NV	NV	0.21 ± 0.01	Kreutzer et al. (2012)
3	**BT608**[1]	Ostrau	9.63 ± 0.96	3.43 ± 0.29	1.95 ± 0.2	NV	NV	NV	0.2 ± 0.01	Kreutzer et al. (2012)
4	**BT609**[1]	Ostrau	7.2 ± 0.99	3.49 ± 0.3	1.96 ± 0.2	NV	NV	NV	0.19 ± 0.01	Kreutzer et al. (2012)
5	**BT610**[1]	Ostrau	9.07 ± 1.07	2.88 ± 0.32	1.84 ± 0.18	NV	NV	NV	0.19 ± 0.01	Kreutzer et al. (2012)
6	**BT611**[1]	Ostrau	7.69 ± 0.86	3.39 ± 0.27	1.83 ± 0.18	NV	NV	NV	0.17 ± 0.01	Kreutzer et al. (2012)
7	**BT612**[1]	Ostrau	8.33 ± 0.9	3.55 ± 0.27	1.84 ± 0.18	NV	NV	NV	0.16 ± 0.01	Kreutzer et al. (2012)
8	**BT613**[1]	Ostrau	6.21 ± 0.84	3.34 ± 0.26	1.93 ± 0.19	NV	NV	NV	0.16 ± 0.01	Kreutzer et al. (2012)
9	**BT614**[1]	Ostrau	9.11 ± 0.88	3.33 ± 0.27	1.74 ± 0.17	NV	NV	NV	0.15 ± 0.01	Kreutzer et al. (2012)
10	**BT615**[1]	Ostrau	8.67 ± 0.86	3.47 ± 0.26	1.68 ± 0.17	NV	NV	NV	0.15 ± 0.01	Kreutzer et al. (2012)
11	**BT616**[1]	Ostrau	8.37 ± 0.97	3.77 ± 0.3	1.65 ± 0.16	NV	NV	NV	0.14 ± 0.01	Kreutzer et al. (2012)
12	**BT617**[1]	Ostrau	6.75 ± 0.86	3.23 ± 0.26	1.75 ± 0.17	10.97 ± 0.55[2]	2.62 ± 0.13[2]	1.84 ± 0.09[2]	0.09 ± 0.01	Kreutzer et al. (2012)
13	**BT618**[1]	Ostrau	11.16 ± 0.93	2.96 ± 0.28	1.56 ± 0.16	10.13 ± 0.51[2]	2.58 ± 0.13[2]	1.65 ± 0.08[2]	0.1 ± 0.01	Kreutzer et al. (2012)
14	**BT619**[1]	Ostrau	9.31 ± 0.97	3.91 ± 0.3	1.52 ± 0.15	10.35 ± 0.52[2]	2.61 ± 0.13[2]	1.65 ± 0.08[2]	0.1 ± 0.01	Kreutzer et al. (2012)
15	**BT620**[1]	Ostrau	9.84 ± 0.98	3.47 ± 0.3	1.85 ± 0.19	12.18 ± 0.61[2]	3.11 ± 0.16[2]	1.89 ± 0.09[2]	0.1 ± 0.01	Kreutzer et al. (2012)
16	**BT621**[1]	Ostrau	10.45 ± 0.93	2.46 ± 0.28	1.88 ± 0.19	12.78 ± 0.64[2]	3.04 ± 0.15[2]	1.99 ± 0.1[2]	0.1 ± 0.01	Kreutzer et al. (2012)
17	**BT622**[1]	Ostrau	11.02 ± 1.03	3.3 ± 0.31	1.84 ± 0.18	12.82 ± 0.64[2]	3.24 ± 0.16[2]	1.97 ± 0.1[2]	0.11 ± 0.01	Kreutzer et al. (2012)
18	**BT623**[1]	Ostrau	9.9 ± 0.98	3.47 ± 0.3	1.66 ± 0.17	NV	NV	NV	0.1 ± 0.01	Kreutzer et al. (2012)
19	**BT624**[1]	Ostrau	13.18 ± 0.93	1.86 ± 0.28	1.98 ± 0.2	NV	NV	NV	0.12 ± 0.01	Kreutzer et al. (2012)
20	**BT625**[1]	Ostrau	11.70 ± 0.90	2.46 ± 0.27	1.85 ± 0.18	NV	NV	NV	0.12 ± 0.01	Kreutzer et al. (2012)
21	**BT626**[1]	Ostrau	10.22 ± 0.86	3.05 ± 0.26	1.69 ± 0.17	NV	NV	NV	0.13 ± 0.01	Kreutzer et al. (2012)
22	**BT706**	Seilitz	11.36 ± 0.9	2.66 ± 0.27	2.09 ± 0.1	NV	NV	NV	0.21 ± 0.01	Meszner et al. (2013)
23	**BT707**	Seilitz	7.12 ± 0.79	3.68 ± 0.24	2.11 ± 0.11	NV	NV	NV	0.19 ± 0.01	Meszner et al. (2013)
24	**BT708**[3]	Seilitz	9.05 ± 0.86	3.3 ± 0.26	2.12 ± 0.11	10.65 ± 0.12	3.2 ± 0.11	2.05 ± 0.04	0.19 ± 0.01	Meszner et al. (2013)
25	**BT709**	Seilitz	8.56 ± 0.93	3.1 ± 0.28	2 ± 0.1	NV	NV	NV	0.18 ± 0.01	Meszner et al. (2013)
26	**BT710**[3]	Seilitz	8.4 ± 0.91	3.27 ± 0.29	1.96 ± 0.1	10.31 ± 0.13	3 ± 0.12	1.95 ± 0.04	0.16 ± 0.01	Meszner et al. (2013)
27	**BT711**[3]	Seilitz	8.79 ± 0.59	3.37 ± 0.18	1.84 ± 0.09	10.73 ± 0.15	3.25 ± 0.15	1.84 ± 0.04	0.15 ± 0.01	Meszner et al. (2013)
28	**BT712**[3]	Seilitz	12.08 ± 0.93	2.7 ± 0.28	1.8 ± 0.09	10.4 ± 0.15	3.04 ± 0.16	1.75 ± 0.04	0.14 ± 0.01	Meszner et al. (2013)
29	**BT713**	Seilitz	9.28 ± 0.93	3.58 ± 0.29	1.82 ± 0.09	NV	NV	NV	0.13 ± 0.01	Meszner et al. (2013)
30	**BT714**	Seilitz	8.23 ± 0.98	3.8 ± 0.3	1.97 ± 0.1	NV	NV	NV	0.13 ± 0.01	Meszner et al. (2013)
31	**BT715**	Seilitz[3]	8.95 ± 1.02	3.93 ± 0.31	1.91 ± 0.1	12.1 ± 0.13	3.26 ± 0.11	1.86 ± 0.04	0.11 ± 0.01	Meszner et al. (2013)
32	**BT716**	Zehren	7.34 ± 0.82	3.09 ± 0.25	1.92 ± 0.1	NV	NV	NV	0.2 ± 0.01	unpublished
33	**BT717**	Zehren	5.87 ± 0.77	3.77 ± 0.23	1.92 ± 0.1	NV	NV	NV	0.19 ± 0.01	unpublished
34	**BT718**	Zehren	7.61 ± 0.93	3.46 ± 0.28	1.93 ± 0.1	NV	NV	NV	0.17 ± 0.01	unpublished
35	**BT719**	Zehren	11.78 ± 0.92	2.85 ± 0.28	2.02 ± 0.1	NV	NV	NV	0.17 ± 0.01	unpublished
36	**BT720**	Zehren	9.51 ± 0.93	2.75 ± 0.28	1.83 ± 0.09	NV	NV	NV	0.13 ± 0.01	unpublished

#	ID	Profile	α-counting		ICP-MS	γ-ray-spectrometry			$\dot{D}_{cosm.}$	Reference
			Th	U	K	Th	U	K		
			[ppm]	[ppm]	[%]	[ppm]	[ppm]	[%]	[Gy ka^{-1}]	
37	**BT752**[1]	DV	10.4 ± 0.93	2.63 ± 0.28	1.65 ± 0.16	11.22 ± 0.13	3.01 ± 0.19	1.68 ± 0.03	0.08 ± 0.01	Fuchs et al. (2012)
38	**BT753**[1]	DV	9.85 ± 0.83	3.97 ± 0.25	1.38 ± 0.14	13.53 ± 0.15	3.65 ± 0.21	1.67 ± 0.03	0.09 ± 0.01	Fuchs et al. (2012)
39	**BT754**	DV	11.85 ± 0.89	3.12 ± 0.27	1.6 ± 0.16	NV	NV	NV	0.1 ± 0.01	Fuchs et al. (2012)
40	**BT755**	DV	8.88 ± 1.15	4.07 ± 0.35	1.7 ± 0.17	NV	NV	NV	0.1 ± 0.01	Fuchs et al. (2012)
41	**BT756**	DV	7.76 ± 0.64	4.18 ± 0.19	1.8 ± 0.18	NV	NV	NV	0.11 ± 0.01	Fuchs et al. (2012)
42	**BT757**	DV	8.42 ± 0.93	3.59 ± 0.29	1.91 ± 0.19	NV	NV	NV	0.11 ± 0.01	Fuchs et al. (2012)
43	**BT758**[1]	DV	11.76 ± 0.76	3.67 ± 0.23	1.85 ± 0.19	11.68 ± 0.17	3.08 ± 0.28	1.97 ± 0.05	0.12 ± 0.01	Fuchs et al. (2012)
44	**BT759**	DV	13.17 ± 1.42	4.94 ± 0.43	2.11 ± 0.21	NV	NV	NV	0.13 ± 0.01	Fuchs et al. (2012)
45	**BT760**	DV	12.37 ± 1.3	3.88 ± 0.4	1.83 ± 0.18	NV	NV	NV	0.14 ± 0.01	Fuchs et al. (2012)
46	**BT761**	DV	13.32 ± 0.93	4.31 ± 0.28	1.91 ± 0.19	NV	NV	NV	0.15 ± 0.01	Fuchs et al. (2012)
47	**BT762**	DV	12.02 ± 0.83	5.3 ± 0.25	2.17 ± 0.22	NV	NV	NV	0.16 ± 0.01	Fuchs et al. (2012)
48	**BT763**	DV	14.28 ± 1.86	3.95 ± 0.56	2.17 ± 0.22	NV	NV	NV	0.17 ± 0.01	Fuchs et al. (2012)
49	**BT764**	DV	11.86 ± 0.83	4.9 ± 0.25	2.11 ± 0.21	NV	NV	NV	0.19 ± 0.01	Fuchs et al. (2012)
50	**BT765**[1]	DV	11.01 ± 0.78	4.93 ± 0.24	1.94 ± 0.19	11.27 ± 0.13	2.8 ± 0.18	1.87 ± 0.04	0.2 ± 0.01	Fuchs et al. (2012)
51	**BT766**	DV	12.34 ± 0.93	4.83 ± 0.24	2.15 ± 0.17	NV	NV	NV	0.21 ± 0.01	Fuchs et al. (2012)
52	**BT835**[4]	Gleina	11.32 ± 0.93	2.39 ± 0.28	1.82 ± 0.09	(7.16 ± 0.14)	NV	(1.82 ± 0.05)	0.17 ± 0.01	Zech et al. (2012)
53	**BT836**[4]	Gleina	8.48 ± 0.93	3.39 ± 0.28	1.75 ± 0.09	(6.93 ± 0.14)	NV	(1.79 ± 0.05)	0.17 ± 0.01	Zech et al. (2012)
54	**BT837**	Gleina	9.24 ± 0.93	3.73 ± 0.28	1.61 ± 0.08	NV	NV	NV	0.15 ± 0.01	Zech et al. (2012)
55	**BT838**[4]	Gleina	8.62 ± 0.71	3.92 ± 0.22	1.59 ± 0.08	(7.69 ± 0.15)	NV	(1.6 ± 0.04)	0.14 ± 0.01	Zech et al. (2012)
56	**BT839**[4]	Gleina	8.58 ± 0.7	3.43 ± 0.21	1.84 ± 0.09	(7.55 ± 0.15)	NV	(1.9 ± 0.05)	0.13 ± 0.01	Zech et al. (2012)
57	**BT840**	Gleina	8.53 ± 0.85	3.46 ± 0.26	1.84 ± 0.09	NV	NV	NV	0.12 ± 0.01	Zech et al. (2012)
58	**BT841**	Gleina	NV	NV	NV	NV	NV	NV	0.12 ± 0.01	-
59	**BT842**	Gleina	9.69 ± 1.3	3.85 ± 0.39	1.9 ± 0.1	NV	NV	NV	0.11 ± 0.01	Zech et al. (2012)
60	**BT843**	Gleina	9.43 ± 1.27	3.55 ± 0.38	1.86 ± 0.09	NV	NV	NV	0.11 ± 0.01	-
61	**BT844**[4]	Gleina	8.51 ± 0.86	3.6 ± 0.26	1.81 ± 0.09	(7.91 ± 0.16)	NV	(1.87 ± 0.05)	0.11 ± 0.01	Zech et al. (2012)
62	**BT845**[4]	Gleina	8.93 ± 0.92	3.44 ± 0.28	1.78 ± 0.09	(7.83 ± 0.16)	NV	(1.87 ± 0.05)	0.11 ± 0.01	-
63	**BT998**	Rottewitz	9.1 ± 0.97	4.1 ± 0.29	1.89 ± 0.09	NV	NV	NV	0.16 ± 0.01	unpublished
64	**BT999**	Rottewitz	12.1 ± 0.93	2.65 ± 0.28	1.84 ± 0.09	NV	NV	NV	0.15 ± 0.01	unpublished
65	**BT1000**	Rottewitz	12.84 ± 0.93	3.02 ± 0.28	1.97 ± 0.1	NV	NV	NV	0.15 ± 0.01	unpublished
66	**BT1001**	Rottewitz	9.31 ± 0.79	3.44 ± 0.24	1.91 ± 0.1	NV	NV	NV	0.15 ± 0.01	unpublished
67	**BT1002**	Rottewitz	11.92 ± 0.93	3.29 ± 0.28	1.89 ± 0.09	NV	NV	NV	0.14 ± 0.01	unpublished
68	**BT1003**	Rottewitz	13.7 ± 0.93	3 ± 0.28	1.76 ± 0.09	NV	NV	NV	0.13 ± 0.01	unpublished
69	**BT1004**	Rottewitz	10.55 ± 0.84	3.41 ± 0.25	1.76 ± 0.09	NV	NV	NV	0.13 ± 0.01	unpublished
70	**BT1005**	Rottewitz	8.53 ± 1.26	4.04 ± 0.38	1.73 ± 0.09	NV	NV	NV	0.12 ± 0.01	unpublished
71	**BT1006**	Rottewitz	8.75 ± 1.26	3.81 ± 0.38	1.78 ± 0.09	NV	NV	NV	0.12 ± 0.01	unpublished
72	**ZEU I** [5]	Zeuchfeld	NV	NV	NV	2.79 ± 0.15	9.5 ± 0.4	1.92 ± 0.1	0.2 ± 0.02	Kreutzer et al. (2012A)

#	ID	Profile	α-counting		ICP-MS	γ-ray-spectrometry			$\dot{D}_{cosm.}$	Reference
			Th	U	K	Th	U	K		
			[ppm]	[ppm]	[%]	[ppm]	[ppm]	[%]	[Gy ka^{-1}]	
73	**ZEU II**[5]	Zeuchfeld	NV	NV	NV	2.55 ± 0.17	9.2 ± 0.4	1.79 ± 0.1	0.16 ± 0.02	Kreutzer et al. (2012A)
74	**ZEU III**[5]	Zeuchfeld	NV	NV	NV	2.77 ± 0.18	10.7 ± 0.4	1.87 ± 0.1	0.15 ± 0.02	Kreutzer et al. (2012A)
75	**ZEU IV**[5]	Zeuchfeld	NV	NV	NV	2.93 ± 0.22	11.3 ± 0.5	2.18 ± 0.1	0.14 ± 0.01	Kreutzer et al. (2012A)
76	**ZEU V**[5]	Zeuchfeld	NV	NV	NV	2.51 ± 0.24	7.9 ± 0.3	1.58 ± 0.1	0.13 ± 0.01	Kreutzer et al. (2012A)
77	**ZEU/SA 1**[5]	Zeuchfeld	NV	NV	NV	0.78 ± 0.07	2.71 ± 0.1	0.94 ± 0.05	0.084 ± 0.008	Kreutzer et al. (2012A)

[1]For total dose rate calculation the values from the α-counting and ICP-MS measurements were taken.

[2]A fixed error of 5% was assumed.

[3]Values from the γ-ray-spectrometry were taken for dose rate calculation.

[4]Due to technical difficulties the values from the γ-ray-spectrometry are not assumed as valid and therefore have not been used for dose rate calculation.

[5]The γ-ray-spectrometry measurements were gratefully financed by Dr. Hans von Suchodoletz and have been carried out at the VKTA Dresden.

M = Mineral; Q = quartz; PM = polymineral; KFS = K-feldspar
NV = no value (not measured)
DV = Dolní Věstonice

Thick source α-counting and ICP-MS measurements have been carried out at the University of Bayreuth.

A.3 Complete list of measured a-values

#	ID	Profile	M	Grain Size [µm]	Signal	n	^{241}Am α-Source	Resetting	a-value
1	**BT594**	Seilitz	Q	4–11	BOSL	NV	NV	NV	NV
2	**BT607**	Ostrau	Q	4–11	BOSL	8/12	Littlemore 721/B	Optical	0.041 ± 0.001
3	**BT608**	Ostrau	Q	4–11	BOSL	NV	NV	NV	NV
4	**BT609**	Ostrau	Q	4–11	BOSL	NV	NV	NV	NV
5	**BT610**	Ostrau	Q	4–11	BOSL	NV	NV	NV	NV
6	**BT611**	Ostrau	Q	4–11	BOSL	1/12	Littlemore 721/B	Optical	0.032 ± 0.001[1]
7	**BT612**	Ostrau	Q	4–11	BOSL	NV	NV	NV	NV
8	**BT613**	Ostrau	Q	4–11	BOSL	9/12	Littlemore 721/B	Optical	0.040 ± 0.001
9	**BT614**	Ostrau	Q	4–11	BOSL	NV	NV	NV	NV
10	**BT615**	Ostrau	Q	4–11	BOSL	NV	NV	NV	NV
11	**BT616**	Ostrau	Q	4–11	BOSL	NV	NV	NV	NV
12	**BT617**	Ostrau	Q	4–11	BOSL	NV	NV	NV	NV
13	**BT618**	Ostrau	Q	4–11	BOSL	8/12	Littlemore 721/B	Optical	0.036 ± 0.001
14	**BT619**	Ostrau	Q	4–11	BOSL	NV	NV	NV	NV
15	**BT620**	Ostrau	Q	4–11	BOSL	NV	NV	NV	NV
16	**BT621**	Ostrau	Q	4–11	BOSL	NV	NV	NV	NV
17	**BT622**	Ostrau	Q	4–11	BOSL	NV	NV	NV	NV
18	**BT623**	Ostrau	Q	4–11	BOSL	2/6	Littlemore 721/B	Optical	0.030 ± 0.002
19	**BT624**	Ostrau	Q	4–11	BOSL	NV	NV	NV	NV
20	**BT625**	Ostrau	Q	4–11	BOSL	6/7	Littlemore 721/B	Optical	0.035 ± 0.001
21	**BT626**	Ostrau	Q	4–11	BOSL	NV	NV	NV	NV
22	**BT706**	Seilitz	Q	4–11	BOSL	NV	NV	NV	NV
23	**BT707**	Seilitz	Q	4–11	BOSL	7/8	Littlemore 721/B	Optical	0.044 ± 0.002
24			PM	4–11	IR_{50}	12/12	Littlemore 721/B	Heating	0.079 ± 0.001
25			PM	4–11	$pIRIR_{225}$	12/12	Littlemore 721/B	Heating	0.118 ± 0.002
26	**BT708**	Seilitz	Q	4–11	BOSL	NV	NV	NV	NV
27	**BT709**	Seilitz	Q	4–11	BOSL	NV	NV	NV	NV
28	**BT710**	Seilitz	Q	4–11	BOSL	8/8	Littlemore 721/B	Optical	0.046 ± 0.002
29	**BT711**	Seilitz	Q	4–11	BOSL	NV	NV	NV	NV
30		Seilitz	PM	4–11	IR_{50}	12/12	Risø DA-15	Heating	0.073 ± 0.001
31		Seilitz	PM	4–11	$pIRIR_{225}$	12/12	Risø DA-15	Heating	0.107 ± 0.002
32	**BT712**	Seilitz	Q	4–11	BOSL	8/8	Littlemore 721/B	Optical	0.040 ± 0.002
33	**BT713**	Seilitz	Q	4–11	BOSL	NV	NV	NV	NV
34			PM	4–11	IR_{50}	12/12	Littlemore 721/B	Heating	0.072 ± 0.001
35			PM	4–11	$pIRIR_{225}$	12/12	Littlemore 721/B	Heating	0.108 ± 0.002
36	**BT714**	Seilitz	Q	4–11	BOSL	NV	NV	NV	NV
37			PM	4–11	IR_{50}	12/12	Littlemore 721/B	Heating	0.075 ± 0.001
38			PM	4–11	$pIRIR_{225}$	12/12	Littlemore 721/B	Heating	0.112 ± 0.001
39	**BT715**	Seilitz	Q	4–11	BOSL	5/6	Littlemore 721/B	Optical	0.030 ± 0.002
40			PM	4–11	IR_{50}	12/12	Risø DA-15	Heating	0.072 ± 0.002
41			PM	4–11	$pIRIR_{225}$	12/12	Risø DA-15	Heating	0.104 ± 0.002
42	**BT716**	Zehren	Q	4–11	BOSL	10/10	Littlemore 721/B	Optical	0.042 ± 0.002
43	**BT717**	Zehren	Q	4–11	BOSL	NV	NV	NV	NV
44	**BT718**	Zehren	Q	4–11	BOSL	NV	NV	NV	NV
45	**BT719**	Zehren	Q	4–11	BOSL	12/12	Littlemore 721/B	Optical	0.036 ± 0.002
46	**BT720**	Zehren	Q	4–11	BOSL	NV	NV	NV	NV
47	**BT752**	DV	Q	4–11	BOSL	13/17	Littlemore 721/B	Optical	0.047 ± 0.002
48	**BT753**	DV	Q	4–11	BOSL	8/9	Littlemore 721/B	Optical	0.048 ± 0.002
49	**BT754**	DV	Q	4–11	BOSL	NV	NV	NV	NV
50	**BT755**	DV	Q	4–11	BOSL	NV	NV	NV	NV
51	**BT756**	DV	Q	4–11	BOSL	NV	NV	NV	NV

#	ID	Profile	M	Grain Size [µm]	Signal	n	^{241}Am α-Source	Resetting	a-value
52	**BT757**	DV	Q	4–11	BOSL	NV	NV	NV	NV
53	**BT758**	DV	Q	4–11	BOSL	11/15	Littlemore 721/B	Optical	0.040 ± 0.001
54	**BT759**	DV	Q	4–11	BOSL	12/18	Littlemore 721/B	Optical	0.038 ± 0.002
55	**BT760**	DV	Q	4–11	BOSL	NV	NV	NV	NV
56	**BT761**	DV	Q	4–11	BOSL	NV	NV	NV	NV
57	**BT762**	DV	Q	4–11	BOSL	NV	NV	NV	NV
58	**BT763**	DV	Q	4–11	BOSL	8/12	Littlemore 721/B	Optical	0.035 ± 0.002
59	**BT764**	DV	Q	4–11	BOSL	NV	NV	NV	NV
60	**BT765**	DV	Q	4–11	BOSL	11/14	Littlemore 721/B	Optical	0.048 ± 0.002
61	**BT766**	DV	Q	90–200	NV	NV	NV	NV	NV
62	**BT835**	Gleina	Q	4–11	BOSL	8/12	Littlemore 721/B	Optical	0.042 ± 0.001
63	**BT836**	Gleina	Q	4–11	BOSL	12/12	Littlemore 721/B	Optical	0.025 ± 0.001
64	**BT837**	Gleina	Q	4–11	BOSL	8/12	Littlemore 721/B	Optical	0.051 ± 0.002
65	**BT838**	Gleina	Q	4–11	BOSL	11/12	Littlemore 721/B	Optical	0.031 ± 0.001
66	**BT839**	Gleina	Q	4–11	BOSL	11/12	Littlemore 721/B	Optical	0.039 ± 0.001
67	**BT840**	Gleina	Q	4–11	BOSL	12/12	Littlemore 721/B	Optical	0.051 ± 0.002
68	**BT841**[2]	Gleina	-	-	-	-	-	-	-
69	**BT842**	Gleina	Q	4–11	BOSL	12/12	Littlemore 721/B	Optical	0.040 ± 0.001
70	**BT843**[2]	Gleina	-	-	-	-	-	-	-
71	**BT844**	Gleina	Q	4–11	BOSL	12/12	Littlemore 721/B	Optical	0.034 ± 0.001
72	**BT845**[2]	Gleina	-	-	-	-	-	-	-
73	**BT998**	Rottewitz	Q	4–11	BOSL	11/12	Littlemore 721/B	Optical	0.034 ± 0.001
74	**BT999**	Rottewitz	Q	4–11	BOSL	12/12	Littlemore 721/B	Optical	0.035 ± 0.001
75	**BT1000**	Rottewitz	Q	4–11	BOSL	12/12	Littlemore 721/B	Optical	0.039 ± 0.001
76	**BT1001**	Rottewitz	Q	4–11	BOSL	12/12	Littlemore 721/B	Optical	0.036 ± 0.001
77	**BT1002**	Rottewitz	Q	4–11	BOSL	12/12	Littlemore 721/B	Optical	0.036 ± 0.001
78	**BT1003**	Rottewitz	Q	4–11	BOSL	12/12	Littlemore 721/B	Optical	0.034 ± 0.001
79	**BT1004**	Rottewitz	Q	4–11	BOSL	11/12	Littlemore 721/B	Optical	0.034 ± 0.001
80	**BT1005**	Rottewitz	Q	4–11	BOSL	12/12	Littlemore 721/B	Optical	0.034 ± 0.001
81	**BT1006**	Rottewitz	Q	4–11	BOSL	12/12	Littlemore 721/B	Optical	0.034 ± 0.001
82	**ZEU I**	Zeuchfeld	Q	4–11	BOSL	11/12	Littlemore 721/B	Optical	0.037 ± 0.001
83	**ZEU II**	Zeuchfeld	Q	200–240	NV	NV	NV	NV	NV
84	**ZEU III**	Zeuchfeld	Q	4–11	BOSL	12/12	Littlemore 721/B	Optical	0.034 ± 0.001
85	**ZEU IV**	Zeuchfeld	Q	38–63	NV	NV	NV	NV	NV
86	**ZEU V**	Zeuchfeld	Q	38–63	NV	NV	NV	NV	NV
87	**ZEU/SA 1**	Zeuchfeld	Q	130–200	NV	NV	NV	NV	NV
88	**ZEU/SA 1**	Zeuchfeld	KFS	130–200	NV	NV	NV	NV	NV

[1] A fixed error was used.

[2]Samples BT841, BT843 and BT845 are duplicated samples for samples BT840, BT842 and BT844 and have not been further treated.

M = Mineral; Q = quartz; PM = polymineral; KFS = K-feldspar

Signal = investigated luminescence signal

BOSL = blue OSL; IR_{50} = IRSL@50 °C; $pIRIR_{225}$ = post IRSL@225 °C

IR-RF = infrared radiofluorescence

Fit = chosen function for dose response curve fitting: EXP = exponential; EXP+LIN = exponential plus linear

NV = no value (not measured)

DV = Dolní Věstonice

Optical = optical bleaching in a solar simulator

Heating = heating in an external furnace at 450 °C for at c. 45 min

All a-values given as mean ± 2σ uncertainty.

Not for all samples an a-value was estimated. Thus, for some studies a mean a-value was calculated, but from that it may appear that the listed a-values are not consistent with the published results.

A.4 Complete list of functions in the R package 'Luminescence'

#	Name	Description	Author
1	`Analyse_SAR.OSLdata()`	Analyse SAR CW-OSL measurements	Sebastian Kreutzer
2	`Calc_CentralDose()`	Apply the central age model (CAM) to a given D_e distribution	Christoph Burow and Rex Galbraith
3	`Calc_CommonDose()`	Apply the common age model to a given D_e distribution	Christoph Burow and Rex Galbraith
4	`Calc_FadingCorr()`	Applying a fading correction according to Huntley and Lamothe (2001) for a given age and a given g-value	Sebastian Kreutzer
5	`Calc_FiniteMixture()`	Apply the finite mixture model (FMM) to a given D_e distribution	Christoph Burow and Rex Galbraith
6	`Calc_FuchsLang2001()`	Calculate D_e applying the method of Fuchs and Lang (2001)	Sebastian Kreutzer
7	`Calc_MinDose3()`	Apply the (un-)logged three parameter minimum dose model (MAM 3) to a given D_e distribution	Christoph Burow and Rex Galbraith
8	`Calc_MinDose4()`	Apply the (un-)logged three parameter minimum dose model (MAM 4) to a given D_e distribution	Christoph Burow and Rex Galbraith
9	`Calc_OSLLxTxRatio()`	Calculate L_x/T_x ratio for a given set of OSL curves	Sebastian Kreutzer
10	`CW2pHMi()`	Transforms a CW-OSL curve in a pHM-OSL curve via interpolation under hyperbolic modulation conditions (Bos and Wallinga, 2012)	Sebastian Kreutzer
11	`CW2pLM()`	Transforms a CW-OSL curve into a pseudo-LM (pLM) curve (e.g. Bulur, 2000)	Sebastian Kreutzer
12	`CW2pLMi()`	Transforms a CW-OSL curve in a pLM-OSL curve via interpolation under linear modulation conditions (Bos and Wallinga, 2012)	Sebastian Kreutzer
13	`CW2pPMi()`	Transforms a CW-OSL curve in a pPM-OSL curve via interpolation under parabolic modulation conditions (Bos and Wallinga, 2012)	Sebastian Kreutzer
14	`fit_CMCurve()`	Nonlinear Least Squares Fit for CW-OSL Curves	Sebastian Kreutzer
15	`fit_LMCurve()`	Non-linear Least Squares (NLS) fit for LM-OSL curves	Sebastian Kreutzer
16	`plot_BINfileData()`	Plot single luminescence curves from a BIN-file object (`readBIN2R()`)	Sebastian Kreutzer
17	`plot_DeDistribution()`	Plot D_e distribution with a kernel density estimate (KDE)	Sebastian Kreutzer
18	`plot_GrowthCurve()`	Fit and plot a growth curve for luminescence data	Sebastian Kreutzer
19	`plot_Histogram()`	Plot a histogram with a separate error plot	Sebastian Kreutzer
20	`plot_RadialPlot()`	Plot a Galbraith's radial plot	Sebastian Kreutzer and Rex Galbraith
21	`readBIN2R()`	Import Risø BIN-file into **R**	Sebastian Kreutzer
22	`Second2Gray()`	Converting values from seconds (s) to Gray (Gy)	Sebastian Kreutzer

All listed functions will be part of the R package 'Luminescence' version 0.2 (submission date to CRAN, December 15th, 2012). The package source code and the manual is available via http://cran.r-project.org/web/packages/Luminescence/index.html and on the CD in the cover of this thesis.

B Emission and detection wavelengths

WAVELENGTHS RELEVANT FOR LUMINESCENCE DATING

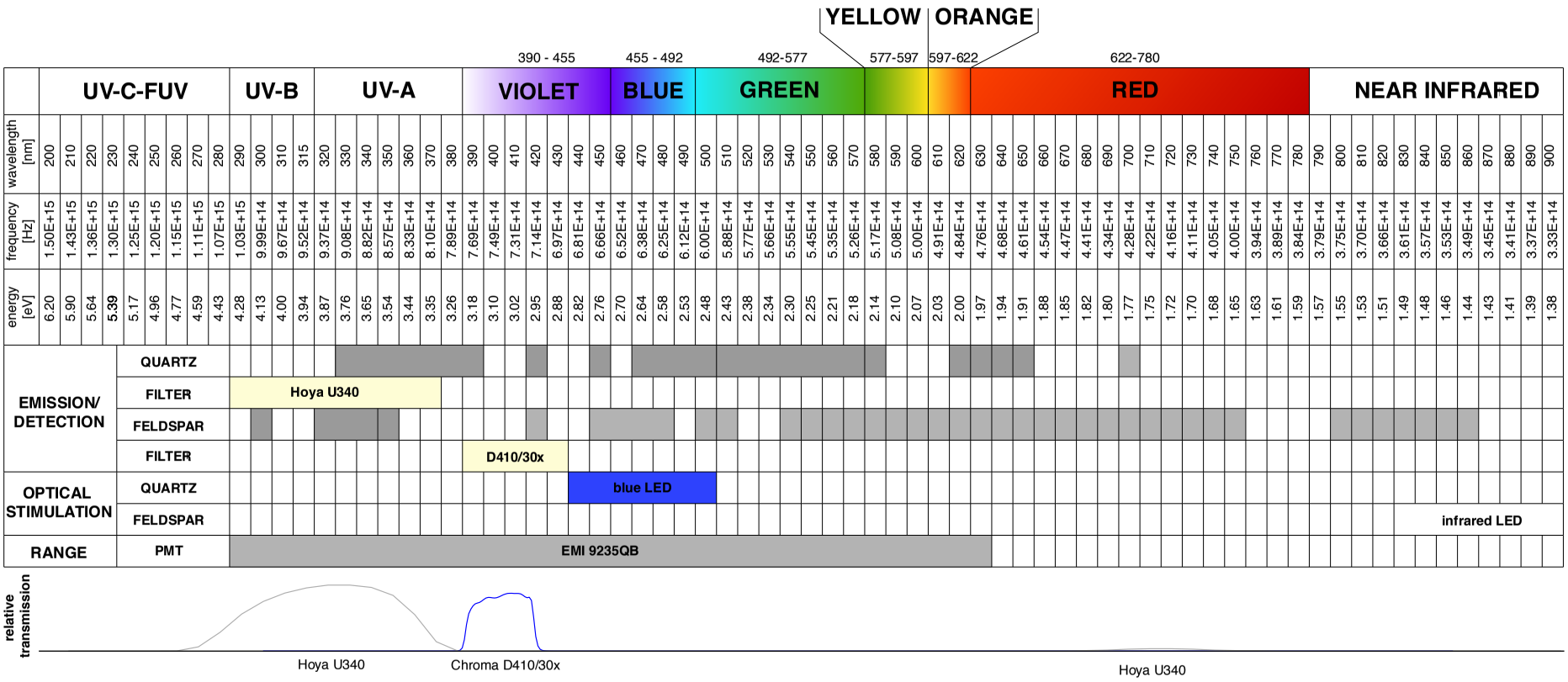

Emission wavelengths taken from Krbetschek et al. (1997)
Spectral wavelengths according to Stöcker (2010)
Filter characteristics taken from the websites of the manufacturers: Hoya U340: http://www.uqgoptics.com/pdf/Hoya%20U-340.pdf [visited: 26.11.2012]
Chroma D410/30x: http://www.chroma.com/product/individual-filters-mirrors/widefield-microscopy/D410_x_30x-EX [visited: 26.11.2012]

SK, 2012

C List of publications

submitted/under review/under revision (status at submission date thesis)

Kreutzer, S., Schmidt, C., DeWitt, R., Fuchs, M., under review. The a-value of polymineral fine grain samples measured with the post-IR IRSL protocol. Radiation Measurements, 1–31. *Finally published in 2014: http://dx.doi.org/10.1016/j.radmeas.2014.04.027*

Meszner, S., **Kreutzer, S.**, Fuchs, M., Faust, D., under revision. Detailed granulometric interpretation of loess sequences – increasingly neglected in quaternary research. Zeitschrift für Geomorphologie, 1–23. *Finally published in 2014: http://dx.doi.org/10.1127/0372-8854/2014/S-00169*

accepted/published

Kreutzer, S., Hülle, D., Thomsen, K.J., Hilgers, A., Kadereit, A., Fuchs, M., 2013. Quantification of cross-bleaching during infrared (IR) light stimulation. Ancient TL 31 (1), 1–10.

Kadereit, A. and **Kreutzer, S.**, 2013. Risø calibration quartz – a challenge for β-source calibration. An applied study with relevance for luminescence dating. Measurement 46 (7), 2238–2250.
doi: http://dx.doi.org/10.1016/j.measurement.2013.03.005

Meszner, S., **Kreutzer, S.**, Fuchs, M., Faust, D., 2013. Late Pleistocene landscape dynamics in Saxony/Germany - Paleoenvironmental reconstruction using loess-paleosol sequences. Quaternary International 296, 95–107.
doi: http://dx.doi.org/10.1016/j.quaint.2012.12.040

Zech, M., **Kreutzer, S.**, Goslar, T., Meszner, S., Krause, T., Faust, D., Fuchs, M., 2013. Technical Note: *n*-Alkane lipid biomarkers in loess: post-sedimentary or syn-sedimentary? Biogeosciences Discuss 9, 9875–9896.
doi: http://dx.doi.org/10.5194/bgd-9-9875-2012

Antoine, P., Rousseau, D.-D., Degeai, J.-P., Moine, O., Lagroix, F., **Kreutzer, S.**, Fuchs, M., Hatté, C., Gauthier, C., Svoboda, J., Lisa, L., 2013. High-resolution record of the environmental response to climatic variations during the last interglacial-glacial cycle in Central Europe: the loess-palaeosol sequence of Dolní Věstonice (Czech Republic), Quaternary Science Reviews 67, 17–38.
doi: http://dx.doi.org/10.1016/j.quascirev.2013.01.014

Schmidt, C. and **Kreutzer, S.**, 2013. Optically stimulated luminescence of amorphous/microcrystalline SiO_2 (silex): basic investigations and potential in archeological dosimetry. Quaternary Geochronology 15, 1–10.
doi: http://dx.doi.org/10.1016/j.quageo.2013.01.005

Fuchs, M., **Kreutzer, S.**, Rousseau, D.-D., Antoine, P., Hatté, C., Lagroix, F., Moine, O., Gauthier, C., Svoboda, J., Lenka, L., 2012. The loess sequence of Dolní Věstonice, Czech Republic: A new OSL based chronology of the Last Climatic Cycle. Boreas, 1–24.
doi: http://dx.doi.org/10.1111/j.1502-3885.2012.00299.x

Kreutzer, S., Lauer, T., Meszner, S., Krbetschek, M.R., Faust, D., Fuchs, M., 2012. Chronology of the Quaternary profile Zeuchfeld in Saxony-Anhalt / Germany – a preliminary luminescence dating study. Zeitschrift für Geomorphologie fast track, 1–21.
doi: http://dx.doi.org/10.1127/0372-8854/2012/S-00112

Kreutzer, S., Schmidt, C., Fuchs, M.C., Dietze, M., Fischer, M., Fuchs, M., 2012. Introducing an R package for luminescence dating analysis. Ancient TL 30 (1), 1–8.
http://www.aber.ac.uk/en/media/ATL---Kreutzer.pdf

Kreutzer, S., Fuchs, M., Meszner, S., Faust, D., 2012. OSL chronostratigraphy of a loess-palaeosol sequence in Saxony/Germany using quartz of different grain sizes. Quaternary

Geochronology 10, 102–109.
doi: http://dx.doi.org/10.1016/j.quageo.2012.01.004

Fuchs, M., **Kreutzer, S.**, Fischer, M., Sauer, D., Sørensen, R., 2012. OSL and IRSL dating of raised beach sand deposits along the southeastern coast of Norway. Quaternary Geochronology 10, 195–200.
doi: http://dx.doi.org/10.1016/j.quageo.2011.11.009

Schmidt, C., **Kreutzer, S.**, Fattahi, M., Bailey, R.M., Zander, A., Zöller, L., 2011. On the luminescence signals of empty sample carriers. Ancient TL 29 (2), 65–74.
doi: http://www.aber.ac.uk/en/media/schmidt_atl29(2)_65-74.pdf

Fuchs, M., Will, M., Kunert, E., **Kreutzer, S.**, Fischer, M., Reverman, R., 2011. The temporal and spatial quantification of Holocene sediment dynamics in a meso-scale catchment in northern Bavaria, Germany. The Holocene 21 (7), 1093–1104.
doi: http://dx.doi.org/10.1177/0959683611400459

D Acknowledgement/Danksagung

Ich bin froh, dass die Liste jener denen ich zu Dank verpflichtet bin, am Ende ziemlich lang geworden ist...:

Mein Dank geht zunächst an den Betreuer dieser Arbeit, Prof. Dr. Markus Fuchs. Sein Beitrag begann mit einem DFG Antrag für ein Projekt in Sachsen zu einem Zeitpunkt, als für mich der Begriff „Lumineszenz“ noch „Science Fiction“ war. Er hat mir über die Jahre meiner Promotion zu jeder Zeit die Unterstützung gegeben, die ich gebraucht habe, und den Druck erhöht, wenn es notwendig war. Aber vor allem hat er mir dabei immer den Freiraum gelassen, meinen eigenen Ideen nachzugehen und meine Vorstellungen umzusetzen. Ein Dank für die Geduld, das Vertrauen über die Zeit und die vielen kritischen, aber immer fairen Diskussionen!

Als Laborleiter hat Manfred Fischer meine ersten Gehversuche im Bayreuther Lumineszenzlabor nicht nur beobachtet, sondern professionell begleitet und zu jeder Zeit unterstützt. Es steht völlig außer Frage, dass ohne seine Hilfe bis heute kein einziges Alter vorliegen würde. Die Liste der vielen begleitenden Gespräche und helfenden Ratschläge bei einer Tasse Espresso ist letztlich sicherlich genau so lang wie jene mit den Science Fiction Filmen, die wir unbedingt noch schauen müssen. Aber: „Nee Kinder, so geht das nicht... .“ Stimmt: Danke!

Diese Arbeit wäre auch nicht möglich gewesen ohne den Rahmen, den mir die Universität Bayreuth und speziell Prof. Dr. Ludwig Zöller am Lehrstuhl Geomorphologie aufgespannt haben. Seine Ratschläge und Ideen haben mir weitergeholfen und das a-Werte Manuskript wäre ohne seinen Vorschlag sicher nicht entstanden.

Dr. Ulrich Hambach hat sich mit mir zusammen sehr geduldig Quarze angeschaut und auf der ein oder anderen Lösstagung meine Lücken am Profil geschlossen.

Danke natürlich auch dem gesamten aktuellen und ehemaligen Lehrstuhlteam. Dies waren und sind: Frau Löbl, PD Dr. Daniel Richter, PD Dr. Klaus-Martin Moldenhauer, Dr. Björn Buggle, Dr. Hans von Suchodoletz, Dr. Michael Zech, Dr. Hao Long, Christian Zeeden, Michael Hark. An Thomas Kolb ein spezieller Dank für die akribische Kontrolle des angehängten Datensalates und die gelegentliche Beratung in allen Rechtslagen.

Auch ohne die gute Zusammenarbeit mit der Dresdner Löss-Gruppe, namentlich Prof. Dr. Dominik Faust und Sascha Meszner, wäre diese Arbeit wohl nie möglich gewesen. Wobei das eigentliche Verständnis für die Qualität der Arbeit von Sascha erst bei Schneeregen in einer verdammt kalten Novembernacht an einer Wand in einem Kalksteinbruch irgendwo in Sachsen begann. Daraus entwickelte sich über die Jahre eine vertrauensvolle Zusammenarbeit mit einer ansteckenden Begeisterung für die Lössforschung. Danke für die Ausdauer bei der für mich immer wieder notwendig gewordenen Einführung in die Geländearbeit und die lokale Löss-Stratigraphie.

Mit Christoph Schmidt verbinden mich viele Forschungsreisen in das Vereinigte Königreich und der Ärger über ein viel zu kleines Waschbecken gepaart mit einer fehlenden Mischbatterie. Danke für die vielen langen und spannenden methodischen Diskussionen sowie die gemeinsame Forschungsarbeit. Und Danke für die vielen ruhig hingenommen und professionell korrigierten physikalischen Fehltritte meinerseits.

To Dr Richard Bailey I would like to express my warmest thanks for the intensive and inspiring time I always had during my visits at the Luminescence Laboratory in Oxford. Thanks also to Dr Jean-Luc Schwenninger and Dr Morteza Fattahi.

Als es wieder einmal eng wurde, konnte ich einen Teil meiner Messungen im Lumineszenzlabor in Heidelberg durchführen. Mein Dank gilt, allen voran, Dr. Annette Kadereit für das Vertrauen in meine Fähigkeiten, akribisches Suchen nach Ungereimtheiten und die wochenlangen Messzeiten. Dank auch an die anderen lokalen Lumigeister: Felizitas, Frau Asmuth und Christian.

Dr. Brigitte John hat mir ursprünglich im Geographiestudium das Interesse an Geoinformationssystemen und Fernerkundung vermittelt, und ich bin dankbar, dass ich ihren trockenen Humor auch in der Zeit als Kollege bei vielen Mensabesuchen genießen durfte.

Mit Steffen hat zwar leider die Poolparty auf dem Dach des Institutsgebäudes am Ende doch nicht mehr stattgefunden, aber es bleiben die schönen Erinnerungen an abendliche Besuche in der Cafeteria und das nächtliche Musizieren im Labor vor einem nochmaligen: „Und weiter geht's!“

Meiner Gießener Kollegin Dr. Johanna Lomax ein Dank für die herzliche Aufnahme in der AG Fuchs und das Vertrauen in meine navigatorischen Fähigkeiten, die uns aber auch vor einem langen Radweg nach Aberystwyth bewahrt haben.

Dem „off-day“ Kommando Maggi und Michael danke für die schönen Momente in der Pension Fröhlich und an Orten in Dresden, die ich noch nicht kannte. @Maggi: Danke für das physisch und virtuell geteilte Büro.

Der Göttinger Doktoren WG Barbara, Björn, Max und Philip für eine immer wieder herzliche Aufnahme und die vielen schönen Stunden in angeregter Diskussion. An Björn ein spezieller Dank für die Annährungsversuche an die hypergeometrische Verteilung am Küchentisch.

Bruder Josef ein Dank für die Möglichkeit der letzten Meter mit beeindruckenden Menschen und die abendlichen vier Zigarettenlängen.

Claudia und Jochen für die Begleitung meines Weges in Bayreuth vom ersten bis zum letzten Moment und die klaren Worte an entscheidenden Stellen. Frederik und Christian danke für die lange Freundschaft und die spontanen Besuche in Bayreuth.

Zum Abschluss geht der Dank an meine Schwester, ihre Familie und meine Eltern für die immer wieder geduldige Unterstützung auf diesem schier endlos langen Weg und an Katrin, ohne die ich wohl nie angefangen hätte.

E Declaration/Erklärung

Hiermit erkläre ich, dass ich diese Arbeit selbständig verfasst und keine anderen als die angegebenen Quellen und Hilfsmittel verwendet habe.

Ich erkläre ferner, dass ich an keiner anderen Hochschule, mit oder ohne Erfolg, als an der Universität Bayreuth versucht habe diese Dissertation einzureichen. Ich habe keine gleichartige Doktorprüfung an einer anderen Hochschule endgültig nicht bestanden.

Gießen, 04.12.2012

Sebastian Kreutzer